Passive Multirate Wave Variables Control for Haptic Applications

by

Naser Yasrebi
B.Sc., University of Tehran, Iran, 2004
M.Sc., University of Tehran, Iran, 2007

A Dissertation Submitted in Partial Fulfillment of the
Requirements for the Degree of

DOCTOR OF PHILOSOPHY

in the Department of Mechanical Engineering

Passive Multirate Wave Variables Control for Haptic Applications

by

Naser Yasrebi
B.Sc., University of Tehran, Iran, 2004
M.Sc., University of Tehran, Iran, 2007

Supervisory Committee

Dr. Daniela Constantinescu, Supervisor
(Department of Mechanical Engineering)

Dr. Afzal Suleman, Departmental Member
(Department of Mechanical Engineering)

Dr. Bradley Buckham, Departmental Member
(Department of Mechanical Engineering)

Dr. Panajotis Agathoklis, Outside Member
(Department of Electrical and Computer Engineering)

Supervisory Committee

Dr. Daniela Constantinescu, Supervisor
(Department of Mechanical Engineering)

Dr. Afzal Suleman, Departmental Member
(Department of Mechanical Engineering)

Dr. Bradley Buckham, Departmental Member
(Department of Mechanical Engineering)

Dr. Panajotis Agathoklis, Outside Member
(Department of Electrical and Computer Engineering)

ABSTRACT

A haptic system is a robotic computer interface which aims to provide tactile feedback for human operators when they manipulate virtual environments (VEs) or remote environments (REs). The tactile feedback is emulated by applying forces, vibrations, or motions to the human users through a haptic device/interface, e.g. a robot arm. Transparency and stability are two important criteria for designing a haptic system. Transparency is related to the realism of user's touch sensation and stability guarantees the safety of the user while interacting with VEs/REs. Because of the nature of the human tactile sensory system, a transparent haptic system demands an update rate greater than 500 Hz, i.e. most commercial haptic devices work at 1 KHz. On the other hand, many haptic applications are multirate systems. The multirate property of a haptic system is due to either the slow update rate of the VE or the impairments of computer networks such as limited transmission bandwidth or packet loss.

Wave transformation is wildly used in teleoperation to cope with both constant and varying time delays. This work aims to use wave transformation to tackle the challenges imposed by multirate property of a haptic system. First, passive multirate wave variables control (PMWVC) is introduced. PMWVC guarantees the passivity of the communication channels through which the fast haptic device is connected to the slow VE/RE. It is shown that to maintain the passivity of the system, aliasing should be avoided in the communication channels, i.e. by using anti-aliasing filters.

Next, PMWVC strategy is applied to two different applications: i) multiuser cooperative haptics and ii) haptic interaction with an unknown VE. In the first application, two users at two different locations manipulate a common virtual object simulated on a central server. The users are connected to the central server through a LAN network. The second application is a single user application in which PMWVC is used to connect the haptic device to an unknown slowly updated VE. Since in this application the VE is unknown, the computational delay of the VE significantly affects the stability of the overall system. To tackle this problem, a nonlinear algorithm based on passivity analysis is proposed. In both examples, numerical and experimental results validating the analytical results are provided. The results show that by using PMWVC, it is possible to significantly improve the performance of a multirate haptic system in terms of transparency and stability.

The second half of this work is devoted to improving the performance of PMWVC in all frequency ranges. In order to study the performance of PMWVC, lifting is used to convert the multirate haptic system to a unirate system. By using this technique, it is shown that velocity estimation plays a critical role in a haptic application with PMWVC, especially in high frequencies. Considering this fact, a method for designing a passive velocity filter in wave domain is proposed.

Finally, a filter bank structure is introduced which enables utilizing a local model in conjunction with PMWVC. In this structure, the outgoing signal sent to the VE is split into two frequency ranges. Low frequency content of the signal is fed to the original VE and high frequency content of the signal is sent to the local model. By using lifting the performance of the proposed structure is studied. The results show that the proposed method improves the transparency of the system in all frequency ranges and unlike utilizing a local model in power domain, it does not impose any restriction on the stability of the system.

Contents

List of Figures

ACKNOWLEDGEMENTS

I would like to sincerely thank my supervisor, Dr. Daniela Constantinescu, for her support and guidance throughout all aspects of my research. It was an excellent privilege for me to work with her and learn from her.

I gratefully thank my supervisory committee members specially Dr. Afzal Suleman and Dr. Bradley Buckham for their help and support during the last months of this work.

I was lucky to be surrounded by a great group of friends and an excellent team of coworkers. In particular, I would like to specially thank Ghazal Hajisalem, Ramtin Rakhsha, and Nima Khadem Mohtaram.

I am very thankful for the financial support of Natural Sciences and Engineering Research Council (NSERC) of Canada, mechanical engineering department, and the Universirty of Victoria.

DEDICATION

I dedicate this thesis to my parents who supported me even from miles away.

Chapter 1

Introduction

1.1 Motivation

1.1.1 Haptics and its Applications

Haptic interfaces (or devices) are robotic computer interfaces through which users can touch, manipulate and feel virtual and/or remote environments. For example, a joystick with force feedback is a haptic interface. Haptic devices can be beneficial in several virtual reality applications, including: medical simulators with force feedback, which can eliminate the need for cadavers and/or animals during surgical training; immersive CAD environments, which can allow engineers to feel a design before building a physical prototype; virtual reality (VR)-based physical rehabilitation programs, which can permit medical personnel to assist remote patients much like they assist patients in traditional therapy programs; computer games with haptic feedback, which can offer a deeper sense of presence in the game environment. Among these applications, medical training has been commercialized. A haptic interface together with a human user and with computer software for generating and rendering the feel of virtual objects (VOs) comprise a haptic system and permits one operator to interact with a virtual environment (VE) using one hand. Because the human user is part of the force control loop, stability and transparency are critical in haptics. Stability guarantees operator's safety. Transparency is related to the realism of user's touch sensations in the VE.

1.1.2 Networked Haptics

Manipulations with two hands and/or cooperation among multiple, potentially remote, users are needed in applications like: supervision of the haptics-based training of a novice resident by an expert surgeon; physical tele-guidance of a remote patient by an occupational therapist; multi-user (on-line) computer games with force feedback. Such manipulations can be enabled by connecting multiple haptic systems together over computer networks like Local Area Networks (LANs), Metropolitan Area Networks (MANs) and the Internet. The connection can be implemented using two different architectures: (i) the client-server architecture shown in Figure 1.1; and (ii) the peer-to-peer architecture depicted in Figure 1.2. In the CS networking scheme, the clients send the user inputs to the server, the server updates the VE state and sends it to the clients, and the clients determine the force feedback corresponding to the updated VE state and apply it to the users. The client-server connectivity is suitable for cooperation among a large number of users [57], but incurs communication delays twice as large as the peer-to-peer connectivity. Furthermore, client-server architecture is desirable in applications that VEs size or cost prohibit their replication at each user (e.g., computationally intensiveVEs which need to run on cluster computers).

In the peer-to-peer networking scheme, each peer computer runs its own copy of the VE, which it updates based on the data received from all other peers. Because it requires data flows between each pair of peers, the peer-to-peer connectivity is suitable for cooperation among a small number of operators [57]. Combinations of the client-server and peer-to-peer architectures can also be used [60, 63].

Networked haptic cooperation removes physical barriers and allows force interactions among distant users which in its turn improves task performance and the sense of immersion [90]. Arguably, the low price and wide accessibility of the Internet (1,668,870,408 users [1]) make it the ideal communications means for networked haptics applications. Unfortunately, Ethernet-based communications links like the Internet are characterized by variable communication delay, jitter, packet loss, and limited packet transmission rate. These characteristics are detrimental to the stability and performance of haptic cooperation. To date, they have hindered networked haptics applications.

1.1.3 Challenges

Stable and transparent networked haptic cooperation is challenging to achieve because stability and transparency place demands on the force control loop that conflict with the characteristics of Ethernet-based networks. Specifically, the human touch requires a force

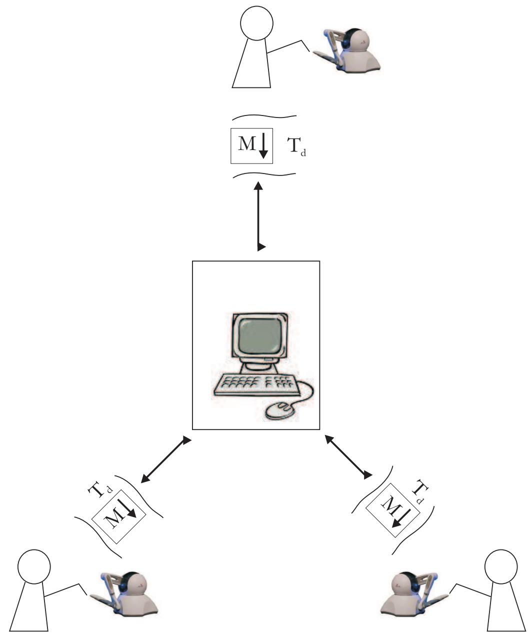

Figure 1.1: Client-server architecture.

refresh rate of at least 500 Hz for convincing [91, 94, 104] interaction with rigid bodies [1]. Furthermore, the force setpoints should be provided at fixed time intervals to ensure the stability of the interaction [24]. Yet, current Ethernet-based networks transmit data packets at frequencies of about 128 Hz [32], with variable delays (due to the packet-switched nature of the communications), and even loose some data packets.

Because these network characteristics hinder the progress of network/Internet-based haptic cooperation, much work has characterized the impact of the communications on stability and realism. The communication delay has been recognized as the major contributor to instability and poor performance in haptic interaction over Internet [3, 6, 18, 30, 41, 43, 47, 65, 74, 103]. Besides degrading stability, the delay in the communication channel may cause drift and thus, incoherency between the states of the different users. Jitter, i.e., the variation in the communication delay, leads to instability [18, 30, 43, 74] and variations in the perceived mass of the manipulated VO [64]. While suitable methods have been proposed to cope with constant time delay, varying time delay remains a challenge. Packet loss threatens stability [30, 43, 50] and can reduce the forces applied to users and change the perceived mass of the VOs [64]. Limited and varying data transfer rate and slowly updated VEs render networked haptic cooperation a multirate system with varying rate. Little attention has been paid to the multirate issue until recently [32].

[1] Lower update rates can be used for haptic rendering of soft VOs.

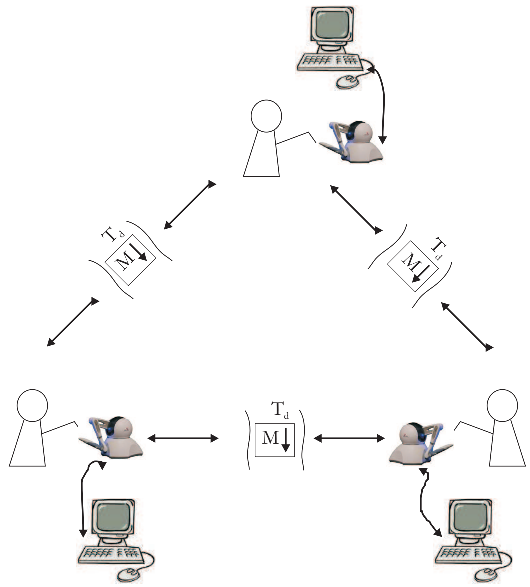

Figure 1.2: Peer-to-peer architecture.

Besides the difficulties due to the network characteristics, haptic cooperation faces challenges due to the different properties of the operators' hands and haptic devices. The uncertainties associated with the physical damping and effective mass of these elements may themselves make haptic cooperation unstable.

The network impairments can be tackled using: (i) computer networking techniques like prediction, compression, buffering, and new effective network protocols; or (ii) classical and modern control tools. Computer networking approaches seek to improve the network performance to bring it closer to the requirements of haptic cooperation. Methods in this category are surveyed in [28, 29]. Control approaches strive to guarantee stability and transparency for the given network performance. The research proposed in this work aims to develop robust controllers for haptic cooperation in clinet-server architecture.

1.2 Statement of the Problem, Objectives and Approach

Limited packet transmission rate, slow update rate of the VE, packet loss, communication time delay, and computational delay converts a unirate haptic system to a multirate system with time delay [42]. This work adopts multirate wave variable control to tackle the problems ensue from the multirate nature of a cooperative haptic system with client-server architecture. Actually, a transparent haptic system requires an update rate greater than 500 Hz [91, 94, 104] and most commercial haptic devices work at 1 Khz. Connecting a fast force feedback loop to a slow or remote VE generates unphysical energy [67, 68] which grows with the sampling time of the VE or update rate of the computer network [67] . The injected energy violates the passivity of the system and has destabilizing effect [32]. The main objectives of this work are to adopt multirate wave control to passively connect the fast force feedback loop to the slow or remote VE and improve the performance of the proposed control strategy in all frequency ranges.

Figure 1.3 depicts the proposed multirate wave variable control strategy. It illustrates that wave [73] (or scattering [6]) variables are transmitted between the haptic interface and the VE, and that the rate change between the fast haptic feedback and the slow VE loops is modeled as wave downsampling and upsampling. In Figure 1.3, notation is used as follows: M is the wave sampling rate drop/increase factor, and is represented as communications downsampling/upsampling factor; $\dot{x}_m$ is the velocity of the haptic interface; $\dot{x}_s$ is the velocity command transmitted to the VE through wave variable communications; F_s is the VE force; F_m is the force applied to the haptic interface by the wave controller; u_m and v_s are the output waves; u_s and v_m are the input waves; and b is the wave impedance. The output and input waves are related to the velocities and forces at the haptic interface (master) and VE (slave) sides via [73]:

$$\begin{array}{ll} u_m(t) = \frac{F_m(t)+b\dot{x}_m(t)}{\sqrt{2b}} & v_s(t) = \frac{-F_s(t)+b\dot{x}_s(t)}{\sqrt{2b}} \\ v_m(t) = \frac{-F_m(t)+b\dot{x}_m(t)}{\sqrt{2b}} & u_s(t) = \frac{F_s(t)+b\dot{x}_s(t)}{\sqrt{2b}} \end{array} . \tag{1.1}$$

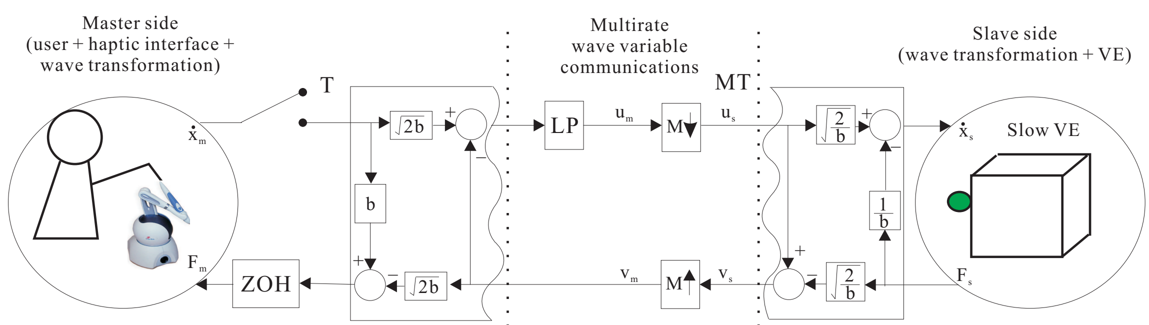

Figure 1.3: Multirate wave variable control of haptic interaction. The drop/increase of the wave sampling rate at the connection between the master side and the slave side is modeled as communications downsampling/upsampling.

The haptic system in Figure 1.3 comprises three main components: (i) the human operator together with the haptic interface, sampler, Zero-Old-Hold (ZOH) and the left side of the wave transformation, hereafter called the master side; (ii) the communication channels;

and (iii) the VE together with the right side of the wave transformation, hereafter called the slave side. If all three components are passive, haptic interaction in slow VEs becomes an interconnection of passive systems and hence, strictly stable [25]. The master and slave sides can be made passive through suitable control [100]. The unirate wave communications are passive for constant transmission delay both for continuous time [6, 73] and discrete time [13] implementation. When rate change happens the passivity of the communication channels is unclear but by making the communication channels passive, it is possible to gaurantee the stability of a haptic system with multirate wave variable control.

This research starts with an investigation of the passivity condition in the communication channels and proposes a method for making the channels passive. Next, the porposed passive multirate wave variables control is applied to two haptic system: i) a multiuser client-server networked haptic system with time delay. 2) haptic interaction with an unknown VE including computational delay which indeed is equivalent to a single-user clinet-server haptic system. Stability and transparency analyses are provided to study the performance of the haptic systems with multirate wave variables control. Multirate state space model [7] and lifting [33] are utilized for this purpose. Second half of the research is devoted to improving the performance of the proposed passive multirate wave control in all frequency ranges. Especially a new filter bank architecture in wave domain is introduced which enables passive velocity filtering of the velocity signal at the master side as well as utilizing a local model in conjunction with passive multirate wave variables control.

1.3 Dissertation Outline

This dissertation is organized as following:

- **Chapter 1** provides the Introduction, which contains the motivation of the work, the statement of the problem, overall objectives and approach. The bulk of the work presented in this thesis is contained in the Appendices. Each Appendix (AE) includes a complete scientific publication. Except for the second paper which is currently under review, all other peer-reviewed papers are published.

- **Chapter 2** includes and overview of the research and previous work done to date on the scientific problem.

- **Chapter 3** The contributions in this dissertation are contained in the five papers provided in Appendices A through E. **Chapter 3** summarizes each one of the articles, explaining the contribution of each publication, and how they are connected in order to meet the objectives of this dissertation.

- **Chapter 4** contains a brief summary of the overall contributions, conclusions, and enumerates avenues of future work for further development.

Chapter 2

State of the Art Review

Users manipulate and sense VEs in haptics similarly to how operators manipulate and sense remote environments in bilateral teleoperation. The haptic interface, the manipulated VO and the VE in haptics play roles analogous to the master robot, the slave robot and the real environment in teleoperation, respectively, as schematically depicted in Figure 2.1. Moreover, networking issues are germane to bilateral teleoperation, which presupposes manipulation and sensing over distance. Therefore, this section presents the state of the art in bilateral teleoperation over the Internet before focusing on haptic cooperation.

2.1 Background: Bilateral teleoperation over the Internet

Passivity-based controllers seek to monitor and control the flow of energy between system components. They have provided good solutions for bilateral teleoperation with constant time delays. Yet, their extensions to addressing the packet-switched network impairments are scarce to date [21]. Passivity-based control of bilateral teleoperation over packet-switched networks is based on wave/scattered communications [6] and on time domain passivity concepts [81]. Passivation of wave/scattering-based communications with time varying, but upper bounded delay was achieved: (i) through wave filters [72]; (ii) through defining a virtual delay and maintaining the delay apparent to the operator almost constant, i.e., within 5% of the virtual delay [55, 77]; (iii) through combining Kalman-based prediction with the monitoring of the energy flow into the communications for small delay variations [69, 70]; and (iv) through a suitable gain in the wave/scattered communications [22, 23, 61]. All approaches lead to designs which assume the worst-case delay throughout the telemanipulation and thus, have suboptimal performance when the actual

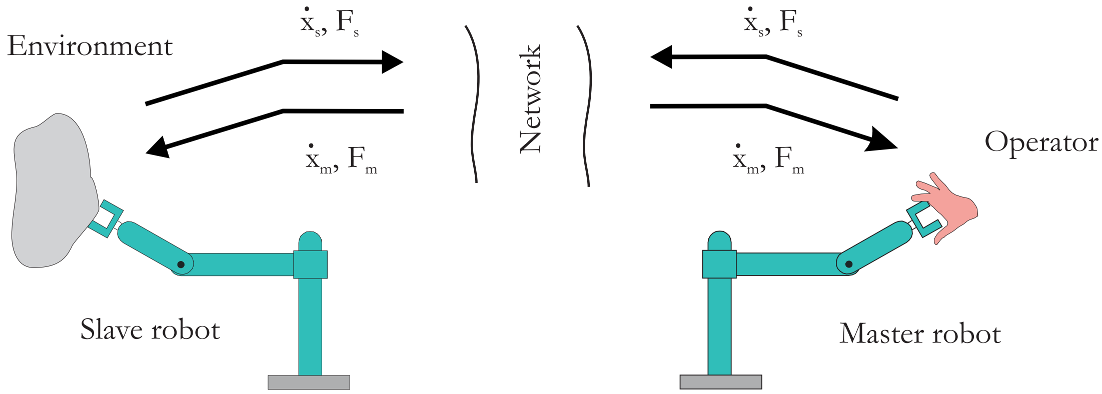

(a) Bilateral teleoperation.

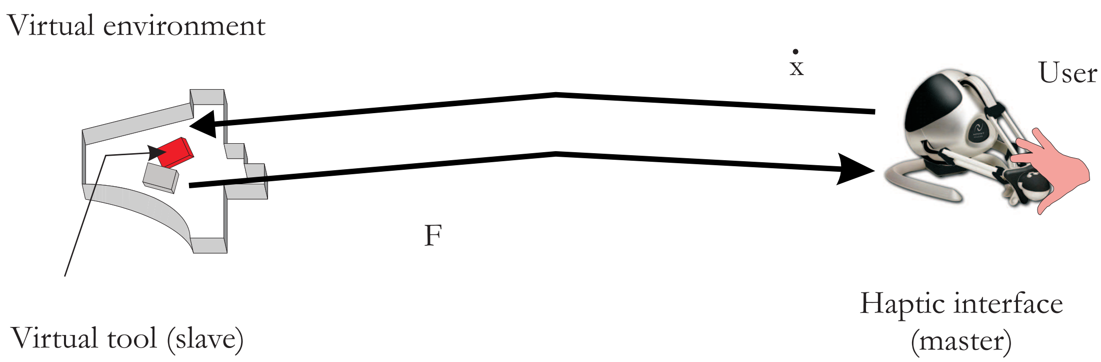

(b) Haptic interaction.

Figure 2.1: Control analogy between a haptic and a teleoperation system.

delay is much smaller than its upper bound. Furthermore, all analyses were performed in continuous time. The gain-based approach was extended through communication management modules in [21] to address both time varying delay and packet losses in continuous and discrete time. The results were restricted to unirate systems and transparency was not discussed. Time domain passivation of communications with variable delay was implemented through adding a passivity observer and a passivity controller to the communications [81]. The observer monitors the energy flow into the communications. The controller adapts the injected damping to dissipate the excess energy when any is observed. Neither the perception nor the limited packet transmission rate were addressed in this approach.

Classical control of bilateral teleoperation with variable delay uses state controllers and proportional-derivative (PD) controllers. State controllers at the local and remote sites were combined with delay compensation in [93]. The compensation strategy adjusts the position command currently received from the human operator based on: (i) the force reflected to the operator at the time when they generated the command; and (ii) the current force between the slave and the remote environment. The state controllers require accurate models of the robots, the environment, and the communication channel. Two conventional PD controllers connects the master and slave robots in [51, 76]. The D-gain was tuned based on the rate of change of the delay in the first controller, and was fixed and selected to ensure stability in the second controller. The P-gain provides position feedback/feedforward and thus, guarantees the master-slave position coordination and static force reflection. Packet loss or the multirate nature of the packet-switched communications were not addressed through the design of the two PD controllers.

Robust control of bilateral teleoperation across the Internet was implemented within the sliding mode and H_∞ frameworks. A sliding mode controller with the nonlinear gains set independently of the changes in the communication delay was presented in [79]. The controller was designed in continuous domain and its transparency was not considered. An H_∞ controller robust to environment and communication delay uncertainties was introduced in [88]. A graphical Nyquist-type procedure permits the computation of the maximum delay uncertainty, for a constant delay, for which the system remains stable in the face of environment uncertainties. A H_∞ and l_1 bilateral teleoperation control design based on a new linear matrix inequality was introduced in [83]. The design presumes unknown and randomly varying communication delay but with a known upper limit, and is applicable to unirate continuous systems.

Besides stability, performance is also a key concern in bilateral teleoperation. Conventional performance requires the teleoperation system to be transparent to the human operator. In other words, the ideal bilateral teleoperator enables the user to feel as if directly interacting with the remote environment. For bilateral teleoperation over the Internet, performance was primarily addressed in the context of scattered/wave-based communications. Therefore, position tracking becomes another important performance indicator. In [106], the wave-based communications were time stamped to ensure position tracking and the energy balance was monitored from the reconstructed input energy at the receiver side to guarantee passivity. The extension in [107] also considers communication blackouts. Packet loss and multiple rates can not be easily incorporated into either approach. In [8], predictors were used to increase the tracking performance of wave-based communications with both constant and varying delay. Prediction requires accurate models of the master and slave robots and of the environment, neither of which are typically readily available. In [75], position tracking was ensured through a PD controller in parallel with scattered communications. User's perception was the concern in [97] and [98]. It was improved by passively tuning the wave impedance on-line in [97], and by feedforwarding the high frequency components of the environment force to the operator in parallel with the wave variables in [98]. The feedforwarding overcome the information lost in the filtering performed by the wave impedance and improves the perception of hard contact.

For teleoperators with conventional communications via velocities and forces, model based, discrete time Linear Quadratic Gaussian (LQG) control was used in [92] to improve the performance of switching from free motion to rigid contact. A similar approach was employed to increase the transparency of cooperative teleoperation during switching in [89]. Neither the multi-rate nature of the cooperative teleoperation over packet-switched networks nor the delay variation were considered in the LQG approaches.

2.2 Cooperative haptics

This section presents the work related to cooperative haptics over computer networks. Haptic cooperation among multiple users was investigated through:

2.2.1 Experimental research

The effect of force feedback on the performance and efficiency of cooperative applications was examined in [90]. The results show that, when provided with haptic and visual feedback, users manipulate VOs faster and more precisely than when provided with visual feedback alone. The impact of time delay on the stability and performance of collaborative networked haptic systems was investigated in [3, 4, 49]. Those studies confirm that communication delays severely decrease the performance of haptic collaboration in terms of stability and transparency.

Two peer-to-peer and one client-server schemes for Internet-based haptic cooperation were studied in [53, 85, 87]. All schemes use virtual coupling[1] [26] coordination between peers and between clients and the server, respectively. In [85], the NIST Net network emulator was used to emulate varying time-delay simulate the communication under the Internet. All three studies concluded that the client-server architecture has better position coherency than the peer-to-peer architecture, but that peer-to-peer architectures can achieve similar position coherency as client-server schemes if suitable tuning of the virtual coupling parameters is possible. Regardless of the architecture, the position discrepancy and the forces rendered to the users increase as the network packet transmission rate decreases.

[1]The virtual coupler is a PD controller whose effect in haptics is to filter the impedances transmitted across the communicationc link.

Similar work with similar results were presented in [84] for constant communication delay. A comparison of virtual coupling, wave variable and time domain passivity control of peer-to-peer haptic cooperation was performed in [86]. It illustrate that tuned virtual coupling achieves the best position coherency, whereas wave variable control renders the most accurate forces to the users.

Practical implementation of multi-user, Internet-based haptics was presented in several works, including Tele-handshake [78], which demonstrate hand shaking supported through client-server communications. A system which allows users to impose forces on each other and on shared VOs was introduced in [20, 40]. A prototype surgical simulation application connected participants in Sweden and Australia over a standard Internet connection in [38, 39]. Collaborative sculpting of virtual clay across the Internet was enabled by the system in [37]. A preliminary networked haptic game implementation allowed online players to feel the handling a basketball in [96]. Collaborative haptic assembly was supported by peer-to-peer and client-server communications in [45], and only by peer-to-peer communications in [34,44,46]. Wave variable-based compensation of constant communication delay and heuristic tuning of the wave impedance was demonstrated in [42] for a multi-DOF haptic system. Most recently, distributed haptic interfaces along with deformable object modeling were used within a collaborative product development and prototyping framework in [60].

2.2.2 Analytical research

The time varying delay problem of haptic cooperation over packet-switched networks was tackled in [9, 10]. The proposed solution employs a Smith-like predictor that, unlike the conventional Smith predictor, does not require the estimation of the time delay. However, precise models of the cooperating haptic interfaces are still needed. Furthermore, the analysis were performed in continuous time.

The multiple rates inherent in haptic cooperation over networks with limited packet transmission bandwidth, like LANs, MANs, and the Internet, were modeled in [32] using the multi-rate state space framework introduced in [7]. Virtual coupling coordination was considered in the analysis. Both analysis and experiments indicate that: (i) stiffer contacts can be rendered to peer users than to remote clients connecting to a centralized VE; and (ii) larger communication delays increase the operator-perceived damping both over peer-to-peer and over client-server architectures. Careful identification of the haptic interfaces is required to compensate for the damping induced by virtually coupling the users among themselves or to the server in the presence of communication delay.

A linear matrix inequalities framework based on passivity and virtual coupling coordination was introduced in [14, 15] for the analysis and design of multi-user/multi-contact haptics systems without communication delay. Sufficient conditions for the passivity of such systems were formulated as linear matrix inequalities. In turn, the matrix inequalities allows the parameterization of a wide class of stabilizing virtual couplers. The framework requires the models of the human operators and haptic devices to guarantee performance. Furthermore, it does not include a transparency analysis.

Compensation, of the negative effect of communication delay on the stability and transparency of networked haptic cooperation, based on state prediction was proposed in [71]. An optimization formulation allows control gains to be selected which maximally enhance performance while maintaining the haptic cooperation stable.

A stability and transparency analysis of networked, cooperative haptic manipulation of a simple spring-mass-damper VE was introduced in [57]. It determines the maximum allowable delay without considering the effects of the zero-order-hold (ZOH), i.e., without considering the sampled-data nature of haptic interaction. Delay compensation based on the identified allowable delay guarantees the performance of the overall system. The impact of the ZOH on the stability results is unclear. The extension of the proposed compensation to cooperative haptic manipulation of more complex VE models is also not straightforward.

Since the developed passive multirate wave communications in this research also applicable to a single-user haptic interaction and on the other hand part of the research is devoted to improving the performance of the passive multirate wave control by using a local model, the next section presents the works related to multirate control of slow VEs as well as the techniques provided up to date for utilizing a local model in haptic systems.

2.3 Multirate haptics

2.3.1 Multirate Control

Multirate control has long been a key strategy for increasing the contact stiffness in slow VEs. However, mostly multirate haptic control with power domain communications has been studied to date. The power domain connection between a fast force feedback loop and a slow VE was shown to generate un-physical energy [67, 68] which grows with the sampling time and the stiffness of the VE [67] and destabilizes the interaction. To increase the contact stiffness provided to users, existing research sought: (i) to decrease the VE sampling time; and (ii) to dissipate the artificial energy via passivity-based multirate control or via hardware.

The VE sampling time was decreased: (i) via efficient collision detection algorithms; and (ii) via local models of interaction. Efficient collision detection algorithms [36, 54, 59] alleviates the collision detection bottleneck typical in rigid VEs with complex geometries and allows the simulation to run at haptic rates. However, the stability of the haptic interaction in VEs employing those algorithms is not guaranteed [36].

The artificial energy due to sampling can be dissipated: (i) via hardware; and (ii) via passivity-based control. Electrical damping [52, 66, 102], magneto-rheological brakes [5] and eddy current brakes [35] were explored to increase the physical damping of the haptic interface and thus, permit stable interaction with stiffer VEs. Hardware approaches can be costly to implement and not trivial to extend to multi degrees of freedom haptic interfaces. Only proof of concept implementations have been presented to date. Passivity-based multirate controllers were devised based on frequency, time and wave domain methods. Frequency domain analysis connects the fast force feedback loop to a slow VE via virtual coupling [67, 68]. The virtual coupler is a conservative design because it dissipates energy throughout the interaction although the slow VE may be active only during certain simulation steps. Time domain analysis aims to dissipate only the spurious energy, via passive sampling-and-hold [16, 80, 82, 95] or via passive-set-position-modulation [56]. Passive sampler-and-holds need to predict the energy balance over a VE step and therefore, assume a sufficiently small VE sampling time [16, 80, 82] or additional physical damping [95]. Passive-set-position-modulation maps the modulated VE position to forces sent to users through a virtual coupler. Hence, for significant VE sampling time, time domain passivity-based multirate controllers still need fixed dissipation in the feedback loop. Wave domain analysis connects the fast force feedback loop to the slow VE via multirate wave communications [19]. The rate drop/increase was modeled as a series of time delays and aliasing was not considered [19].

2.3.2 Local Model

A key approach to enabling a fast force control loop in the presence of computational delay of the virtual environment exploits a fast local model of interaction either in conjunction with the original slow virtual environment [12, 17] or in its place [48, 62, 101]. In essence, the fast local model is a simulation with reduced numerical complexity that computes the force feedback at typical haptic frequencies and thus, increases the stability and transparency of the haptic interaction. Local models of interaction were proposed for haptic manipulation both of rigid [27] and of deformable [11, 12, 48, 58, 62] virtual environments. Since this work does not address the development of a local model of interaction, the reader is referred to [48] for a recent comprehensive overview.

A local model can be used in various architectures in conjunction with diverse control strategies. In [12], a local model comprising a fixed stiffness was used together with virtual coupling [2, 25] control. Lifting [33] was employed to derive the closed loop stability of a multirate simulation with the constant stiffness local model [12], and to show that the simulation loop is stable if the local stiffness is lower than the stiffness of the slow virtual environment. The results in [12] indicate that a fixed stiffness local model cannot be used to increase the gain of the force feedback loop and thus, to increase the range of contact impedances that can be rendered to users interacting in slowly updated virtual environments. In [62], pre-computed passive local models substitutes the slow virtual environment and a switching between the local models was devised to passively activate them. The resulting passive interaction forces guarantee stable interaction, and the physical accuracy of the pre-specified local models ensures fidelity. The passive activation of the local models [62] guarantees the stability of the haptic manipulation of any slowly updated deformable virtual environment but requires passive local models to be pre-defined. In [17, 48], a real-time technique was offered to generate a lower-order approximation of a full order virtual environment model. The lower-order-approximation local model was used in conjunction with the full-order virtual environment in [17], and was used in place of the full-order environment in [48]. Substituting a local model for a slow virtual environment improves the stability of the haptic interaction [62], but the transparency of the interaction hinges on the accuracy of the local model. Oftentimes no guarantee is provided for such accuracy. Using a local model in conjunction with the slow virtual environment may threaten the stability of the haptic system [12].

Chapter 3

Summary of Contributions

The contributions in this dissertation are contained in the five papers provided in Appendices A through E. This chapter summarizes these contributions and explains how they are connected toward the aims of the present work.

3.1 Passive Multirate Wave Communications for Haptic Interaction in Slow Virtual Environments (Appendix A)

Phase lag introduced in the control loop by the slow update rate of VEs or the limited packet transmission rate of computer networks can make a haptic interaction unstable. To overcome this problem, a multirate wave variable control framework is adopted for multirate haptic interaction. In the multirate wave variables framework, wave communications are used to connect the force control loop which runs at the fast 1-KHz haptic frequency to the remote VE or/and the VE which runs at a slow and fixed frequency. In this framework, the change of the sampling rate occurs in the wave communications. To investigate the effect of the rate change, an analysis of the discrete-time energy balance in the wave communications is performed. The rate changes in outgoing and incoming channels are modeled by a domwnsampler and an upsampler respectively. By using Parseval's theorem it is shown that the communication channels remain passive in the absence of aliasing. An illustrative numerical example is provided to prove that aliasing can violate the passivity of the communication channels, i.e. by injecting unphysical energy to the system. It is concluded that avoiding aliasing is the passivity condition for the wave communications in the presence of rate change. Hence, by using a low-pass anti-aliasing filter whose cutoff frequency is less than the update rate of the wave communications, it is possible to guarantee the passivity of the multirate wave variables framework. The obtained passivity condition is validated through a numerical example in which multirate wave variables frame work with anti-aliasing low-pass filter are used, i.e. a multirate haptic system with passive multirate wave communications. In this example, the stability region of the haptic system for different cutoff frequencies and sampling drop rate factors is obtained. The stability region is compared with the passivity region of the wave communications derived in the first part.

Lifting [33] is used to study the performance of the proposed control strategy in frequency domain. By using lifting the multirate haptic system with wave control is converted to a unirate system and its frequency response is compared with the frequency response of an ideal haptic ineraction, i.e. fast direct coupling control. The results show that by increasing wave impedance in low frequency the response of the haptic system with wave control gets closer to the the response of the ideal system whereas in high frequency by increasing wave impedance the response of the system deviates from the response of the ideal system.

Finally, the performance of passive multirate wave communication is checked experimentally. In the experiments, the Z-width of a haptic system with direct coupling control is compared with the Z-wdith of the same haptic system with passive multirate wave communications. The results show that by using passive multirate wave communications, it is possible to render stiffer contacts to the users and passive wave variables control provides a robust solution for multirate haptic systems.

The main contributions of this part of the research are:

- An analysis of the discrete-time energy balance in the multirate wave channels which reveals that they are passive only if the rate drop does not introduce aliasing.
- Analytical and numerical verification of the passivity condition for multirate wave communications connecting a fast haptic feedback loop to VEs with various stiffnesses and update rates.
- A frequency domain analysis of the transparency of multirate wave variable control of haptic interaction in slow VEs.
- Experimental validation of the ability of passive multirate wave communications to render stiffer slow VEs than direct coupling. The experiments also illustrate that the

haptic interaction in a slow VE with multirate wave communications can become unstable when the decrease of the wave sampling rate introduces aliasing.

For further information, the reader is directed to Appendix A. In the next part of this research, the developed passive multirate wave communications is applied to a client-server cooperative haptic system with two users.

3.2 Centralized Multirate Wave Variables Control of Haptic Cooperation in Rigid Virtual Environments (Appendix B)

This part of the work is concerned with increasing the realism of haptic cooperation among client users connected to a centralized VE over a LAN or a high-speed MAN. To enable the clients to cooperatively manipulate stiffer centralized virtual objects across networks with packet update rates lower than the rate of force control loops and in the presence of time delay, the users are connected to the central server through passive multirate wave communications, introduced in the first part of this research. The multirate state space model [7] is used to derive the stability region for a cooperative haptic system with two remote users. The stability regions are obtained for i) different time delays, and ii) different cutoff frequencies of the low-pass anti-aliasing filter which is used to maintain the passivity of the wave communications. Also, in order to compare the performance of passive multirate wave variables with the traditional cooperative control strategy, i.e. direct coupling, stability regions for different time delays are obtained for a cooperative haptic system with traditional control. The analysis predicts two important advantages of passive multirate wave variables control over traditional multirate control of centralized haptic cooperation: (i) it enables users to manipulate much stiffer virtual objects together and hence, it increases the realism of haptic cooperation in centralized virtual environments; and (ii) it renders a maximum stiffness of the virtual environment that is unaffected by the network delay. Hence, the stability analysis suggests that passive multirate wave variables communications have benefits for multirate haptic cooperation similar to their benefits for haptic manipulation of slowly updated virtual environments. On the other hand, the results show that by using inappropriate low-pass filter, i.e. a low pass filter with cutoff frequency greater than the update rate of the communication channels, the stability region shrinks. The analytical results are validated experimentally. In the experiments two remote users are asked to move a common virtual cube along a prespecified trajectory. The virtual cube is simulated on a central server and the users are connected to the central server though a LAN. The experiments are repeated for different time delays in the communication channels.

On the other hand, the initial force feedback in the experiments was to noisy. To get smoother force feedback, a First-Order-Hold (FOH) expander in the wave communications is used in place of a Zero-Order-Hold (ZOH) expander. The results show that FOH significantly mitigated the force feedback noise. By carrying out time domain passivity analysis, it is shown that utilizing a FOH expander in the wave communications does not violate the passivity of the system.

The main contributions of this part of the research are:

- A stability analysis of centralized haptic cooperation with passive multirate wave variables communications that considers the constant delay and the bandwidth limitation of the LAN/MAN networks.
- A comparative analysis of the stability of passive multirate wave variables control to the stability of traditional control of centralized haptic cooperation.
- Experimental validation of the analytical results which proof that stiffer contact compared to traditional control strategy is achievable.
- Using a FOH expander in place of a ZOH expander to alleviate the force feedback noise.

For further information, the reader is directed to Appendix B. The second half of the research is devoted to dealing with problems ensue from utilizing passive multirate wave variables control. The problems to be addressed are: i) computational delay due to connecting a wave variable controller to an unknown VE, ii) noisy force feedback due to noisy velocity signal, and iii) poor performance at some frequency ranges. In the next part of this research the problem of connecting passive wave variable control to an unknown VE is investigated.

3.3 Passive Wave Variable Control of Haptic Interaction with an Unknown Virtual Environment (Appendix C)

This part of the work proposes a technique for passively connecting a wave variable controller to an unknown VE. A VE is considered unknown when its properties such as damping and/or stiffness are unknown or its mathematical model is not available. Since the velocity command decoded on the slave side is a function of both the incoming wave variable and the force output of the VE and on the other hand also the force output of the VE depends on the decoded velocity command, an algebraic loop shows up when wave communication is used to connect a haptic interface to a VE. To study the effect of the algebraic loop on the stability of a haptic system, the Jury-Marden stability criterion is used to analyze the stability of a haptic interaction with a virtual wall for two cases: i) the algebraic loop can be unwrapped, either through iteration or through exploiting the model of the virtual environment; and (ii) the algebraic loop is eliminated through one step computational delay when the VE is unknown and/or a slow simulation update rate precludes the use of iteration. To simplify the analysis and reduce the number of parameters the wall parameters are converted to non-dimensional parameters. The results show that the computational delay significantly decreases the stability region of a haptic interaction system. On the other hand by performing a time domain passivity analysis, the amount of unphysical energy injected to the feedback loop by the computational delay is derived. By using the result of passivity analysis an algorithm is proposed to compensate the destabilizing effect of the computational delay and to guarantee passive connection of the wave variable communication to an unknown VE. Lastly, the analytical results are validated via controlled experiments.

The main contributions of this part of the research are:

- Non-dimensional Jury-Marden stability analysis of the haptic interaction with a virtual wall with computational delay and without computational delay
- Time domain passivity analysis of the slave side of wave communications including computational delay
- Developing an algorithm to compensate the nonphysical energy injected by computational delay
- experimental validation of the performance of the proposed algorithm

For further information, the reader is directed to Appendix C.

3.4 Passive Velocity Filtering for Haptic Applications with Wave Control (Appendix D)

This part of the research is concerned with designing a passive velocity filtering for haptic applications with passive multirate wave variables control. When passive wave variables control is used, the velocity of the haptic interface is directly fedback to the human operator with a large gain, i.e. wave impedance. To study the effect of the wave impedance on the performance of a haptic system with wave control, lifting [33] is used to convert the multirate system to a unirate system. Then, the frequency response of the unirate system is obtained. The results show that in low frequencies, increasing the wave impedance improves the performance of the haptic interaction but in high frequencies by increasing wave impedance the frequency response of the haptic system deviates from the frequency response of the ideal haptic interaction. On the other hand, since the velocity signal provided by most haptic devices is noisy, the direct feedback of the velocity signal results in a noisy force feedback to the user. By low-pass filtering the velocity signal, it is possible to tackle the problems induced by direct velocity feedback but low-pass filtering imposes phase lag to the control loop and can make the system unstable. To overcome these problems, this part of the research proposes a new filter bank architecture for passive velocity filtering. In this architecture, the outgoing wave variable in the master side is split into two signals by using low-pass and high-pass filters. The output of the low-pass filter is fed to the slowly updated/remote VE and the output of the high-pass filter is used to passively filter the velocity signal. Actually, by some manipulations it is shown that having a high-pass filter in the wave domain is equivalent to having a low-pass filter in the direct velocity feedback loop. By passivity analysis of the proposed filter bank architecture, the passivity condition of the proposed architecture is derived. Since available filters are not ideal, the design of the filters are formulated as a minimax problem based on the passivity condition. By using lifting, the performance of the proposed architecture is studied in frequency domain and it is shown that the proposed architecture improves the performance of the system in high frequencies. The analytical results are confirmed experimentally, especially the effectiveness of the proposed design method and appropriate performance of the filtering scheme in terms of noise removal.

The main contributions of this part of the research are:

- Introducing a new filter bank architecture for velocity filtering
- Time domain passivity analysis of the proposed architecture

- Formulating the filter design problem as a minimax problem
- Frequency response analysis of the proposed architecture
- experimental validation of the analytical results

For further information, the reader is directed to Appendix D.

3.5 Wave Filter Bank for High Fidelity Passive Multirate Haptic Interaction with Slowly Updated Virtual Environments (Appendix E)

This part of the work proposes a new filter bank structure for utilizing a local model of interaction in the application with passive multirate wave communications. The proposed structure comprises a low-pass and a band-pass filter. The outgoing wave signal in the master side is split into two signals by using these filters. The output of the low-pass filter is sent to the remote or slowly updated VE and the output of the band-pass filter is fed to the local model of interaction. In order to obtain the frequency response of the system, lifting [33] is used to convert the multirate haptic system to a unirate system. The results show that the filter bank structure with local model improves the transparency of the system in high frequencies, but have little effect on the performance of the system in low frequencies. Increased transparency in low frequencies is achieved via adding an additional term to the returning wave at the master side v_m [31]:

$$v_m = v_m - K_p(x_m - x_s), \tag{3.1}$$

where K_p is a constant gain, and x_m and x_s are the position of the haptic device and the position of its avatar in the virtual environment, respectively. On the other hand this extra term might have destabilizing effect on the system. By using lifting and converting the multirate system including the extra term to a unirate system, the stability region for various local model parameters, VE parameters, and K_p is derived. The result shows that the local model parameters and K_p has little impact on the stability of the overall system and even by adding a local model of interaction higher stiffness is achievable in the VE. The performance of the proposed structure is investigated in frequency domain. The results show that the filter bank structure with position feedback significantly improves the performance of a haptic system in both low and high frequencies and in some frequencies the response of the haptic system with filter bank structure matches with the response of the ideal system. Finally, the analytical results are confirmed by experimental results.

The main contributions of this part of the research are:

- Introducing a new filter bank architecture for utilizing a local model of interaction in wave domain
- Stability analysis of the proposed structure
- Frequency response analysis of the proposed filter bank architecture
- Experimental validation of the analytical results

For further information, the reader is directed to Appendix E.

Chapter 4

Conclusion and Future works

This dissertation is devoted to developing a robust control framework for multirate networked haptic applications. Limited packet transmission rate, slow Virtual environment (VE), packet loss, transmission delay, and computational delays make a networked haptic system a multirate system with time delay. To tackle these problems, this work adopts multirate wave variables framework. In this framework, instead of power variables, i.e. force and velocity, wave variables are exchanged between the fast force loop control and the remote/ slow VE and the rate change occurs in the communication channels. This work starts with an investigation of passivity condition in the wave variables communications channels. Time domain passivity analysis shows that the communication channels are passive if aliasing due to rate change does not happen. To avoid aliasing and guarantee the passivity of the communication channels, an anti-aliasing lowpass filter whose cutoff frequency is less than the update rate of the communication channels is used before the rate change. The performance of the proposed passive multirate wave variables control (PMWVC) is examined numerically and experimentally. The results proof that by using PMWVC, it is possible to render much stiffer contact to the users compared to direct coupling control and by appropriate filtering the system is robust against rate change in the communication channels.

In the next part of this work, the proposed PMWVC is applied to a cooperative haptic system. In this haptic system, two remote users cooperatively manipulated a common virtual cube simulated on a central server. The clients are connected to the server through a LAN network. By using multirate state space model, the stability regions of the system are obtained for different time delays and different cutoff frequencies of the anti-aliasing lowpass filter. The results show that compared to the traditional control strategy, higher stiffness can be rendered to the users and the maximum stiffness is unaffected by the time delay. On the other hand, the results confirm the passivity condition obtained in the first part of the research because by choosing a cutoff frequency greater than the network rate, i.e. packet transmission rate, the stability region shrinks significantly. Experiments are provided to support the analyses.

From the results of the first and second part of this research it can be concluded that PMWVC provides a robust solution for cooperative haptic applications with rate change and constant time delay. The second half of the research is devoted to addressing the problems ensue from using PMWVC in a haptic system.

First, the problem of connecting wave communications to an unknown VE is addressed. Indeed, connecting passive multirate wave communication to an unknown VE results in an algebraic loop. The algebraic loop is eliminated by imposing one step computational delay to the salve side of the wave transformation. The stability analysis of a haptic system with an unknown VE shows that the computational delay significantly shrinks the stability region. On the other hand, time domain passivity is performed to study the effect of the computational delay on the passivity of the connection. The result shows that the computational delay injects unphysical energy to the system. Based on the passivity analysis an algorithm for passive connection of the wave communication to an unknown VE is proposed. The performance of the proposed algorithm is examined experimentally. The experimental results indicate that the proposed algorithm removes the injected energy and makes the system stable.

In the next part of the research, a filter bank structure for passive velocity filtering is proposed. In this structure the outgoing wave variables is split into two frequency ranges using lowpass and highpass filters. The output of the lowpass filter is sent to the slow/remote VE and the output of the highpass filter is used to filter the velocity. The design of the filter bank structure is formulated as a minimax problem. Lifting is used to study the transparency of the proposed structure and the performance of the velocity filter is examined experimentally.

In the last part of the research, another filter bank structure is proposed for utilizing a local model of interaction with PMWVC to improve the performance of a haptic system with PMWVC in all frequencies. The proposed filter bank structure comprises of a lowpass and a bandpass filter. The output of the lowpass filter is fed to the slow/remote VE and the output of the bandpass filter is fed to a fast local model. For improving the performance of the system in low frequencies an additional term, the difference between the position of the haptic interface and the position of its avatar in the VE, is added to the incoming wave variable. Again, lifting is used to investigate the performance of the proposed structure in frequency domain. The results show that the proposed structure significantly improves the transparency of the system. On the other hand the stability region of the system is derived for different parameters of the VE, local model, and the gain of the additional term. The results proof that utilizing a local model in this structure has little impact on the stability of the overall system.

The experimental and analytical results suggest that the proposed amendment to PMWVC in the second half of the research makes it applicable to wider range of haptic applications, provides smoother force feedback to the user, and significantly improves the transparency of the haptic system in all frequency ranges.

The passive multirate wave communications share the limitations of wave variables controllers [73, 99]. They: (i) may suffer from position drift; (ii) may degrade perception via wave reflections; and (iii) cannot provide ideal kinesthetic coupling [108] because of their intervening impedance, which acts as a spring inversely proportional to the VE sampling time [73] and eliminates high frequencies from the forces rendered to users. Position drift can be diminished via transmitting wave integrals together with the wave signals [73], via modulation of the outgoing wave [73], or via adding user-perceived and environment forces [105] to the outgoing wave. Wave reflections are opportunely eliminated by the proposed anti-aliasing filter. As it is shown in Appendex A and Appendix E, the transparency of the haptic system with PMWVC hinges on the wave impedance. Although PMWVC gaurantees the passivity of the system, wave impedance must be tuned for the best performance of the haptic system and this is the main weakness of the proposed frame work.

Extending the results to time varying multirate systems and formulating the design of the proposed filter bank structure in the last part of the research as an optimal control problem can be considered as the future works. Currently the filters of the proposed filter bank structure are selected heuristically. Also all analyses and experiments in this research are restricted to one degree of freedom (DOF) or 3 DOF point interactions. Extending the results to include more degrees of freedom with virtual body twists and wrenches is considered among the future works.

Bibliography

[1] http://www.internetworldstats.com.

[2] R. J. Adams and B. Hannaford. Stable haptic interaction with virtual environments. *IEEE Transactions on Robototics and Automation*, 5(3):465–474, 1999.

[3] M. O. Alhalabi, S. Horiguchi, and S. Kunifuji. An experimental study on the effects of network delay in cooperative shared haptic virtual environment. *Computers and Graphics*, 27(2):205 – 213, 2003.

[4] R. S. Allison, J. E. Zacher, D. Wang, and J. Shu. Effects of network delay on a collaborative motor task with telehaptic and televisual feedback. In *International Conference on Virtual Reality Continuum and Its Applications in Industry*, pages 375–381, Singapore, 2004.

[5] J. An and D.-S. Kwon. Stability and performance of haptic interfaces with active/passive actuators - theory and experiments. *Intnernational Journal of Robotic Research*, 25(11):1121–1136, 2006.

[6] R. J. Anderson and M. W. Spong. Bilateral control of teleoperators with time delay. *IEEE Transactions on Automatic Control*, 34(5):494–501, 1989.

[7] M. Araki and K. Yamamoto. Multivariable multirate sampled-data systems: State-space description, transfer characteristics, and Nyquist criterion. *IEEE Transactions on Automatic Control*, 31(2):145–154, 1986.

[8] H. Arioui, A. Kheddar, and S. Mammar. A predictive wave-based approach for time delayed virtual environment haptics systems. In *11th IEEE International Workshop on Robot and Human Interactive Communication*, Berlin, Germany, 2002.

[9] H. Arioui, A. Kheddar, and S. Mammar. Stable shared virtual environment haptic interaction under time-varying delay. In *8th IEEE Methods and Models in Automation and Robotics*, Szczecin, Poland, 2002.

[10] H. Arioui, S. Mammar, and T. Hamel. A Smith-prediction based haptic feedback controller for time delayed virtual environments systems. In *American Control Conference*, pages 4303–4308, Anchorage, Alaska, 2002.

[11] R. Balaniuk. A differential method for the haptic rendering of deformable objects. In *ACM Symposium on Virtual Reality Software and Technology*, pages 297–304, Limassol, Cyprus, 2006.

[12] F. Barbagli, D. Prattichizzo, and K. Salisbury. A multirate approach to haptic interaction with deformable objects single and multipoint contacts. *International Journal of Robotic Research*, 24(9):703–715, 2005.

[13] P. Berestesky, N. Chopra, and M. W. Spong. Discrete time passivity in bilateral teleoperation over the Internet. In *IEEE International Conference of Robotics and Automation*, pages 4557– 4564, New Orleans, LA, 2004.

[14] G. Bianchini, M. Orlandesi, and D. Prattichizzo. An LMI framework for analysis and design of multi-dimensional haptic systems. In *47th IEEE Conference on Decision and Control*, pages 4564–4569, 2008.

[15] G. Bianchini, M. Orlandesi, and D. Prattichizzo. Stability analysis and design of multi-dimensional haptic systems. In *Symposium on Haptic Interfaces for Virtual Environment and Teleoperator Systems*, pages 177–184, Reno, NV, 2008.

[16] G. Borghesan, A. Macchelli, and C. Melchiorri. Interconnection and simulation issues in haptics. *IEEE Transactions on Haptics*, 3(4):266–279, 2010.

[17] M. C. Cavusoglu. Multirate simulation for high fidelity haptic interaction with deformable objects in virtual environments. In *IEEE International Conference on Robotics and Automation*, pages 2458–2465, 2000.

[18] J. Cheong, S. I. Niculescu, A. Annaswamy, and M. A. Srinivasan. Motion synchronization in virtual environments with shared haptics and large time delays. In *World Haptics Conference*, pages 277–282, Pisa, Italy, 2005.

[19] Ch. Cho, J. B. Song, and M. Kim. Stable haptic display of slowly updated virtual environment with multirate wave transform. *IEEE/ASME Transactions on Mechatronics*, 13(5):566–575, 2008.

[20] H. R. Choi, B. H. Choi, and S. M. Ryew. Haptic display in the virtual collaborative workspace shared by multiple users. In *6th IEEE International Workshop on Robot and Human Communication*, pages 478–483, Sendai, Japan, 1997.

[21] N. Chopra, P. Berestesky, and M. W. Spong. Bilateral teleoperation over unreliable communication networks. *IEEE Transactions on Control Systems Technology*, 16(2):304–313, 2008.

[22] N. Chopra and M. W. Spong. Delay-independent stability for interconnected nonlinear systems with finite L_2 gain. In *46th IEEE Conference on Decision and Control*, pages 3847–3852, New Orleans, LA, 2007.

[23] N. Chopra, M. W. Spong, and M. Buss. Bilateral teleoperation over Internet: the time varying delay problem. In *American Control Conference*, pages 168–173, Denver, CO, 2003.

[24] J. E. Colgate and J. M. Brown. Factors affecting the Z-Width of a haptic display. In *IEEE Conference on Robotics and Automation*, pages 3205–3210, San Diego, CA, 1994.

[25] J. E. Colgate and G. G. Schenkel. Passivity of a class of sampled-data systems: Application to haptic interfaces. *Journal of Robotic Systems*, 14(1):37–47, 1997.

[26] J. E. Colgate, M. C. Stanley, and J. M. Brown. Issues in the haptic display of tool use. In *IEEE/RSJ International Conference on Intelligent Robots and Systems*, pages 140–145, Los Alamitos, CA, 1995.

[27] D. Constantinescu, S.E. Salcudean, and E.A. Croft. Local model of interaction for haptic manipulation of rigid virtual worlds. *International Journal of Robotic Research*, 24(10):789–804, 2005.

[28] D. Delaney, T. Ward, and S. McLoone. On consistency and network latency in distributed interactive applications: A survey part I. *Presence: Teleoperators and Virtual Environments*, 15(2):218–234, 2006.

[29] D. Delaney, T. Ward, and S. McLoone. On consistency and network latency in distributed interactive applications: A survey part II. *Presence: Teleoperators and Virtual Environments*, 15(4):465–482, 2006.

[30] P. Dev, D. Harris, D. Gutierrez, A. Shah, and S. Senger. End-to-end performance measurement of Internet based medical applications. In *Annual Symposium of the American Medical Informatics Association*, pages 205–209, San Antonio, Tex, 2002.

[31] N. Diolaiti, G. Niemeyer, and N. A. Tanner. Wave haptics: Building stiff controllers from the natural motor dynamics. *International Journal of Robotics Reseasrch*, 26(1):5–21, 2007.

[32] M. Fotoohi, S. Sirouspour, and D. Capson. Stability and performance analysis of centralized and distributed multi-rate control architectures for multi-user haptic interaction. *International Journal of Robotics Research*, 26(9):977–994, 2007.

[33] B.A. Francis and T.T. Georgiou. Stability theory for linear time-invariant plants with periodic digital controllers. *IEEE Transactions on Automatic Control*, 33(9):820–832, 1988.

[34] M. Glencross, C. Jay, J. Feasel, L. Kohli, M. Whitton, and R. Hubbold. Effective cooperative haptic interaction over the Internet. In *IEEE Virtual Reality Conference*, pages 115–122, Charlotte, NC, 2007.

[35] A. Gosline and V. Hayward. Eddy current brakes for haptic interfaces: design, identification, and control. *IEEE/ASME Transactions on Mechatronics*, 13(6):669 –677, 2008.

[36] A. Gregory, M.C. Lin, S. Gottschalk, and R. Taylor. Fast and accurate collision detection for haptic interaction using a three degree-of-freedom force-feedback device. *Computational Geometry: Theory and Applications*, 15(1-3):69–89, 2000.

[37] C. Gunn. Collaborative virtual sculpting with haptic feedback. *Virtual Reality*, 10(2):73–83, 2006.

[38] C. Gunn, M. Hutchins, and M. Adcock. Combating latency in haptic collaborative virtual environments. *Presence: Teleoperators and Virtual Environments*, 14(3):313–328, 2005.

[39] C. Gunn, M. Hutchins, D. Stevenson, M. Adcock, and P. Youngblood. Using collaborative haptics in remote surgical training. In *World Haptics Conference*, pages 481–482, Los Alamitos, CA, USA, 2005.

[40] J. P. Hespanha, M. Mclaughlin, G. S. Sukhatme, M. Akbarian, R. Garg, and W. Zhu. Haptic collaboration over the Internet. In *Fifth Phantom Users Group Workshop*, pages 9–13, New York City, NY, 2000.

[41] K. Hikichi, I. Arimoto, H. Morino, K. Sezaki, and Y. Yasuda. Evaluation of adaptation control for haptics collaboration over the Internet. In *5th Phantom Users' Group Workshop*, Okinawa, Japan, 2000.

[42] S. Hirche and M. Buss. Packet loss effects in passive telepresence systems. In *43rd IEEE Conference on Decision and Control*, pages 4010–4015, Paradise Islands, The Bahamas, 2004.

[43] T. Hudson, M. C. Weigle, K. Jeffay, and R. M. Taylor. Experiments in best-effort multimedia networking for a distributed virtual environment. In *Multimedia Computing and Networking*, pages 88–98, San Jose, CA, 2001.

[44] R. Iglesias, S. Casado, and T. Gutierrez. Simultaneous remote haptic collaboration for assembling tasks. *Multimedia Systems*, 13:263–274, 2008.

[45] R. Iglesias, S. Casado, T. Gutierrez, A. Garcia-Alonso, K. M. Yap, W. Yu, and A. Marshall. A Peer-to-peer architecture for collaborative haptic assembly. In *10th IEEE International Symposium on Distributed Simulation and Real-Time Applications*, pages 25–34, 2006.

[46] R. Iglesias, E. Prada, A. Uribe, A. Garcia-Alonso, S. Casado, and T. Gutierrez. Assembly simulation on collaborative haptic virtual environments. In *15th International Conference in Central Europe on Computer Graphics, Visualization and Computer Vision*, pages 241–247, Plzen, Czech Rep., 2007.

[47] M. Ishihara and N. Negishi. Effect of feedback force delays on the operation of haptic displays. *IEEE Transactions on Electrical and Electronic Engineering*, 3(1):151–153, 2008.

[48] Paul Jacobs, Michael J. Fu, and M. Cenk Cavusoglu. High fidelity haptic rendering of frictional contact with deformable objects in virtual environments using multi-rate simulation. *International Journal of Robotics Research*, 29(14):1778–1792, 2010.

[49] C. Jay, M. Glencross, and R. Hubbold. Modeling the effects of delayed haptic and visual feedback in a collaborative virtual environment. *ACM Transactions on Computer-Human Interaction*, 14(2):8–41, 2007.

[50] K. Jeffay, T. Hudson, and M. Parris. Beyond audio and video: Multimedia networking support for distributed, immersive virtual environments. In *27th Euromicro Conference*, pages 300–307, Warsaw, Poland, 2001.

[51] H. Kawada and T. Namerikawa. Bilateral control of nonlinear teleoperation with time varying communication delays. In *American Control Conference*, pages 189–194, Seattle, WA, 2008.

[52] M. Kawai and T. Yoshikawa. Haptic display with an interface device capable of continuous-time impedance display within a sampling period. *IEEE/ASME Transactions on Mechatronics*, 9(1):58 –64, 2004.

[53] J. Kim, H. Kim, B. K. Tay, M. Muniyandi, M. A. Srinivasan, J. Jordan, J. Mortensen, M. Oliveira, and M. Slater. Transatlantic touch: A study of haptic collaboration over long distance. *Presence: Teleoperators and Virtual Environments*, 13(3):328–337, 2004.

[54] Y.J. Kim, M.A. Otaduy, M.C. Lin, and D. Manocha. Six-degree-of-freedom haptic rendering using incremental and localized computations. *Presence: Teleoperators and Virtual Environments*, 12(3):277–295, 2003.

[55] K. Kosuge, H. Murayama, and K. Takeo. Bilateral feedback control of telemanipulators via computer network . In *International Conference on Intelligent Robots and Systems*, volume 3, pages 1380–1385, 1996.

[56] D. Lee and K. Huang. Passive-set-position-modulation framework for interactive robotic systems. *IEEE Transactions on Robotics*, 26(2):354–369, 2010.

[57] I. Lee and S. Choi. Discrimination of visual and haptic rendering delays in networked environments. *International Journal of Control, Automation and Systems*, 7(1):25–31, 2009.

[58] K. Lee and D.Y. Lee. MIMO output estimation with reduced multirate sampling for real-time haptic rendering. *IEEE Transactions on Robotics*, 23(3):481–493, 2007.

[59] M.C. Lin and M.A. Otaduy. Sensation-preserving haptic rendering. *IEEE Computer Graphics and Applications*, 25(4):8–11, 2005.

[60] S. Lin, R. J. Narayan, and Y. S. Lee. Hybrid client-server architecture and control techniques for collaborative product development using haptic interfaces. *Computers in Industry*, In Press, Corrected Proof: Available online at http://www.elsevier.com, 2009.

[61] R. Lozano, N. Chopra, and M. W. Spong. Passivation of force reflecting bilateral teleoperators with time varying delay. In *8th Mechatronics Forum*, pages 24–26, Twente, Netherlands, 2002.

[62] M. Mahvash and V. Hayward. High-fidelity passive force-reflecting virtual environments. *IEEE Transactions on Robotics*, 21(1):38–46, 2005.

[63] J. Marsh, M. Glencross, S. Pettifer, and R. Hubbold. A network architecture supporting consistent rich behavior in collaborative interactive applications. *IEEE Transactions on Visualization and Computer Graphics*, 12(3):405–416, 2006.

[64] A. Marshall, M. K. Yap, and W. Yu. Providing QoS for networked peers in distributed haptic virtual environments. *Advances in Multimedia*, 2008, 2008.

[65] S. Matsumoto, I. Fukuda, H. Morino, K. Hikichi, K. Sezaki, and Y. Yasuda. Influences of network issues on haptic collaboration in shared virtual environments. In *5th Phantom Users' Group Workshop*, pages 22–24, Aspen, Colo, 2000.

[66] J.S. Mehling, J.E. Colgate, and M.A. Peshkin. Increasing the impedance range of a haptic display by adding electrical damping. In *IEEE 1st Joint World Haptic Conference*, pages 257–262, 2005.

[67] B.E. Miller, J.E. Colgate, and R.A. Freeman. Environment delay in haptic systems. In *IEEE International Conference on Robotics and Automation*, pages 2434–2439, 2000.

[68] B.E. Miller, J.E. Colgate, and R.A. Freeman. Guaranteed stability of haptic systems with nonlinear virtual environments. *IEEE Transactions on Robotics and Automation*, 16(6):712–719, 2000.

[69] S. Munir and W. J. Book. Internet-based teleoperation using wave varibales with prediction. *IEEE/ASME Transaction on Mechatronics*, 7(2):124–133, 2002.

[70] S. Munir and W. J. Book. Control techniques and programming issues for time delayed Internet based teleoperation. *Journal of Dynamic Systems, Measurement, and Control*, 125(2):205–214, 2003.

[71] S. Niakosari and S. Sirouspour. Improving transparency in network-based haptics. In *World Haptics 2009 - Third Joint EuroHaptics conference and Symposium on Haptic Interfaces for Virtual Environment and Teleoperator Systems*, pages 547–552, Washington, DC, 2009.

[72] G. Niemeyer and J.-J. E. Slotine. Towards force-reflecting teleoperation over the Internet. In *Proceedings IEEE International Conference on Robotics and Automation*, volume 3, pages 1909–1915, 1998.

[73] G. Niemeyer and J.-J.E. Slotine. Telemanipulation with time delays. *International Journal of Robotic Research*, 23(9):873–890, 2004.

[74] H. Nishino, S. Yamabiraki, Y. M. Kwon, Y. M. Okada, and K. Utsumiya. A distributed virtual reality framework for Korea-Japan high-speed network testbed. In *20th International Conference on Advanced Information Networking and Applications*, pages 433–438, Vienna, Austria, 2006.

[75] E. Nuno, L. Basanez, R. Ortega, and M. W. Spong. Position tracking for non-linear teleoperators with variable time delay. *International Journal of Robotics Research*, 28(7):895–910, 2009.

[76] E. Nuno, R. Ortega, N. Barabanov, and L. Basanez. A globally stable PD controller for bilateral teleoperators. *IEEE Transactions on Robotics*, 24(3):753–758, 2008.

[77] R. Oboe. Web-interfaced, force-reflecting teleoperation systems. *IEEE Transactions on Industrial Electronics*, 48(6):1257–1265, 2001.

[78] M. Osama and A. S. Horiguchi. Tele-Handshake: A cooperative shared haptic virtual environment. In *EuroHaptics*, pages 60–64, Birmingham, UK, 2001.

[79] J. H. Park and H. C. Cho. Sliding-mode controller for bilateral teleoperation with varying time delay. In *International Conference on Advanced Intelligent Mechatronics*, pages 311–316, 1999.

[80] J.-H. Ryu, Y.S. Kim, and B. Hannaford. Sampled-data and continuous-time passivity and stability of virtual environments. *IEEE Transactions on Robotics*, 20(4):772–776, 2004.

[81] J. H. Ryu, D. S. Kwon, and B. Hannaford. Stable teleoperation with time-domain passivity control. *IEEE Transactions on Robotics and Automation*, 20:1863–1869, 2004.

[82] J.-H. Ryu, C. Preutsche, B. Hannaford, and G. Hirzinger. Time domain passivity control with reference energy following. *IEEE Transactions on Control Systems Technology*, 13(5):737–742, 2005.

[83] M. S. Sadeghi, H. R. Momeni, and R. Amirifar. H_∞ and L_1 control of a teleoperation system via LMIs. *Applied Mathematics and Computation*, 206(2):669 – 677, 2008.

[84] G. Sankaranarayanan and B. Hannaford. Virtual coupling schemes for position coherency in networked haptic environments. In *1st IEEE/RAS-EMBS International Conference on Biomedical Robotics and Biomechatronics*, pages 853–858, Pisa, Italy, 2006.

[85] G. Sankaranarayanan and B. Hannaford. Comparison of performance of virtual coupling schemes for haptic collaboration using real and emulated Internet connections. In *1st International Conference on Robot Communication and Coordination*, pages 1–8, Athens, Greece, 2007.

[86] G. Sankaranarayanan and B. Hannaford. Experimental comparison of Internet haptic collaboration with time-delay compensation techniques. In *IEEE International Conference on Robotics and Automation*, pages 206–211, Pasadena, CA, 2008.

[87] G. Sankaranarayanan and B. Hannaford. Experimental Internet haptic collaboration using virtual coupling schemes. *Symposium on Haptic Interfaces for Virtual Environment and Teleoperator Systems*, pages 259–266, 2008.

[88] O. Sename and A. Fattouh. Robust H_∞ control of a bilateral teleoperation system under communication time-delay. In *IFAC World Congress*, pages 311–316, Prague, Czech, 2005.

[89] A. Shahdi and S. Sirouspour. Model-based decentralized control of time delay teleoperation systems. *International Journal of Robotics Research*, 28(3):376–394, 2009.

[90] X. Shen, J. Zhou, A. E. Saddik, and N. D. Georganas. Architecture and evaluation of tele-haptic environments. In *8th IEEE International Symposium on Distributed Simulation and Real Time Applications*, pages 53–60, Budapest, Hungary, 2004.

[91] K. B. Shimoga. A survey of perceptual feedback issues in dexterous telemanipulation. II. Finger touch feedback. In *IEEE Virtual Reality Annual International Symposium*, pages 271–279, Seattle, WA, 1993.

[92] S. Sirouspour and A. Shahdi. Discrete-time Linear Quadratic Gaussian control for teleoperation under communication time delay. *The International Journal of Robotics Research*, 25(2):187–202, 2006.

[93] E. Slawinski, J. F. Postigo, and V. Mut. Bilateral teleoperation through the Internet. *Robotics and Autonomous Systems*, 55(3):205 – 215, 2007.

[94] R. Souayed, D. Gaiti, W. Yu, G. Dodds, and A. Marshall. Experimental study of haptic interaction in distributed virtual environments. In *Eurohapics*, pages 260–266, Munich, Germany, 2004.

[95] S. Stramigioli, C. Secchi, A.J. van der Schaft, and C. Fantuzzi. Sampled data systems passivity and discrete port-Hamiltonian systems. *IEEE Transactions on Robotics*, 21(4):574–587, 2005.

[96] M. Y. Sung, Y. Yoo, K. Jun, N. J. Kim, and J. Chae. Experiments for a collaborative haptic virtual reality. In *16th International Conference on Artificial Reality and Telexistence*, pages 174–179, 2006.

[97] N. A. Tanner and G. Niemeyer. Online tuning of wave impedance in telerobotics. In *IEEE Conference on Robotics, Automation and Mechatronics*, pages 7–12, Singapore, 2004.

[98] N. A. Tanner and G. Niemeyer. Improving perception in time-delayed telerobotics. *International Journal of Robotics Research*, 24(8):631–644, 2005.

[99] N. A. Tanner and G. Niemeyer. Improving perception in time-delayed telerobotics. *International Journal of Robotics Research*, 24(8):631–644, 2005.

[100] N.A. Tanner and G. Niemeyer. Practical limitations of wave variable controllers in teleoperation. In *IEEE Conference on Robotics, Automation and Mechatronics*, pages 25–30, 2004.

[101] Daniel Wang, Yuru Zhang, Yuhui Wang, Yuan-Shin Lee, Peijun Lu, and Yong Wang. Cutting on triangle mesh: Local model-based haptic display for dental preparation surgery simulation. *IEEE Transactions on Visualization and Computer Graphics*, 11:671–683, 2005.

[102] D.W. Weir, J.E. Colgate, and M.A. Peshkin. Measuring and increasing Z-width with active electrical damping. In *IEEE symposium on Haptic interfaces for virtual environment and teleoperator systems*, pages 169 –175, 2008.

[103] A. Yamaguchi, K. Natori, and K. Ohnishi. An analysis of the impedance perceived by an operator in multilateral control system under constant communication time delay. In *2009 IEEE International Conference on Industrial Technology*, pages 1–6, Washington, DC, 2009.

[104] K. M. Yap, V. Marshall, V. Yu, G. Dodds, Q. Gu, and R. T. Souayed. Characterising distributed haptic virtual environment network traffic flows. In *Eurohapics*, pages 297–310, Lannion, France, 2007.

[105] Yongqiang Ye and P.X. Liu. Improving trajectory tracking in wave-variable-based teleoperation. *IEEE/ASME Transaction on Mechatronics*, 15(2):321–326, 2010.

[106] Y. Yokokohji, T. Imaida, and T. Yoshikawa. Bilateral control with energy balance monitoring under time-varying communication delay. In *IEEE International Conference on Robotics and Automation*, pages 2684–2689, San Francisco, CA, 2000.

[107] Y. Yokokohji, T. Tsujioka, and T. Yoshikawa. Bilateral control with time-varying delay including communication blackout. In *10th Symposium on Haptic Interfaces for Virtual Environment and Teleoperator Systems*, pages 2684–2689, Orlando, FL, 2002.

[108] Y. Yokokohji and T. Yoshikawa. Bilateral control of master-slave manipulators for ideal kinesthetic coupling: formulation and experiment. *IEEE Transactions on Robotics and Automation*, 10(5):605–20, 1994.

Appendix A: Passive Multirate Wave Communications for Haptic Interaction in Slow Virtual Environments

Naser Yasrebi, Daniela Constantinescu

Department of Mechanical Engineering, University of Victoria, Victoria, Canada

E-mail: nyasrebi@uvic.ca, danielac@me.uvic.ca.

Abstract

Haptic interaction in slow virtual environments (VEs) can become unstable due to the phase lag introduced in the control loop by the slow update rate of the VE. Increasing the physical damping and/or limiting the contact stiffness rendered to users can mitigate the destabilizing effect of the low VE update rate. However, large physical damping and compliant virtual contacts decrease the sense of presence in VEs, especially during interaction with rigid virtual objects. To increase the maximum virtual contact stiffness can be rendered to users without increasing the interface damping, this paper proposes a control strategy based on multirate wave communications between a haptic interface and a VE updated at a slow and fixed rate. The multirate wave communications are shown to be guaranteed passive only if the decrease of the wave sampling rate at the connection between the haptic interface and the VE does not cause aliasing. Therefore, an anti-aliasing low-pass filter is placed before the wave rate drop in the communications. The passivity condition is verified analytically and numerically for multirate haptic interaction in VEs with various contact stiffnesses and update rates. The transparency of haptic interaction in slow VEs to which users connect via passive multirate wave communications is investigated analytically in the frequency domain. Experiments validate that passive multirate wave communications can render stiffer contact in slow VEs than conventional direct coupling, and illustrate the destabilizing effect of the aliasing caused by the sampling rate drop in the communications.

keywords: Haptics, slow virtual environments, wave variables, multirate control.

1 Introduction

This paper aims to enhance the realism of haptic interaction in VEs updated at a slow and fixed rate. In slow VEs, the update rate of the simulation limits the contact stiffness that can be stably displayed to users [1, 2] and thus, degrades the fidelity of haptic feedback. To increase the maximum virtual stiffness which can be rendered to users who manipulate slow VEs, this paper connects the haptic interface to the VE simulation through passive multirate wave communications.

Multirate control has long been a key strategy for increasing the contact stiffness in slow VEs. However, mostly multirate haptic control with power domain communications has been studied to date. The power domain

IEEE/ASME Transactions on Mechatronics, vol.18, no.1, pp.328-336, Feb. 2013

connection between a fast force feedback loop and a slow VE has been shown to generate un-physical energy [3, 4] which grows with the sampling time and the stiffness of the VE [3] and destabilizes the interaction. To increase the contact stiffness provided to users, existing research has sought: (i) to decrease the VE sampling time; and (ii) to dissipate the artificial energy via passivity-based multirate control or via hardware.

The VE sampling time has been decreased: (i) via efficient collision detection algorithms; and (ii) via local models of interaction. Efficient collision detection algorithms [5, 6, 7] alleviate the collision detection bottleneck typical in rigid VEs with complex geometries and allow the simulation to run at haptic rates. However, the stability of haptic interaction in VEs employing those algorithms is not guaranteed [5]. Local models of interaction have been offered for haptic manipulation both of rigid [8] and of deformable [9, 10, 11, 12, 13, 14, 15, 16] VEs, for use in conjunction with the delayed VE [9, 11], or in its place [12, 10, 16]. However, stability guarantees have been provided only in [11], based on multirate analysis, and in [12], based on passivity arguments. The local model [11] is suitable only for high fidelity haptic feedback in compliant VEs because it lacks damping and would lead to large oscillations when stiff contacts are initiated. The local models [12] are also restricted to interaction with deformable VEs until a technique for pre-specifying local models of rigid body interaction is devised.

The artificial energy due to sampling can be dissipated: (i) via hardware; and (ii) via passivity-based control. Electrical damping [17, 18, 19], magneto-rheological brakes [20] and eddy current brakes [21] have been explored to increase the physical damping of the haptic interface and thus, permit stable interaction with stiffer VEs. Hardware approaches can be costly to implement and not trivial to extend to multi degrees of freedom haptic interfaces. Only proof of concept implementations have been presented to date. Passivity-based multirate controllers have been devised based on frequency, time and wave domain methods. Frequency domain analysis has connected the fast force feedback loop to a slow VE via virtual coupling [3, 4]. The virtual coupler is a conservative design because it dissipates energy throughout the interaction although the slow VE may be active only during certain simulation steps. Time domain analysis has aimed to dissipate only the spurious energy, via passive sampling-and-hold [22, 23, 24, 25] or via passive-set-position-modulation [26]. Passive sampler-and-holds need to predict the energy balance over a VE step and therefore, assume a sufficiently small VE sampling time [22, 23, 25] or additional physical damping [24]. Passive-set-position-modulation maps the modulated VE position to forces sent to users through a virtual coupler. Hence, for significant VE sampling time, time domain passivity-based multirate controllers still need fixed dissipation in the feedback loop. Wave domain analysis has connected the fast force feedback loop to the slow VE via multirate wave communications [27]. The rate drop/increase has been modeled as a series of time delays and aliasing has not been considered [27].

This paper adopts a multirate wave variable control framework for haptic interaction in slow VEs. In the multirate wave variable framework, the force control loop runs at the fast 1 KHz haptic frequency, the VE runs at a slow and fixed frequency, and the change of the sampling rate occurs in the wave variable communications. The first contribution of this work is an analysis of the discrete time energy balance in the multirate wave channels which reveals that they are passive only if the rate drop does not introduce aliasing. To ensure passive multirate wave channels, this paper places an anti-aliasing low-pass wave filter before the rate drop in the communications. Low-pass wave filtering has previously been used in [28] to overcome instability due to a hold-last-sampler addressing packet loss in packet-switched communications. However, the low-pass filters [28] have been designed heuristically, whereas the low-pass filter in this paper results from time domain energy considerations and guarantees passive multirate wave communications. The second contribution is the analytical and numerical verification of the passivity condition for multirate wave communications connecting a fast haptic feedback loop to VEs with various stiffnesses and update rates. The third contribution is a frequency domain analysis of the transparency of multirate wave variable control of haptic interaction in slow VEs. The fourth contribution is the experimental validation of the ability of passive multirate wave communications to render stiffer slow VEs than direct coupling. The experiments also illustrate that the haptic interaction in a slow VE with multirate wave communications can become unstable when the decrease of the wave sampling rate introduces aliasing.

The proposed passive multirate wave communications have several advantages. (i) Unlike controllers that enforce passive sampling-and-hold of power domain signals [22, 23, 24, 25], they maintain an exact energy balance without requiring prediction and without assuming a sufficiently small VE sampling time. (ii) They neither depend on a passive numerical integrator whose extension to rigid body interaction is unclear, like the passive set-position-modulation strategy [26], nor require pre-computed local models of interaction, like the passivity-based control in [12]. Therefore, the passive multirate wave communications should be extensible to 6DOF haptic interaction in slow VEs provided body twists and wrenches are mapped to 6DOF wave variables as in [29]. Future work will investigate this extension. (iii) As shown in Section 3, the passive multirate wave communications are practical to implement. They require only a low-pass filter with gain limited below unity and cutoff frequency half the update rate of the slow VE to be placed in the forward wave path before the wave sampling frequency drops.

The passive multirate wave communications share the limitations of wave variables controllers [30, 31]. They: (i) may suffer from position drift; (ii) may degrade perception via wave reflections; and (iii) cannot provide ideal kinesthetic coupling [32] because of their intervening impedance, which acts as a spring inversely proportional to the VE sampling time [30] and eliminates high frequencies from the forces rendered to users. Position drift can be diminished via transmitting wave integrals together with the wave signals [30], via modulation of the outgoing wave [30], or via adding user-perceived and environment forces [33] to the outgoing wave. Wave reflections are opportunely eliminated by the proposed anti-aliasing filter. High frequency forces can be applied to users via asymmetric wave communications with force [31] or acceleration [34] feedback, or via reusing the energy dissipated by the anti-aliasing wave filter in a local model of interaction. Work in progress is investigating the latter option. Future work will also address the passivity of wave communications for haptic interaction in slow VEs with variable update rate.

In the remainder of the paper, Section 2 introduces the multirate model of haptic interaction in slow VEs. Section 3 derives the passivity condition for multirate wave communications. Section 4 checks this condition analytically and numerically for multirate haptic interaction in slow VEs with various contact stiffness and sampling rates. Section 5 investigates the transparency of haptic interaction in slow VEs with passive multirate wave communications. Section 6 offers experimental support to the analysis. Section 7 presents the conclusions of this work.

2 Problem definition

2.1 Multirate wave transformation

This work uses wave variable control [30] to tackle the change of sampling rate which arises in a haptic system due to a slow VE. Figure 1 depicts the proposed multirate wave variable control strategy. It illustrates that wave [30] (or scattering [35]) variables are transmitted between the haptic interface and the slow VE, and that the rate change between the fast haptic feedback and the slow VE loops is modeled as wave downsampling and upsampling. In Figure 1, notation is used as follows: M is the wave sampling rate drop/increase factor, and is represented as communications downsampling/upsampling factor; $\dot{x}_m$ is the velocity of the haptic interface; $\dot{x}_s$ is the velocity command transmitted to the VE through wave variable communications; F_s is the VE force; F_m is the force applied to the haptic interface by the wave controller; u_m and v_s are the output waves; u_s and v_m are the input waves; and b is the wave impedance. The output and input waves are related to the velocities and forces at the haptic interface (master) and VE (slave) sides via [30]:

$$\begin{array}{ll} u_m(t) = \frac{F_m(t)+b\dot{x}_m(t)}{\sqrt{2b}} & v_s(t) = \frac{-F_s(t)+b\dot{x}_s(t)}{\sqrt{2b}} \\ v_m(t) = \frac{-F_m(t)+b\dot{x}_m(t)}{\sqrt{2b}} & u_s(t) = \frac{F_s(t)+b\dot{x}_s(t)}{\sqrt{2b}} \end{array} . \tag{1}$$

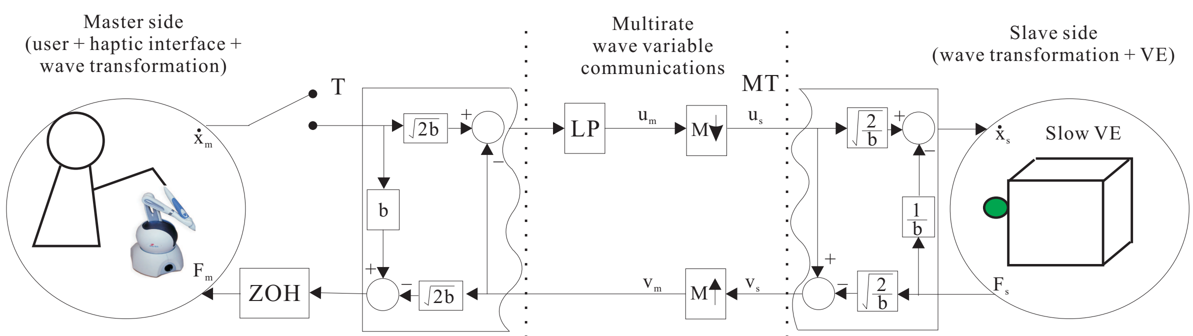

Figure 1: Multirate wave variable control of haptic interaction in a slow VE. The drop/increase of the wave sampling rate at the connection between the master side and the slave side is modeled as communications downsampling/upsampling.

The haptic system in Figure 1 comprises three main components: (i) the human operator together with the haptic interface, sampler, Zero-Old-Hold (ZOH) and the left side of the wave transformation, hereafter called the master side; (ii) the communication channels; and (iii) the VE together with the right side of the wave transformation, hereafter called the slave side. If all three components are passive, haptic interaction in slow VEs becomes an interconnection of passive systems and hence, strictly stable [1]. The master and slave sides can be made passive through suitable control [36]. The unirate wave communications are passive for constant transmission delay both for continuous time [35, 30] and discrete time [37] implementation. The discrete time passivity condition for multirate wave communications is derived in Section 3, and requires aliasing to be prevented when the wave sampling rate drops at the connection between the fast haptic feedback loop and the slow VE loop.

3 Passivity condition for multirate wave communications

Hereafter, a wave downsampler and upsampler pair is used to model the change of the wave sampling rate that occurs in the wave communications that connect a fast haptic loop to a slow VE loop, as shown in Figure 1. The aliasing due to the wave rate drop is also considered in the time domain passivity analysis below.

The two-port mechanical system with velocities $\dot{x}_m(t)$ and $\dot{x}_s(t)$, forces $F_m(t)$ and $F_m(t)$, and initial energy $E(0)$ depicted in Figure 1 is passive iff it obeys [30]:

$$\begin{aligned}&\int_0^t (F_m(t)\dot{x}_m(t) - F_s(t)\dot{x}_s(t))\,dt + E(0) \geq 0\\ &\forall t, \quad \text{admissible } F_m(t),\, F_s(t).\end{aligned} \tag{2}$$

This two-port system employs wave domain communications. If continuous time implementation is assumed and the communications rate drop and increase are ignored, the passivity condition of the two-port system can be written as [30]:

$$\begin{aligned}&\int_0^t \frac{1}{2}\left(u_m^T(t)u_m(t) + v_s^T(t)v_s(t)\right)dt\\ &\geq \int_0^t \frac{1}{2}\left(u_s^T(t)u_s(t) + v_m^T(t)v_m(t)\right)dt\\ &\forall t, \quad \text{admissible } u_m(t),\, v_m(t).\end{aligned} \tag{3}$$

In other words, the continuous time wave communications are passive if the energy provided by the output waves is less than the energy received via the input waves [30].

After defining truncated signals via:

$$u_\theta(\tau) = \begin{cases} 0 & \text{if } \tau < 0 \\ u(\tau) & \text{if } 0 \leq \tau \leq \theta \\ 0 & \text{if } \tau > \theta \end{cases}, \tag{4}$$

the passivity condition in Equation (3) can be written for discrete time wave communications as:

$$\begin{aligned}\Delta E(t) &= \frac{1}{2}\left[\sum_{k=0}^{N} u_{m_t}^2(kT)\cdot T - \sum_{i=0}^{N/M} u_{s_t}^2(iMT)\cdot MT\right]\\ &+ \frac{1}{2}\left[\sum_{i=0}^{N/M} v_{s_t}^2(iMT)\cdot MT - \sum_{k=0}^{N} v_{m_t}^2(kT)\cdot T\right]\\ &\geq 0 \quad \forall t \geq 0,\end{aligned} \tag{5}$$

where $\Delta E(t)$ is the energy stored in the multirate wave communications at time t, T is the sampling interval of the haptic loop, N is the signal length before the wave rate drop, and the rate drop factor M relates the VE sampling interval T_{VE} to the control sampling interval T via $T_{VE} = MT$. For simplicity, only MT is used in place of T_{VE} in Equation (5) and in the remainder of the paper.

Given the definition of the truncated signals in Equation (4), Equation (5) can also be written as:

$$\begin{aligned}\Delta E(t) &= \frac{1}{2}\left[\sum_{k=-\infty}^{\infty} u_{m_t}^2(kT)\cdot T - \sum_{i=-\infty}^{\infty} u_{s_t}^2(iMT)\cdot MT\right] \\ &+ \frac{1}{2}\left[\sum_{i=-\infty}^{\infty} v_{s_t}^2(iMT)\cdot MT - \sum_{k=-\infty}^{\infty} v_{m_t}^2(kT)\cdot T\right] \\ &\geq 0 \quad \forall t \geq 0. \end{aligned} \tag{6}$$

Since the ZOH expander is used to increase the sampling rate, the $v_{m_t}(kT)$ and $v_{s_t}(iMT)$ wave signals are related via:

$$v_{m_t}(kT) = v_{s_t}(iMT), \quad \text{for} \quad (i-1)M \leq k < iM. \tag{7}$$

It follows that:

$$\sum_{k=-\infty}^{\infty} v_{m_t}^2(kT)\cdot T = \sum_{i=-\infty}^{\infty} v_{s_t}^2(iMT)\cdot MT, \tag{8}$$

which shows that the ZOH rate increase is passive.

From Equations (6) and (8), the passivity condition for the multirate wave communications can be written as:

$$\begin{aligned}\Delta E(t) &= \frac{1}{2}\left[\sum_{k=-\infty}^{\infty} u_{m_t}^2(kT)\cdot T - \sum_{i=-\infty}^{\infty} u_{s_t}^2(iMT)\cdot MT\right] \\ &\geq 0 \quad \forall t, \quad \text{admissible } u_{m_t}(t),\, u_{s_t}(t), \end{aligned} \tag{9}$$

and, after application of Parseval's theorem the second term in Equation (9) becomes:

$$\sum_{i=-\infty}^{\infty} u_{s_t}^2(iMT)\cdot MT = \frac{TM}{2\pi}\int_{-\pi}^{\pi} |U_s(e^{j\Omega})|^2 d\Omega, \tag{10}$$

where U_s is the discrete-time Fourier transform of u_{s_t}.

If the maximum frequency in u_{m_t} is $|\Omega_{max}| < \frac{\pi}{M}$, then the drop of the wave sampling rate does not introduce aliasing in the multirate wave transformation shown in Figure 1, and:

$$|U_m\left(e^{j\Omega}\right)| = 0 \quad \forall \Omega > \frac{\pi}{M}. \tag{11}$$

Moreover, in the absence of aliasing [38]:

$$U_s(e^{j\Omega}) = \frac{1}{M} U_m(e^{\frac{j\Omega}{M}}) \quad \forall |\Omega| < \Omega_{max} < \frac{\pi}{M}. \tag{12}$$

Using Equations (11) and (12), Equation (10) can be further manipulated to give:

$$\begin{aligned}&\frac{TM}{2\pi}\int_{-\pi}^{\pi} |U_s(e^{j\Omega})|^2 d\Omega = \frac{T}{2\pi M}\int_{-\pi}^{\pi} |U_m(e^{j\frac{\Omega}{M}})|^2 d\Omega \\ &= \frac{T}{2\pi}\int_{-\pi}^{\pi} |U_m(e^{j\frac{\Omega}{M}})|^2 d\frac{\Omega}{M} = \frac{T}{2\pi}\int_{\frac{-\pi}{M}}^{\frac{\pi}{M}} |U_m(e^{j\Omega_1})|^2 d\Omega_1 \\ &= \frac{T}{2\pi}\int_{-\pi}^{\pi} |U_m(e^{j\Omega_1})|^2 d\Omega_1 = \sum_{i=-\infty}^{\infty} u_{m_t}^2(n)T, \end{aligned} \tag{13}$$

which shows that $\Delta E(t) = 0$ and the multirate wave transformation is passive when the rate drop introduces no aliasing.

When the decrease of the wave sampling rate causes aliasing, Equation (12) does not hold and the energy stored in the multirate wave communications, $\Delta E(t)$ in Equation (9), can be positive or negative depending on the aliasing-induced phase change [39]. Experimental validation that aliasing may or may not inject energy in the multirate wave communications is presented in Section 6. To ensure a passive multirate wave transformation, this paper prevents aliasing by placing an anti-aliasing low-pass filter with gain limited below unity before the rate drop in the forward wave path from the device to the slow VE. The filter does not endanger stability because the passivity of the wave variables is unaffected by delays or phase lag [30], and adds dissipation that prevents sustained oscillations if its gain is less than unity.

Section 4 presents an example where aliasing injects energy into the multirate wave communications and thus, into the haptic interaction system. Section 6 demonstrates the need for the anti-aliasing wave filter via experiments.

4 Verification of the passivity condition

4.1 Example multirate wave transformation with aliasing

This section verifies the necessity of the passivity condition derived in Section 3 through a counterexample. For ease of computation, the VE is considered twice as slow as the force control loop, $M = 2$. The frequency content of the exemplary wave signal u_{m_t} sampled at the haptic frequency is shown in Figure 2(a), and is such that $\Omega_{max} > \frac{\pi}{2}$ and $|U_m| = \alpha$ for $|\Omega| < \Omega_{max}$. As shown in Figure 2(b), the decrease of the wave sampling rate in the forward path from the haptic device to the slow VE expands the spectral images of u_{m_t} by a factor $M = 2$, causing them to overlap, and therefore, introducing aliasing into u_{s_t} (Figure 2).

The energy stored in the exemplary multirate wave transformation is computed by investigating the two terms in Equation (9) separately. After applying Parseval's theorem, the first term can be written as:

$$\sum_{k=-\infty}^{\infty} u_{m_t}^2(kT)T = \frac{T}{2\pi}\int_{-\pi}^{\pi}|U_m(e^{j\Omega})|^2 d\Omega$$
$$= \frac{T}{2\pi}\int_{-\Omega_{max}}^{\Omega_{max}}|U_m(e^{j\Omega})|^2 d\Omega = \frac{T\alpha^2\Omega_{max}}{\pi}. \tag{14}$$

After applying the downsampling theorem in the Z-domain:

$$U_s(e^{j\Omega}) = \frac{1}{2}(U_m(e^{j\frac{\Omega}{2}}) + U_m(e^{j\frac{\Omega}{2}-j\pi})) \tag{15}$$

and Parseval's theorem, the second term in Equation (9) can be written as:

$$\sum_{i=0}^{\infty} u_s^2(i\cdot 2T)\cdot 2T = \frac{2T}{2\pi}\int_{\pi}^{\pi}|U_s(e^{j\Omega})|^2 d\Omega$$
$$= \frac{T}{4\pi}\int_{-\pi}^{\pi}|(U_m(e^{j\frac{\Omega}{2}}) + U_m(e^{j\frac{\Omega}{2}-j\pi}))|^2 d\Omega$$
$$= \frac{T}{4\pi}\int_{2(\Omega_{max}-\pi)}^{2(\pi-\Omega_{max})}|U_m(e^{j\frac{\Omega}{2}})|^2 d\Omega$$
$$+\frac{T}{4\pi}\int_{-\pi}^{2(\Omega_{max}-\pi)}|U_m(e^{j\frac{\Omega}{2}}) + U_m(e^{j\frac{\Omega}{2}-j\pi})|^2 d\Omega$$
$$+\frac{T}{4\pi}\int_{2(\pi-\Omega_{max})}^{\pi}|U_m(e^{j\frac{\Omega}{2}}) + U_m(e^{j\frac{\Omega}{2}-j\pi})|^2 d\Omega. \tag{16}$$

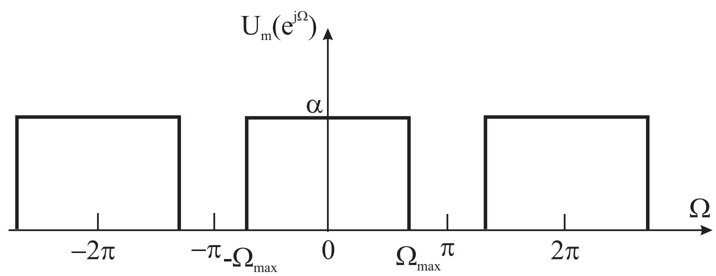

(a)

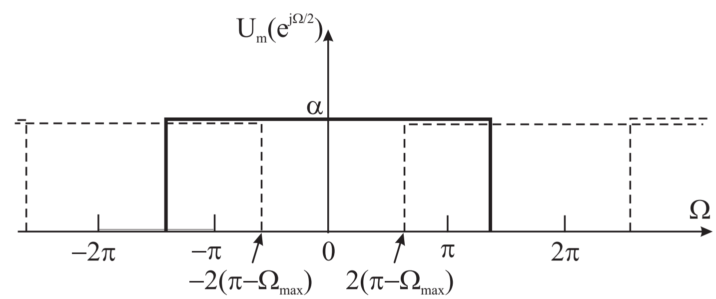

(b)

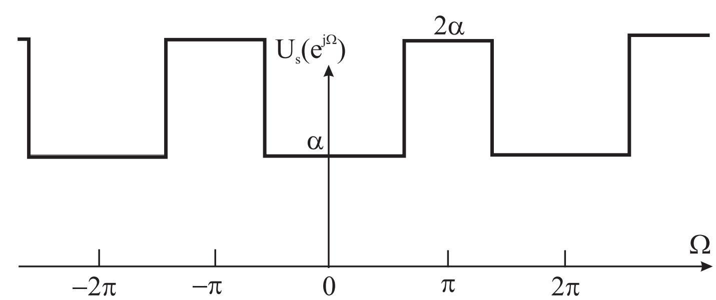

(c)

Figure 2: Frequency content of a sampled wave signal with aliasing.

After considering Figure 2(c), Equation (16) is simplified to:

$$\sum_{i=-\infty}^{\infty} u_s^2(i \cdot 2T) \cdot 2T = \frac{T\alpha^2(\pi - \Omega_{max})}{\pi} + \frac{T\alpha^2(2\Omega_{max} - \pi)}{\pi} + \frac{T\alpha^2(2\Omega_{max} - \pi)}{\pi} = \frac{T\alpha^2(3\Omega_{max} - \pi)}{\pi}, \tag{17}$$

and the energy balance in the communication channels becomes:

$$\Delta E = \sum_{k=-\infty}^{\infty} u_m^2(kT) \cdot T - \sum_{i=-\infty}^{\infty} u_s^2(i \cdot 2T) \cdot 2T = \frac{T\alpha^2\Omega_{max}}{\pi} - \frac{T\alpha^2(3\Omega_{max} - \pi)}{\pi} = -\frac{T\alpha^2(2\Omega_{max} - \pi)}{\pi} < 0. \tag{18}$$

Equation (18) shows that aliasing caused by the decrease of the wave sampling rate can inject energy into the system and thus, destabilize the haptic interaction in a slow VE.

4.2 Numerical example

In this section, the stability region for an example haptic system with multirate wave communications is computed using: (i) the passivity condition of the multirate wave transformation derived in this paper; and (ii) the eigenvalues of the state transition matrix of the multirate state space realization of the haptic system derived as in [40].

The example haptic system includes a virtual wall connected through multirate wave communications with wave impedance $b = 25$ Ns/m to a haptic interface with mass $m_{HD} = 0.15$ kg and $b_{HD} = 0$ Ns/m. The transfer function of the slow VE is:

$$H_{VE}(z) = \frac{KT_{VE}}{2}\frac{z+1}{z-1}, \tag{19}$$

where K is the virtual stiffness. In the absence of computational delay, the transfer function of the slave side is:

$$\frac{V_s(z)}{U_s(z)} = \frac{b - H(z)}{b + H(z)} = \frac{(2b - KT_{VE})z - (2b + KT_{VE})}{(KT_{VE} + 2b)z + (KT_{VE} - 2b)}. \tag{20}$$

After substitution of $z = e^{j\Omega}$ and algebraic manipulation, Equation (20) gives:

$$\left\| \frac{V_s(z)}{U_s(z)} \right\| = 1, \tag{21}$$

which shows that the slave side is passive independent of the VE sampling time and stiffness. A similar argument holds for the master side and its transfer function $\frac{U_m(z)}{V_m(z)}$. Since the slave and master sides are passive, suitable low-pass wave filtering of the multirate wave communications ensures their passivity and thus, guarantees the stability of the example haptic system.

Figure 3 plots the stability regions for the example haptic system for different wave sampling rate drop factors M, up to 10, and for different cutoff frequencies λ_c of a first-order anti-aliasing low-pass wave filter:

$$H_f(s) = \frac{a}{s+a}, \tag{22}$$

where a is a constant. Since the filter is not ideal, λ_c is considered to be the frequency at which the magnitude response of the filter is -20 dB. The stability regions in this figure are the areas under the plotted curves, and are derived: (i) by imposing passive communications through anti-aliasing low-pass wave filtering (dotted line); and (ii) by imposing closed loop stability for different values of the VE stiffness K (continuous lines).

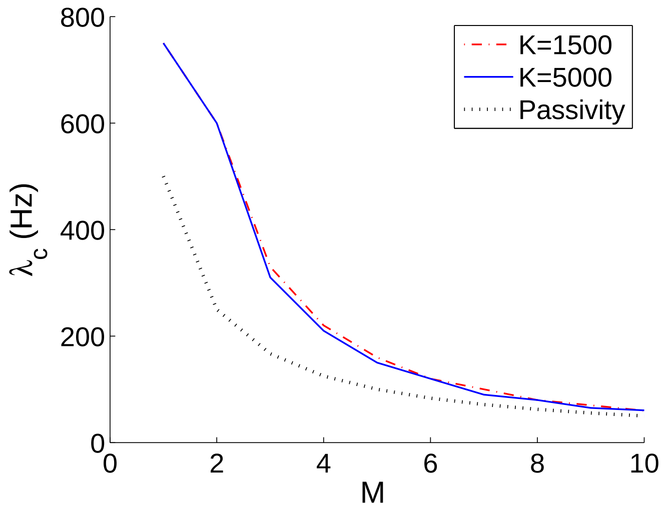

Figure 3: Stability regions for the example haptic system with multirate wave communications derived: (i) by imposing passive communications (dotted line); (ii) by imposing closed loop stability for different VE stiffness values K (continuous lines).

As Figure 3 illustrates, all stability regions show the same trend and stability depends on the wave sampling rate drop factor, M. As expected, the stability region obtained by feedback interconnection of passive sub-systems is more restrictive than the closed-loop stability region of the haptic interaction in a specific slow VE.

5 Transparency analysis

This section uses the transmitted admittance:

$$H(z) = \frac{X_m(z)}{F_h(z)} \tag{23}$$

to compare the transparency of haptic interaction in a slow VE to which the user connects via passive multirate wave communications to the transparency of the "ideal" interaction in a fast VE to which the user connects via direct coupling. The transmitted admittance of the haptic system with passive multirate wave communications is computed after converting the multirate system in Figure 1 to a unirate system using lifting [41]. In the analysis, the haptic device has mass $m_{HD} = 0.15$ kg and physical damping $b_{HD} = 1$ Ns/m. The VE has stiffness $K = 3500$ N/m and damping $B = 25$ Ns/m, and is updated at 50 Hz.

Figure 4 plots the transmitted admittance versus the normalized frequency: for the "ideal" interaction in the fast VE (dotted line); and for the interaction in the slow VE with passive multirate wave communications and with various wave impedance b (continuous lines). The magnitude of the transmitted admittance in this figure indicates the inverse of the transmitted stiffness, $\frac{1}{K_m}$.

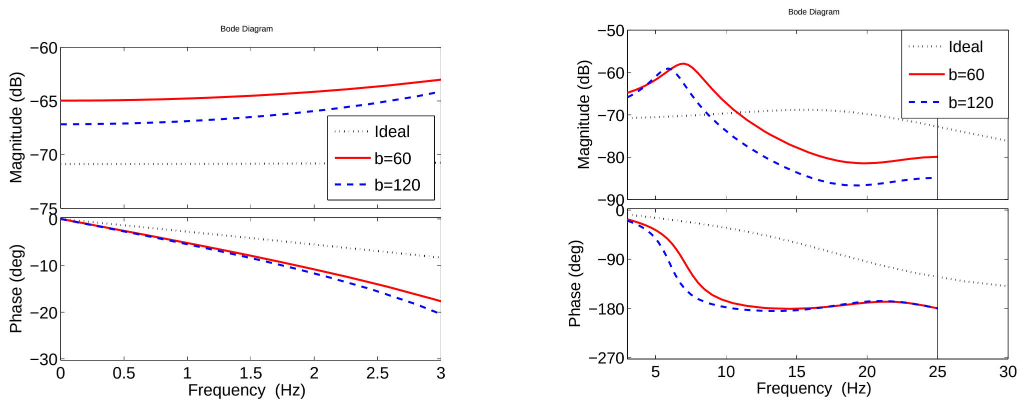

(a) Low frequencies.

(b) High frequencies.

Figure 4: Frequency response of transmitted admittance for different wave impedances and frequency ranges, and for a VE updated at 50 Hz and having stiffness $K = 3500$ N/m and damping $B = 25$ Ns/m.

Figure 4(a) plots the transmitted admittance in the low low frequency range, i.e., during enduring contact with the VE. It illustrates that passive multirate wave communications transmit lower stiffness to users interacting in slow VEs than direct coupling transmits to users interacting in fast VEs. Figure 4(a) also shows that the transmitted stiffness, i.e., the performance of passive multirate wave communications, increases as the wave impedance b increases. This is expected because, in low frequencies, the wave channels behave like a spring with stiffness [30]:

$$K_{comm} = \frac{b}{T_{VE}}. \tag{24}$$

Figure 4(b) plots the transmitted admittance in the high frequency range, i.e., when new contacts are established. It shows that a larger wave impedance can increase the stiffness transmitted to the operator during short-lived contacts. Whether users perceive this increase requires further investigation.

6 Experiments

This section presents two sets of experimental interactions with a slow virtual wall through a Phantom Omni haptic interface. In the experiments, the haptic device is connected to a personal computer running Windows Vista on an Intel Core 2 Duo CPU at 2.67GHz with 2 GB RAM. The slow virtual wall runs as a C++ console application on the same computer. The console application has two threads: (i) a fast thread which runs the master side including the low level control of the haptic interface and the filtering of the outgoing wave variable, u_m; and (ii) a slow thread which runs the VE simulation including the graphics on the slave side. The OPENHAPTICS^{TM} API is used to run the haptic thread at 1 KHz and the VE thread at 50 Hz. Since the console application runs on the Windows operating system, exact sampling time cannot be guaranteed. However, the observed variation of the sampling time is negligible.

In both sets of experiments, a constant force $F_h = 1$ N is applied to the handle of the haptic interface as the operator input to ensure the "same" user during successive interactions. According to Section 3, the wave communications need to be low-pass filtered using a filter with cutoff frequency less than $\frac{1}{(2)(0.02)\text{ s}} = 25$ Hz before their sampling rate drops from the high haptic rate to the slow VE rate to eliminate aliasing and thus, ensure their passivity. An IIR-Butterworth filter, designed according to the specifications in Table 1 and using the Digital Filter Design toolbox in Matlab, is used in the experiments.

Table 1: Anti-alising wave filter specifications for the experiments and performance analysis.

Filter	Passband	Stopband	Passband	Stopband
	Freq (Hz)	Freq (Hz)	Amp (dB)	Amp (dB)
LP	25	50	20	40

The results of the first set of experiments are presented in Figure 5. This figure plots the experimental Z-width of the Phantom Omni interface obtained for the cases that the device is connected to the slow virtual wall: (i) via direct coupling (dotted line); and (ii) via passive multirate wave variables (solid line). The results in Figure 5 demonstrate that multirate wave variable control can render contacts at least four times as stiff as direct coupling to operators who use a Phantom Omni device to touch a virtual wall updated at 50 Hz.

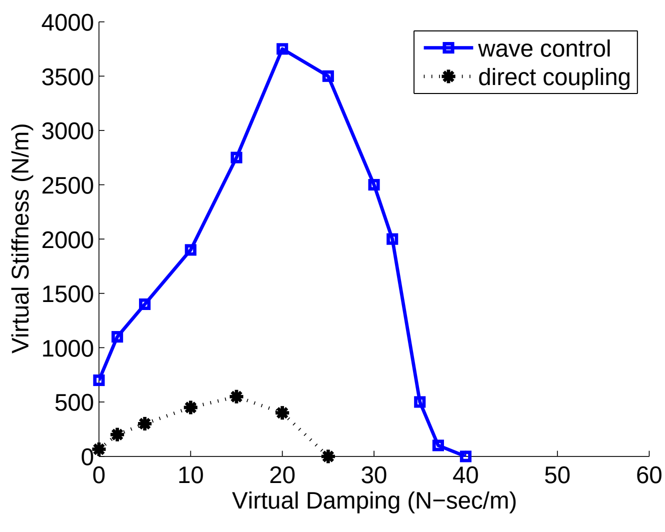

Figure 5: Z-width of the Phantom Omni device derived when (i) multirate wave transformation free of aliasing (solid line) and (ii) direct coupling (dotted line) are used to connect the haptic interface to a virtual wall updated at 50 Hz.

The second set of experiments investigates interactions of the Phantom Omni with a slow virtual wall via passive multirate wave communications and via multirate wave communications with aliasing caused by the wave sampling rate drop, respectively. In these interactions, the slow virtual wall has stiffness $K = 3500$ N/m and damping $B = 25$ Ns/m, and the wave impedance is $b = 80$ Ns/m. The low-pass filter has a cutoff frequency 25 Hz in the first experiment, and it has a cutoff frequency 250 Hz in the second experiment. According to Section 3, the multirate wave communications are free of aliasing and thus guaranteed passive in the first experiment, and they include aliasing and are not guaranteed passive in the second experiment.

The interactions with the slow virtual wall via passive multirate wave communications and via multirate wave communications with aliasing are presented in Figures 6 and 7, respectively. In these figures, x_m is the position of the haptic interface, x_s is the position command in the slow VE, F_m is the force fed back to the operator, and F_s is the force computed in the VE. Note that the haptic device settles on the virtual wall, i.e., the interaction is stable, when controlled via passive multirate communications (Figure 6). In contrast, a limit cycle-like behavior arises and the interaction is unstable when controlled via multirate wave communications with aliasing caused by the wave sampling rate drop (Figure 7). The results in Figure 7 illustrate that aliasing can have a destabilizing effect and thus, confirm the sufficiency of the condition derived for the passivity of the multirate wave communications in Section 3.

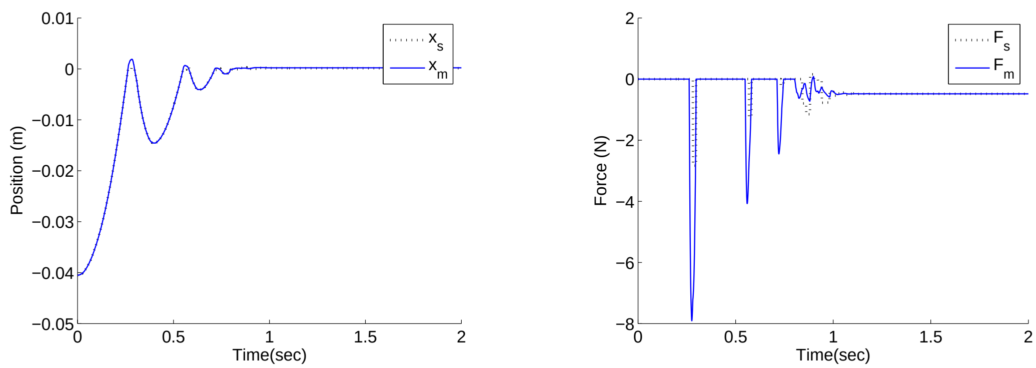

(a) Positions of the device x_m, and commanded in the VE x_s.

(b) Forces applied to the user F_m, and computed in the VE F_s.

Figure 6: Experimental interaction with a slow virtual wall ($K = 3500$ N/m, $B = 25$ Ns/m, $T_{VE} = 0.02$ s) via passive multirate wave communications. The low-pass filter has cutoff frequency $\lambda_c = 25$ Hz.

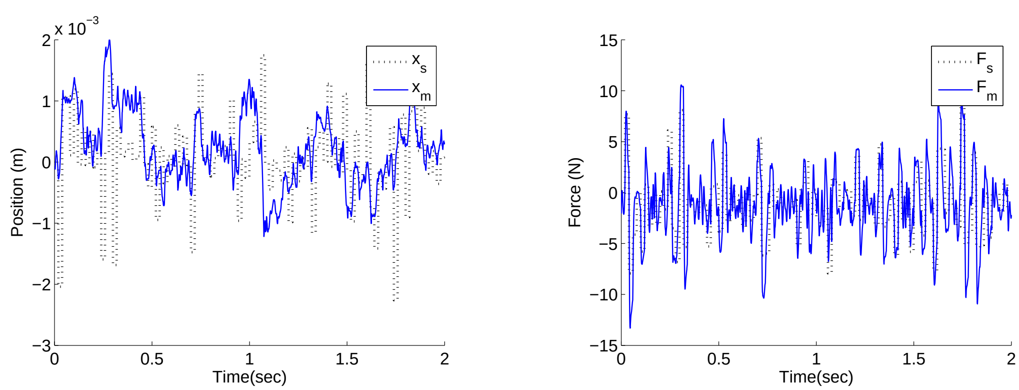

(a) Positions of the device x_m, and commanded in the VE x_s.

(b) Forces applied to the user F_m, and computed in the VE F_s.

Figure 7: Experimental interaction with a slow virtual wall ($K = 3500$ N/m, $B = 25$ Ns/m, $T_{VE} = 0.02$ s) via multirate wave communications with aliasing. The low-pass filter has cutoff frequency $\lambda_c = 250$ Hz.

Further confirmation that elimination of aliasing is sufficient to guarantee the passivity of multirate wave communications is offered by a set of experiments in which the hand input is set to be a chirp signal with frequency range $0-10$ Hz. The hand input is applied for 30 s and the VE has stiffness $K = 3500$ N/m, damping $B = 25$ Ns/m and sampling time $T_{VE} = 0.02$ s. The multirate wave communications are low-pass filtered with various cutoff frequencies using filters with specifications given in Table 2. The energy balance $\Delta E = E_1 - E_2$ is observed during the experiments, where E_1 is the energy after the filter and before the downsampler, and E_2 is the energy after the downsampler. Figure 8 plots the minimum energy balance during the interaction ΔE_{min} and the energy balance at the end of the interaction ΔE_{final} for the various filter cutoff frequencies. Note in this figure that: (1) the filters with cutoff frequencies 10 Hz and 25 Hz maintain the energy balance zero or positive throughout the interaction; (2) some filters with larger cutoff frequencies (50 Hz and 250 Hz in these experiments) may also maintain a positive energy balance throughout or during certain periods of the interaction. Hence, aliasing does not necessary inject energy in the multirate wave communications, but avoiding it guarantees their passivity.

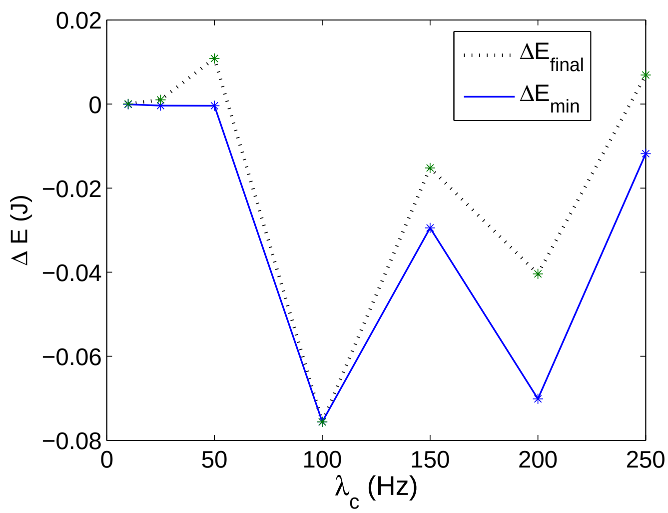

Figure 8: The final (dotted line) and minimum (continuous line) energy balance ΔE of the downsampler during experimental interaction with a slow VE ($K = 3500$ N/m, $B = 25$ Ns/m, $T_{VE} = 0.02$ s) for a 30 s chirp input with frequency range $0-10$ Hz, for various filter cutoff frequencies λ_c.

7 Conclusions

This paper has proposed passive multirate wave communications for increasing the contact stiffness that can be stably rendered to users interacting in slow VEs. It has shown that multirate wave communications are passive only if aliasing is prevented when the wave sampling rate drops in the forward path from the haptic device to the slow VE. This passivity condition has been derived by computing the energy stored in the multirate wave communications. The paper has ensured passive multirate wave communications through anti-aliasing low-pass filtering of the wave signal before its sampling rate drops in the forward path from the haptic device to the slow VE. Experiments have verified that: (i) compared to direct coupling, passive multirate wave communications can

Table 2: Filter specifications for the experiment with chirp hand input.

Filter	Passband Freq (Hz)	Stopband Freq (Hz)	Passband Amp (dB)	Stopband Amp (dB)
LP_1	10	25	20	40
LP_2	25	50	20	40
LP_3	50	100	20	40
LP_4	100	150	20	40
LP_5	150	200	20	40
LP_6	200	250	20	40
LP_7	250	300	20	40

render stiffer virtual contacts to operators interacting in a slow VE using a Phantom Omni haptic device; and (ii) the haptic interaction can become unstable unless the aliasing caused by the sampling rate drop in the forward wave path is prevented.

Future work will seek: to reuse the energy dissipated by the anti-aliasing wave filter to improve transparency; to extend the passive multirate wave communications to 6DOF haptics; and to consider interaction in VEs with variable update rate.

Acknowledgement

This work has been supported by the National Sciences and Engineering Research Council of Canada (NSERC).

REFERENCES

[1] J. E. Colgate and G. G. Schenkel. Passivity of a class of sampled-data systems: application to haptic interfaces. *J Robotic Syst*, 14(1):37–47, 1997.

[2] J.J. Abbott and A.M. Okamura. Effects of position quantization and sampling rate on virtual-wall passivity. *IEEE T Robotics*, 21(5):952–964, 2005.

[3] B.E. Miller, J.E. Colgate, and R.A. Freeman. Environment delay in haptic systems. In *IEEE Int Conf Robot Autom*, pages 2434–2439, 2000.

[4] B.E. Miller, J.E. Colgate, and R.A. Freeman. Guaranteed stability of haptic systems with nonlinear virtual environments. *IEEE T Robot Autom*, 16(6):712–719, 2000.

[5] A. Gregory, M.C. Lin, S. Gottschalk, and R. Taylor. Fast and accurate collision detection for haptic interaction using a three degree-of-freedom force-feedback device. *Computational Geometry: Theory and Applications*, 15(1-3):69–89, 2000.

[6] Y.J. Kim, M.A. Otaduy, M.C. Lin, and D. Manocha. Six-degree-of-freedom haptic rendering using incremental and localized computations. *Presence: Teleoperators and Virtual Environments*, 12(3):277–295, 2003.

[7] M.C. Lin and M.A. Otaduy. Sensation-preserving haptic rendering. *IEEE Computer Graphics and Applications*, 25(4):8–11, 2005.

[8] D. Constantinescu, S.E. Salcudean, and E.A. Croft. Local model of interaction for haptic manipulation of rigid virtual worlds. *Int J Rob Res*, 24(10):789–804, 2005.

[9] M. C. Cavusoglu. Multirate simulation for high fidelity haptic interaction with deformable objects in virtual environments. In *IEEE Int Conf Robot Autom*, pages 2458–2465, 2000.

[10] Daniel Wang, Yuru Zhang, Yuhui Wang, Yuan-Shin Lee, Peijun Lu, and Yong Wang. Cutting on triangle mesh: Local model-based haptic display for dental preparation surgery simulation. *IEEE T Vis Comp Graphics*, 11:671–683, 2005.

[11] F. Barbagli, D. Prattichizzo, and K. Salisbury. A multirate approach to haptic interaction with deformable objects single and multipoint contacts. *Int J Robot Res*, 24(9):703–715, 2005.

[12] M. Mahvash and V. Hayward. High-fidelity passive force-reflecting virtual environments. *IEEE T Robotics*, 21(1):38–46, 2005.

[13] R. Balaniuk. A differential method for the haptic rendering of deformable objects. In *ACM Symp Virt Real Software Technology*, pages 297–304, Limassol, Cyprus, 2006.

[14] K. Lee and D.Y. Lee. MIMO output estimation with reduced multirate sampling for real-time haptic rendering. *IEEE T Robotics*, 23(3):481–493, 2007.

[15] P. Fong. Sensing, acquisition, and interactive playback of data-based models for elastic deformable objects. *Int J Rob Res*, 28(5):630–655, 2009.

[16] Paul Jacobs, Michael J. Fu, and M. Cenk Cavusoglu. High fidelity haptic rendering of frictional contact with deformable objects in virtual environments using multi-rate simulation. *Int J Rob Res*, 29(14):1778–1792, 2010.

[17] M. Kawai and T. Yoshikawa. Haptic display with an interface device capable of continuous-time impedance display within a sampling period. *IEEE/ASME T Mechatronics*, 9(1):58 –64, 2004.

[18] J.S. Mehling, J.E. Colgate, and M.A. Peshkin. Increasing the impedance range of a haptic display by adding electrical damping. In *IEEE 1st World Haptic Conf Symp*, pages 257–262, 2005.

[19] D.W. Weir, J.E. Colgate, and M.A. Peshkin. Measuring and increasing Z-width with active electrical damping. In *IEEE Symp Haptic Interf Virt Env Teleop Syst*, pages 169 –175, 2008.

[20] J. An and D.-S. Kwon. Stability and performance of haptic interfaces with active/passive actuators - theory and experiments. *Int J Robotic Res*, 25(11):1121–1136, 2006.

[21] A. Gosline and V. Hayward. Eddy current brakes for haptic interfaces: design, identification, and control. *IEEE/ASME T Mechatronics*, 13(6):669 –677, 2008.

[22] J.-H. Ryu, Y.S. Kim, and B. Hannaford. Sampled-data and continuous-time passivity and stability of virtual environments. *IEEE T Robotics*, 20(4):772–776, 2004.

[23] J.-H. Ryu, C. Preutsche, B. Hannaford, and G. Hirzinger. Time domain passivity control with reference energy following. *IEEE T Control Syst Tech*, 13(5):737–742, 2005.

[24] S. Stramigioli, C. Secchi, A.J. van der Schaft, and C. Fantuzzi. Sampled data systems passivity and discrete port-Hamiltonian systems. *IEEE T Robotics*, 21(4):574–587, 2005.

[25] G. Borghesan, A. Macchelli, and C. Melchiorri. Interconnection and simulation issues in haptics. *IEEE T Haptics*, 3(4):266–279, 2010.

[26] D. Lee and K. Huang. Passive-set-position-modulation framework for interactive robotic systems. *IEEE T Robotics*, 26(2):354–369, 2010.

[27] Ch. Cho, J. B. Song, and M. Kim. Stable haptic display of slowly updated virtual environment with multirate wave transform. *IEEE/ASME T Mechatronics*, 13(5):566–575, 2008.

[28] S. Hirche and M. Buss. Packet loss effects in passive telepresence systems. In *43rd IEEE Conf Dec Control*, pages 4010–4015, Paradise Islands, The Bahamas, 2004.

[29] M. Alise, R.G. Roberts, D.W. Repperger, C.A. Moore, and S. Tosunoglu. On extending the wave variable method to multiple-DOF teleoperation systems. *IEEE/ASME T Mechatronics*, 14(1):55–63, 2009.

[30] G. Niemeyer and J.-J.E. Slotine. Telemanipulation with time delays. *Int J Rob Res*, 23(9):873–890, 2004.

[31] N. A. Tanner and G. Niemeyer. Improving perception in time-delayed telerobotics. *Int J Rob Res*, 24(8):631–644, 2005.

[32] Y. Yokokohji and T. Yoshikawa. Bilateral control of master-slave manipulators for ideal kinesthetic coupling: formulation and experiment. *IEEE T Robot Autom*, 10(5):605–20, 1994.

[33] Yongqiang Ye and P.X. Liu. Improving trajectory tracking in wave-variable-based teleoperation. *IEEE/ASME T Mechatronics*, 15(2):321–326, 2010.

[34] N. A. Tanner and G. Niemeyer. High-frequency acceleration feedback in wave variable telerobotics. *IEEE/ASME T Mechatronics*, 11(2):119–127, 2006.

[35] R. J. Anderson and M. W. Spong. Bilateral control of teleoperators with time delay. *IEEE T Automat Contr*, 34(5):494–501, 1989.

[36] N.A. Tanner and G. Niemeyer. Practical limitations of wave variable controllers in teleoperation. In *IEEE Conf Robot Automat Mechatronics*, pages 25–30, 2004.

[37] P. Berestesky, N. Chopra, and M. W. Spong. Discrete time passivity in bilateral teleoperation over the Internet. In *IEEE Int Conf Robot Autom*, pages 4557– 4564, New Orleans, LA, 2004.

[38] J. G. Proakis and D. G. Manolakis. *Digital Signal Processing : Principles, Algorithms, and Applications*. Upper Saddle River, EUA : Prentice-Hall, 1996.

[39] S. W. Smith. *Digital signal processing. A practical guide for engineers and scientists.* Newnes - Elsevier Science, 2003.

[40] M. Araki and K. Yamamoto. Multivariable multirate sampled-data systems: State-space description, transfer characteristics, and Nyquist criterion. *IEEE T Automat Contr*, 31(2):145–154, 1986.

[41] B.A. Francis and T.T. Georgiou. Stability theory for linear time-invariant plants with periodic digital controllers. *IEEE T Automat Contr*, 33(9):820–832, 1988.

Appendix B: Centralized Multirate Wave Variables Control of Haptic Cooperation in Rigid Virtual Environments

Naser Yasrebi, Daniela Constantinescu

Department of Mechanical Engineering, University of Victoria, Victoria, Canada

E-mail: nyasrebi@uvic.ca, danielac@me.uvic.ca.

Abstract

Centralized control of networked haptic cooperation offers higher consistency of the virtual world than distributed control, but renders much more limited contact stiffness and thus, provides decreased fidelity in rigid virtual environments. To increase the realism of force feedback in centralized rigid virtual environments, this paper proposes a passive multirate wave variables control strategy that supports cooperative manipulations of stiff virtual objects over a network with constant delay and with limited packet update rate, like a local area network (LAN) or a high-speed metropolitan area network (MAN). The paper demonstrates through analysis and experiments that passive multirate wave variables control has two important advantages compared to traditional multirate centralized control: (i) it maintains the haptic cooperation stable in much stiffer virtual environments; and (ii) it renders to users a maximum contact stiffness that is unaffected by the network delay. These results indicate that centralized control of haptic cooperation in rigid virtual environments can achieve similar fidelity to descentralized control when the cooperating client users are connected to the server through passive multirate wave variables communications.

keywords: haptic cooperation, centralized control, passive multirate wave variables control.

1 INTRODUCTION

Force feedback can enhance task performance in virtual reality applications which require cooperation among multiple networked users [1]. Promising applications include surgical training [2], telerehabilitation [3, 4, 5], cooperative virtual reality-based industrial design [6, 7], and immersive online computer games [8]. Yet, only a limited number of cooperative haptic manipulations have been reported to date [9, 10, 6, 7, 11, 2]. The wide spread use of haptic cooperation over distance is still hampered by significant challenges arising from the network characteristics. As demonstrated by several experimental studies [12, 13, 14, 15, 11], transmission delay, jitter, packet loss and low transmission rate lead to non-deterministic and multirate communications which threaten the realism and stability of the cooperation.

Control strategies have been proposed to stabilize haptic cooperation supported both through peer-to-peer and through client-server communications. In [10], a peer synchronization scheme has combined linear compensation with Smith prediction. The scheme is proven stable for constant transmission delay, no packet loss and a packet transmission rate equal to the update rate of the force feedback loop. Experimentally, the scheme [10] also demonstrates robustness to delay variation. In [16], a method to adjust the force feedback gains at the clients has been proposed which compensates for perceptual distortions due to packets arriving at the haptic frequency with constant delay. In [17], haptic cooperation has been investigated assuming that the remote users exchange position and force information over communications with constant and relatively small transmission delay and constant and limited transmission rate, like those provided by LANs and high-speed MANs. The analysis in [17] has shown that centralized control renders significantly lower virtual stiffness to the remote users compared to distributed control.

Multirate control has been employed for increasing the contact stiffness rendered both to users interacting with slowly updated virtual environments [18, 19, 20, 21, 22, 23, 24], and to cooperating users connected over a network with low packet update rate [17]. However, work in multirate haptic manipulation of slowly updated virtual environments has not considered communication delays, and research in multirate centralized haptic co-operation has analyzed the stability of the interaction solely between networked users passing position and force information to each other. The analysis has concluded that even small communication delays severely limit the contact stiffness stably rendered to networked users exchanging position and force data. The interaction between networked users exchanging wave variables [25, 26] has been investigated only empirically and only for distributed unirate control of the cooperation [3, 11, 27]. Neither a stability analysis nor a methodology for selecting the wave impedance and the environment stiffness have been presented.

This work is concerned with increasing the realism of haptic cooperation among client users connected to a centralized rigid virtual environment over a LAN or a high-speed MAN. Centralized control is advantageous in applications that involve many users because it offers high consistency of the virtual environment [16]. Furthermore, centralized control is required in applications that demand virtual environments whose size or cost prohibit their replication at each user (e.g., computationally intensive virtual environments which need to run on cluster computers). LAN and high-speed MAN networks offer connectivity over a limited distance, but can nevertheless support multi-user haptic cooperations deployed over the internal network of an organization, e.g., military training [8] and virtual reality-based industrial design [6, 7]. In this work, increased realism of centralized haptic cooperation in rigid virtual environments is achieved through enlarging the maximum stiffness of the virtual objects that client users can manipulate together over a LAN or a high-speed MAN.

To enable the clients to cooperatively manipulate stiffer centralized virtual objects across networks with packet update rates lower than the rate of the clients' force control loops, this paper connects the users to the central server through passive multirate wave variables communications. The key contributions of the paper are: (i) a stability analysis of centralized haptic cooperation with passive multirate wave variables communications that considers the constant delay and the bandwidth limitation of the LAN/MAN networks, in which the jitter and packet loss are negligible and can be ignored in analysis and delay is constant [28]; (ii) a comparative analysis of the stability of passive multirate wave variables control to the stability of traditional control of centralized haptic cooperation; and (iii) the experimental validation of the analytical results. For the stability investigations, the paper develops the state space model of centralized haptic cooperation with passive multirate wave communications using the lifting approach in [29]. Thereafter, it derives the stability region of haptic cooperation between two clients based on the eigenvalue analysis of the closed-loop state transition matrix. The analysis predicts two important advantages of passive multirate wave variables control over traditional multirate control of centralized haptic cooperation: (i) it enables users to manipulate much stiffer virtual objects together and hence, it increases the realism of haptic cooperation in centralized rigid virtual environments; and (ii) it renders a maximum stiffness of the virtual environment that is unaffected by the network delay. Hence, the stability analysis suggests that passive multirate wave variables communications have benefits for multirate haptic cooperation similar to their benefits for haptic manipulation of slowly updated virtual environments [24]. Controlled experiments as well as experimental manipulations of a centralized virtual cube by two cooperating clients validate the analytical predictions. Initial controlled experimental results have been presented in [30].

The paper introduces the centralized passive multirate wave variables control architecture for haptic cooperation among multiple clients in Section 2. In Section 3, it develops the multirate state-space model of centralized haptic cooperation with passive multirate wave variables control. In Section 4, it contrasts the stability of passive wave variables control to the stability of non-passive wave variables control and to the stability of traditional control for haptic cooperation between two clients connected to the server across a LAN or a high-speed MAN. In Section 5, it supports the analytical results through controlled experiments and through experimental manipulations of a centralized virtual cube by two client users. The paper ends with conclusions and directions for future work.

2 CENTRALIZED HAPTIC COOPERATION with PASSIVE MULTI-RATE WAVE VARIABLES

Figure 1 shows the centralized control architecture investigated in this paper. For clarity of presentation, only the connection between client i and the centralized virtual object is detailed in this figure. As depicted in Figure 1, the cooperating users connect to the centralized virtual environment as remote clients, via wave variables [25, 26] controllers. For realistic force interactions within rigid virtual environments, the clients' force control loops need to run at a frequency of about 1 KHz. However, Ethernet-based LAN and high-speed MAN networks currently offer packet update rates of the order of 125 Hz [17]. Running the local force control loops at the required high haptic update rate in the presence of a lower packet update rate makes the haptic cooperation system in Figure 1 a system with two rates[1]: (i) the fast rate of the clients' force feedback loops, with sampling interval T_c, this rate depends on the haptic device specifications which for most commercial haptic devices is equal to 1 KHz and can be considered as the available feedback force bandwidth.; (ii) and the slow rate of network updates, with sampling interval T_n. A third rate may be present in centralized haptic cooperation when the sampling interval of the virtual environment T_{VE} is different from the sampling interval both of the force control loops and of the network updates. In this work, the virtual environment sampling interval is considered equal to the network sampling interval,

[1] Haptic cooperation over a network with constant packet loss and Hold-Last-Sample implementation [31] can also be modeled as a system with two rates.

$T_{VE} = T_n$, and centralized haptic cooperation is modeled as a system with two rates. However, the analysis can be extended to allow for $T_{VE} \neq T_n$. In Figure 1, the transition between the fast sampling interval of the force control loop at client i and the slow network packet update rate is modeled through the downsampler M↓ and upsampler M↑ placed in the communications. LP is a low-pass wave filter with output y_{fi} and cutoff frequency f_c less than the network packet update rate. The low-pass wave filter eliminates aliasing due to downsampling and, thus, ensures the passivity of the multirate wave transformation [24].

The remaining notation is used as follows: m_{HDi}, b_{HDi}, x_{HDi}, and $\dot{x}_{\mathrm{HDi}}$ are the mass, damping, position and velocity of the haptic device of client i; f_{hi} is the force applied by client i to their haptic interface; f_{i} is the force feedback applied by the haptic interface to client i; x_{si}, and $\dot{x}_{\mathrm{si}}$ are the position and velocity of the avatar of client i in the centralized virtual environment; m_{O}, b_{O}, x_{O}, and $\dot{x}_{\mathrm{O}}$ are the mass, damping, position and velocity of the centralized virtual object cooperatively manipulated by the p clients; K_{i}, B_{i} and f_{si} are the stiffness, damping, and the interaction force at the contact between the virtual object and the client i's avatar in the centralized virtual environment; b is the wave impedance; u_{ci} and u_{si} are the wave signals sent by client i to the server and received by the server from client i, respectively; v_{si} and v_{ci} are the wave signals sent by the server to client i and received by client i from the server, respectively; T_{d} is the communication delay.

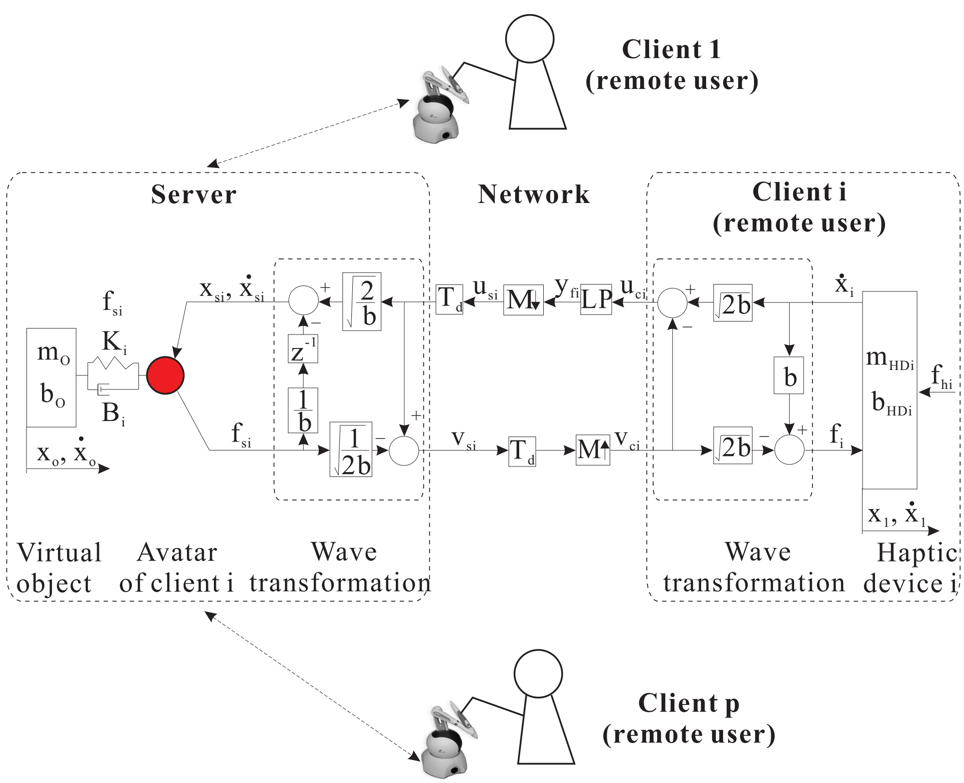

Figure 1: Centralized passive multirate wave variables control of haptic cooperation among p remote clients. Only the connection between client i and the centralized virtual object is presented in detail.

The dynamics of the haptic cooperation system in Figure 1 comprise the dynamics of the p client haptic devices and those of the centralized virtual object:

$$\begin{array}{rcl} m_{\text{HDi}}\ddot{x}_{\text{i}} + b_{\text{HDi}}\dot{x}_{\text{i}} & = & f_{\text{hi}} - f_{\text{i}}, \quad i = 1, \ldots, p \\ m_{\text{O}}\ddot{x}_{\text{O}} + b_{\text{O}}\dot{x}_{\text{O}} & = & \sum_{i=1}^{p} f_{\text{si}} \end{array} . \tag{1}$$

In Equation (1):

- $\ddot{x}_{\text{i}}$ and $\ddot{x}_{\text{O}}$ are the accelerations of the client i's haptic device and of the centralized virtual object, respectively;

- the force feedback to client i, f_{i}, is decoded at the client's site from the wave signal v_{ci}:

$$f_{\text{i}} = b\dot{x}_{\text{i}} - \sqrt{2b}v_{\text{ci}} = f_{\text{bi}} - \sqrt{2b}v_{\text{ci}}, \tag{2}$$

  where $f_{\text{bi}} = b\dot{x}_{\text{i}}$ is calculated at the fast rate of the force control loop, and $-\sqrt{2b}v_{\text{ci}}$ is computed at the slow rate of packet updates;

- the interaction force between the avatar of client i and the virtual object is computed on the server via:

$$f_{\text{si}} = K_{\text{i}}(x_{\text{si}} - x_{\text{O}}) + B_{\text{i}}(\dot{x}_{\text{si}} - \dot{x}_{\text{O}}) \tag{3}$$

  after decoding the velocity command $\dot{x}_{\text{si}}$ from the wave signal u_{si}:

$$\dot{x}_{\text{si}} = \sqrt{\frac{2}{b}}u_{\text{si}} + \frac{-f_{\text{si}}(t - T_n)}{b}, \tag{4}$$

  and integrating it in discrete time to obtain the position command x_{si}. Note in Equation (4) and in Figure 1 that a delay equal to the network update interval T_n has been inserted in the path from f_{si} to $\dot{x}_{\text{si}}$ at the server to avoid the algebraic loop typical when decoding velocity from wave signals.

The wave variables transmitted between client i and the server are given by [32]:

$$\begin{array}{rcl} u_{\text{ci}} & = & \sqrt{2b}\dot{x}_{\text{i}} - v_{\text{ci}} \\ v_{\text{si}} & = & u_{\text{si}} - \sqrt{\frac{2}{b}}f_{\text{si}} \end{array} , \tag{5}$$

and the following relations hold between the wave variables at the server and at client i at time t:

$$\begin{array}{l} u_{\text{si}}(t) = u_{\text{ci}}(t - T_d)(M \downarrow) \\ v_{\text{ci}}(t) = v_{\text{si}}(t - T_d)(M \uparrow) \end{array} . \tag{6}$$

The discrete time implementation of the controller, virtual environment, and communications make the system in Equation (1) a sampled-data system. The limitation of the communication ports make it a system with two rates: the (fast) rate of the force control loops at the clients, with sampling interval $T_c = 0.001$ s; and the (slow) rate of network packet updates, with sampling interval $T_n = 0.008$ s. Its stability is investigated in the following section using the multirate state-space approach introduced in [29] and applied to haptic cooperation between networked users exchanging position and force data in [17].

3 MULTIRATE STATE-SPACE MODEL of CENTRALIZED HAPTIC COOPERATION with PASSIVE MULTIRATE WAVE VARIABLES CONTROL

The multirate state-space approach [29] uses a lifting technique to derive the state matrix of a closed loop multirate system starting from the state-space continuous time open loop dynamics. Thereafter, it investigates stability by determining the control parameters for which all eigenvalues of the closed loop state matrix have magnitude less than unity. For centralized haptic cooperation, the open loop dynamics comprise the dynamics of the clients, haptic devices and centralized virtual object in Equation (1). The details of how the lifting technique [29] is used to derive the multirate state-space model of haptic cooperation inclusive of computational and network delay can be found in [17]. In this section, its application to centralized haptic cooperation is detailed only in as much as needed to incorporate the passive multirate wave variables communications.

3.1 Continuous time state-space open loop dynamics

The approach [29] distinguishes the system inputs and outputs based on the rate at which they are updated. For centralized haptic cooperation among p clients, Equations (1) to (3), the distinction leads to the state-space dynamics:

$$\begin{aligned}
\dot{\mathbf{x}}_{n_0\times 1}(t) &= \mathbf{A}_{n_0\times n_0}\cdot\mathbf{x}_{n_0\times 1}(t)+\begin{bmatrix}\mathbf{B}_{c_{n_0\times ncu}} & \mathbf{B}_{n_{n_0\times nnu}}\end{bmatrix}\cdot\begin{pmatrix}\mathbf{u}_{c_{ncu\times 1}}(t)\\ \mathbf{u}_{n_{nnu\times 1}}(t)\end{pmatrix}\\
\begin{pmatrix}\mathbf{y}_{c_{ncy\times 1}}(t)\\ \mathbf{y}_{n_{ny\times 1}}(t)\end{pmatrix} &= \begin{bmatrix}\mathbf{C}_{c_{ncy\times n_0}}\\ \mathbf{C}_{n_{ny\times n_0}}\end{bmatrix}\cdot\mathbf{x}_{n_0\times 1}(t)
\end{aligned} \tag{7}$$

where: indices c and n are used to denote signals sampled at the control and network intervals, T_c and T_n, respectively; the state $\mathbf{x}_{n_0\times 1}=\mathbf{x}_{(2p+2)\times 1}=\begin{pmatrix}x_1 & \dot{x}_1 & \cdots & x_{\mathrm{p}} & \dot{x}_{\mathrm{p}} & x_{\mathrm{O}} & \dot{x}_{\mathrm{O}}\end{pmatrix}^T$ includes the positions and velocities of the haptic devices and centralized virtual object; the fast inputs (sampled at the control interval T_c) are $\mathbf{u}_{c_{ncu\times 1}}=\mathbf{u}_{c_{p\times 1}}=\begin{pmatrix}f_{\mathrm{b}1} & \cdots & f_{\mathrm{bp}}\end{pmatrix}^T$; the slow inputs (sampled at the network interval T_n) are $\mathbf{u}_{n_{nnu\times 1}}=\mathbf{u}_{n_{2p\times 1}}=\begin{pmatrix}v_{\mathrm{c}1} & \cdots & v_{\mathrm{cp}} & f_{\mathrm{s}1} & \cdots & f_{\mathrm{sp}}\end{pmatrix}^T$; the fast outputs are $\mathbf{y}_{c_{ncy\times 1}}=\mathbf{y}_{c_{(2p+2)\times 1}}=\begin{pmatrix}x_1 & \dot{x}_1 & \cdots & x_{\mathrm{p}} & \dot{x}_{\mathrm{p}} & x_{\mathrm{O}} & \dot{x}_{\mathrm{O}}\end{pmatrix}^T$; the slow outputs are $\mathbf{y}_{n_{ny\times 1}}=\mathbf{y}_{n_{(2p+2)\times 1}}=\begin{pmatrix}x_1 & \dot{x}_1 & \cdots & x_{\mathrm{p}} & \dot{x}_{\mathrm{p}} & x_{\mathrm{O}} & \dot{x}_{\mathrm{O}}\end{pmatrix}^T$; and the system matrices are given in the Section 6. For cooperation between two clients, as considered in the stability analysis and in the experiments, $p=2$, $n_0=6$, $n_{cu}=2$, $n_{nu}=4$, $n_{cy}=6$, and $n_{ny}=6$. Since asymptotic stability of the closed loop is investigated in this work, exogenous hand inputs are ignored in the analysis.

3.2 Multirate state-space open loop dynamics

Assuming that the control T_c and network T_n sampling intervals are synchronized and commensurate, it follows that they obey $T_c=l_c\tau_0=T_0/N_c$ and $T_n=l_n\tau_0=T_0/N_n$, where l_c and l_n are positive integers whose largest common measure is one, whereas N_c and N_n are positive integers with largest common measure one and least common multiple N_0. Specifically, $T_c = 0.001$ s and $T_n = 0.008$ s in this paper, and thus $\tau_0 = 0.001$ s, $T_0 = 0.008$ s, $l_c = 1$, $l_n = 8$, $N_c = 8$, $N_n = 1$, and $N_0 = 8$. Then, the discrete time realization of the open loop system in Equation (7) can be written in the form [29]:

$$\begin{aligned} \mathbf{x}_{\mathrm{D}}[k+1] &= \mathbf{A}_{\mathrm{D}}\,\mathbf{x}_{\mathrm{D}}[k] + \mathbf{B}_{\mathrm{D}}\,\mathbf{u}_{\mathrm{D}}[k] \\ \mathbf{y}_{\mathrm{D}}[k] &= \mathbf{C}_{\mathrm{D}}\,\mathbf{x}_{\mathrm{D}}[k] + \mathbf{D}_{\mathrm{D}}\,\mathbf{u}_{\mathrm{D}}[k] \end{aligned}, \tag{8}$$

where the discrete state comprises the continuous time states sampled at τ_0 intervals:

$$\mathbf{x}_{\mathrm{D}_{N_0 \cdot n_0}}[k] = \begin{pmatrix} \mathbf{x}_{n_0}\left((k-1)T_0 + \tau_0\right) \\ \mathbf{x}_{n_0}\left((k-1)T_0 + 2\tau_0\right) \\ \vdots \\ \mathbf{x}_{n_0}\left(kT_0\right) \end{pmatrix}, \tag{9}$$

the input vector $\mathbf{u}_{\mathrm{D}}[k] = \left(\mathbf{u}_{\mathrm{D}_c}[k]^T \quad \mathbf{u}_{\mathrm{D}_n}[k]^T\right)^T$ includes the fast inputs:

$$\mathbf{u}_{\mathrm{D}_{c_{N_c \cdot ncu}}}[k] = \begin{pmatrix} \mathbf{u}_{c_{ncu}}\left(kT_0 + T_c\right) \\ \vdots \\ \mathbf{u}_{c_{ncu}}\left(kT_0 + (N_c - 1)T_c\right) \end{pmatrix} \tag{10}$$

and the slow inputs:

$$\mathbf{u}_{\mathrm{D}_{n_{N_n \cdot nnu}}}[k] = \begin{pmatrix} \mathbf{u}_{n_{nnu}}\left(kT_0 + T_n\right) \\ \vdots \\ \mathbf{u}_{n_{nnu}}\left(kT_0 + (N_n - 1)T_n\right) \end{pmatrix}, \tag{11}$$

the output vector $\mathbf{y}_{\mathrm{D}}[k] = \left(\mathbf{y}_{\mathrm{D}_c}[k]^T \quad \mathbf{y}_{\mathrm{D}_n}[k]^T\right)^T$ includes the fast outputs:

$$\mathbf{y}_{\mathrm{D}_{c_{N_c \cdot ncy}}}[k] = \begin{pmatrix} \mathbf{y}_{c_{ncy}}\left(kT_0\right) \\ \vdots \\ \mathbf{y}_{c_{ncy}}\left(kT_0 + (N_c - 1)T_c\right) \end{pmatrix} \tag{12}$$

and the slow outputs:

$$\mathbf{y}_{\mathrm{D}_{n_{N_n \cdot nny}}}[k] = \begin{pmatrix} \mathbf{y}_{n_{nny}}\left(kT_0\right) \\ \vdots \\ \mathbf{y}_{n_{nny}}\left(kT_0 + (N_n - 1)T_n\right)() \end{pmatrix} \tag{13}$$

and the matrices $\mathbf{A}_{\mathrm{D}}$, $\mathbf{B}_{\mathrm{D}}$, $\mathbf{C}_{\mathrm{D}}$, and $\mathbf{D}_{\mathrm{D}}$ are computed starting from the continuous time system matrices as described in detail in [29] and [17].

3.3 Multirate state-space open loop dynamics with passive wave transformations

Centralized haptic cooperation with passive wave variables control requires the server to decode velocity commands from wave signals. As shown in Equation (4) and Figure 1, the decoding uses the delayed force $f_{\mathrm{si}}(t - T_{VE})$, in this work is set to be equal to network rate $T_{VE} = T_n$. Because time delays can be incorporated into discrete time dynamics without difficulty, the passive wave transformations are included directly in the multirate realization of the open loop dynamics of haptic cooperation in this work. The integration is performed through adding the dynamics of the users' avatars and the dynamics of the low-pass wave filters.

For client i, the dynamics of their avatar are:

$$\begin{aligned} \dot{x}_{\text{si}}(k+1) &= \frac{K_{\text{i}}\left(x_{\text{si}}(k)-x_{\text{O}}(k)\right)+B_{\text{i}}\left(\dot{x}_{\text{si}}(k)-\dot{x}_{\text{O}}(k)\right)}{b}+\sqrt{\frac{2}{b}}u_{si}(k) \\ x_{\text{si}}(k+1) &= T_{\text{n}}\dot{x}_{\text{si}}(k)+x_{\text{si}}(k), \end{aligned} \tag{14}$$

whereas the dynamics of their anti-aliasing filter are:

$$\begin{aligned} \dot{x}_{\text{fi}} &= -f_c x_{\text{fi}}+u_{\text{ci}} \\ y_{\text{fi}} &= f_c x_{\text{fi}} \end{aligned} . \tag{15}$$

The dynamics in Equations (14) and (15) are incorporated into the multirate open loop haptic cooperation through augmenting:

- the discrete state with the discrete time vectors of avatar states $\mathbf{x}_{\text{Ds}}$ and of filter states $\mathbf{x}_{\text{Df}}$:

$$\mathbf{x}_{\text{Dw}}[k]=\begin{pmatrix} \mathbf{x}_{\text{D}_{N_0 n_0\times 1}}[k] \\ \mathbf{x}_{\text{Ds}_{N_n 2p\times 1}}[k] \\ \mathbf{x}_{\text{Df}_{N_c p\times 1}}[k] \end{pmatrix}, \tag{16}$$

- the discrete input with the discrete time vectors of incoming waves at the server $\mathbf{u}_{\text{Ds}}$ and of filter inputs $\mathbf{u}_{\text{Df}}$:

$$\mathbf{u}_{\text{Dw}}[k]=\begin{pmatrix} \mathbf{u}_{\text{D}_{(N_c n_{cu}+N_n n_{nu})\times 1}}[k] \\ \mathbf{u}_{\text{Ds}_{N_n p\times 1}}[k] \\ \mathbf{u}_{\text{Df}_{N_c p\times 1}}[k] \end{pmatrix}, \tag{17}$$

- and the discrete output with the discrete time vectors of wave signals sent by the clients $\mathbf{u}_{\text{Dc}}$, of wave signals sent by the server $\mathbf{v}_{\text{Ds}}$, of interaction forces between the centralized virtual object and the avatars $\mathbf{f}_{\text{Ds}}$, and of filter outputs $\mathbf{y}_{\text{Df}}$:

$$\mathbf{y}_{\text{Dw}}[k]=\begin{pmatrix} \mathbf{y}_{\text{D}_{(N_c n_{cy}+N_n n_{ny})\times 1}}[k] \\ \mathbf{u}_{\text{Dc}_{N_c p\times 1}}[k] \\ \mathbf{v}_{\text{Ds}_{N_n p\times 1}}[k] \\ \mathbf{f}_{\text{Ds}_{N_n p\times 1}}[k] \\ \mathbf{y}_{\text{Df}_{N_n p\times 1}}[k] \end{pmatrix}. \tag{18}$$

In Equations (16) to (18), the discrete time state, input and output vectors which represent the dynamics of the wave transformations and the anti-aliasing filters are obtained through sampling, at their respective sampling interval, the continuous time vectors of avatar states $\mathbf{x}_{\text{s}_{2p\times 1}}=\begin{pmatrix} x_{\text{s1}} & \dot{x}_{\text{s1}} & \cdots & x_{\text{sp}} & \dot{x}_{\text{sp}} \end{pmatrix}^T$, of filter states $\mathbf{x}_{\text{f}_{p\times 1}}=\begin{pmatrix} x_{\text{f1}} & \cdots & x_{\text{fp}} \end{pmatrix}^T$, of incoming waves at the server $\mathbf{u}_{\text{s}_{p\times 1}}=\begin{pmatrix} u_{\text{s1}} & \cdots & u_{\text{sp}} \end{pmatrix}^T$, of filter inputs $\mathbf{u}_{\text{f}_{p\times 1}}=$

$\begin{pmatrix} u_{c1} & \cdots & u_{cp} \end{pmatrix}^T$, of waves sent by clients $\mathbf{u}_{c_{p\times 1}} = \begin{pmatrix} u_{c1} & \cdots & u_{cp} \end{pmatrix}^T$, of waves sent by the server $\mathbf{v}_{s_{p\times 1}} = \begin{pmatrix} v_{s1} & \cdots & v_{sp} \end{pmatrix}^T$, of interaction forces between the centralized virtual object and the avatars $\mathbf{f}_{s_{p\times 1}} = \begin{pmatrix} f_{s1} & \cdots & f_{sp} \end{pmatrix}^T$, and of filter outputs $\mathbf{y}_{f_{p\times 1}} = \begin{pmatrix} y_{f1} & \cdots & y_{fp} \end{pmatrix}^T$.

Then, the multirate open loop dynamics of centralized haptic cooperation between two users with passive wave communications become:

$$\begin{aligned} \mathbf{x}_{Dw}[k+1] &= \mathbf{A}_{Dw}\,\mathbf{x}_{Dw}[k] + \mathbf{B}_{Dw}\,\mathbf{u}_{Dw}[k] \\ \mathbf{y}_{Dw}[k] &= \mathbf{C}_{Dw}\,\mathbf{x}_{Dw}[k] + \mathbf{D}_{Dw}\,\mathbf{u}_{Dw}[k] \end{aligned}, \tag{19}$$

where the system matrices $\mathbf{A}_{Dw}$, $\mathbf{B}_{Dw}$, $\mathbf{C}_{Dw}$, and $\mathbf{D}_{Dw}$ are given in Section 6. The computational delays at the clients and the server, and the network delays, are incorporated into the multirate model by augmenting the input vector with the delayed input signals, as proposed in [17]. The new system matrices $\tilde{\mathbf{A}}_{Dw}$, $\tilde{\mathbf{B}}_{Dw}$, $\tilde{\mathbf{C}}_{Dw}$, and $\tilde{\mathbf{D}}_{Dw}$ are used in the stability analysis after the outputs are connected to the inputs through the feedback law:

$$\mathbf{u}_{Dw}[k] = \mathbf{F}_{Dw}\,\mathbf{y}_{Dw}[k], \tag{20}$$

where the feedback gain matrix $\mathbf{F}_{Dw}$, given in Section 6, is computed as in [29], and depends on the wave impedance.

Lastly, the state transition matrix for the multirate closed loop system $\mathbf{A}^{cl}_{Dw}$ is determined via:

$$\mathbf{A}^{cl}_{Dw} = \tilde{\mathbf{A}}_{Dw} + \tilde{\mathbf{B}}_{Dw}\,\mathbf{F}_{Dw}\left(\mathbf{I} - \tilde{\mathbf{D}}_{Dw}\,\mathbf{F}_{Dw}\right)^{-1}\tilde{\mathbf{C}}_{Dw} \tag{21}$$

and the parameter pairs (K_1, K_2) for which all its eigenvalues have magnitude smaller than unity are determined. The K_1 and K_2 parameters represent the stiffness of contact between the centralized virtual object and the users' avatars for which passive multirate wave variables control maintains the haptic cooperation stable.

4 STABILITY REGION of CENTRALIZED HAPTIC COOPERATION with PASSIVE MULTIRATE WAVE VARIABLES CONTROL

Because LANs and high-speed MANs are characterized by communication delays which are a small integer (up to four) multiple of the network packet update interval T_n and jitter and packet loss are neglegible [17], the stability region of passive multirate wave variables control of haptic cooperation between two users interacting across such a network is derived for constant delays $T_d = 0, \ldots, 3T_n$ in this section. Furthermore, the delays are assumed equal in all paths, i.e., from both clients to the server and from the server to both clients; the wave impedance is $b = 25$ Ns/m; the contacts between the virtual object and the clients' avatars have damping $B_i =$ 10 Ns/m; the haptic devices have mass $m_{HDi} = 0.25$ kg and negligible damping, $b_{HDi} = 0$ Ns/m; the cooperatively manipulated virtual object has $m_O = 2$ kg and no damping, $b_O = 0$ Ns/m; the network packet update interval is $T_n = 0.008$ s; the sampling interval of the clients' force control loops is $T_c = 0.001$ s; and two anti-aliasing wave filters, with cutoff frequencies $f_{c1} = 50$ Hz and $f_{c2} = 100$ Hz, are selected to ensure passivity of the multirate wave transformation [24].

Figure 2 illustrates the stability region, colored area, for centralized passive multirate wave variables control of haptic cooperation for both wave filters and for network delays of up to three network packet update intervals. Note in this figure that: (i) the network delay has little impact on the maximum stiffness of the manipulated virtual object; and (ii) users can cooperate in stiffer virtual environments when the cutoff frequency of the anti-aliasing wave filters is $f_{c1} = 50$ Hz than when it is $f_{c2} = 100$ Hz. This is because the wave filters are non-ideal, first order low-pass filters. Hence, they totaly eliminate frequencies above the network update rate $\frac{1}{T_n} = 125$ Hz and, thus, ensure passivity of the multirate wave communications [24], only when their cutoff frequency is sufficiently lower than the network rate, $f_c < \frac{1}{T_n}$.

The stability region for centralized multirate direct coupling control [17] of the same cooperative manipulation is plotted in Figure 3, colored area. A comparison between Figure 2 and Figure 3 suggests two advantages of passive multirate wave variables control over direct coupling control: it maintains the haptic cooperation stable in centralized virtual environments that are much stiffer and whose maximum stiffness is largely unaffected by the network delay.

5 EXPERIMENTS

This section validates the stability analysis in Section 4: (i) through controlled experiments; and (ii) through experiments with human users. In all experiments, two Phantom Omni haptic devices are connected to two client personal computers (PCs) running Windows Vista on Intel Core 2 Duo CPU at 2.67GHz with 2 GB RAM. The client PCs communicate via the UDP protocol to the server PC, also running Windows Vista on Intel Core 2 Duo CPUs at 2.67GHz with 2 GB RAM. The one degree of freedom virtual environment runs as a C++ console application on the server PC. The network environment is simulated via the Wide Area Network Emulator (WANem) [33] on a fourth PC running Linux. As depicted in Figure 4, the virtual environment contains a virtual cube having mass $m_O = 2$ kg and moving along the x-axis, and the avatars of the two cooperating clients. The update intervals of the network and of the virtual environment are $T_n = 0.008$ s, and the sampling interval of the client force control loops is $T_c = 0.001$ s. The wave impedance is $b = 25$ Ns/m, and the stiffness and damping of the virtual contacts are $K_1 = K_2 = 500$ N/m and $B_1 = B_2 = 10$ Ns/m, respectively. The multirate wave transformations are rendered passive through anti-aliasing wave filters with cutoff frequency $f_c = 50$ Hz. The force feedback to the clients is turned off when the avatars are not in contact with the virtual cube.

In the controlled experiments, the client users are replaced by forces equal to 1 N applied to the device handles through motor commands. The controlled forces ensure the initial conditions and the "same user" during successive cooperative manipulations. Because the haptic devices are impedance-type interfaces and the controlled forces eliminate the adaptive human damping from the control loop, the controlled experiments represent a worst case for stability of haptic cooperation system. Figure 5 plots the experimental results obtained during the controlled cooperative haptic manipulation of the virtual cube under centralized passive multirate wave variables control with various network delays. In Figure 5, x_1 and x_2 are the positions of the haptic interfaces, x_{s1} and x_{s2} are the position commands in the centralized virtual environment, f_{s1} and f_{s2}, are the interaction forces between the virtual cube and the users' avatars, and f_1 and f_2 are the forces fed back to the two clients. The results in

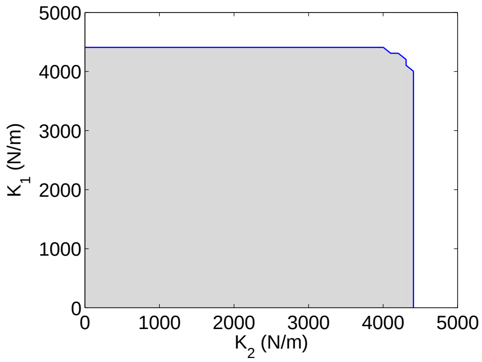

(a) $T_d = 0$, $f_{c1} = 50$ Hz.

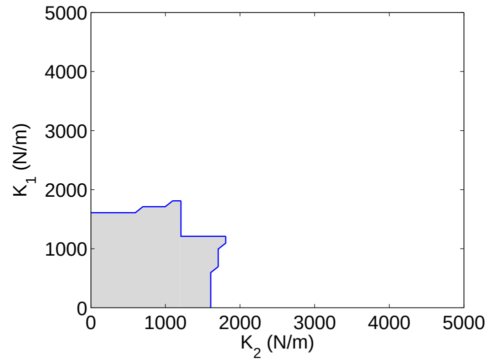

(b) $T_d = 0$, $f_{c2} = 100$ Hz.

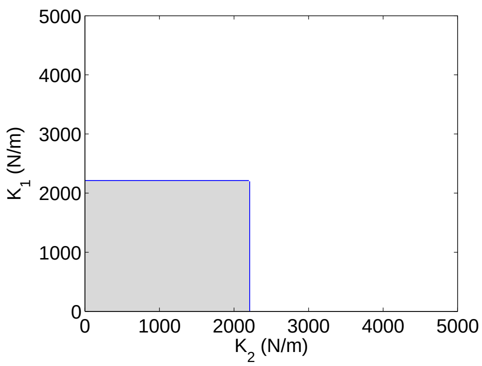

(c) $T_d = T_n$, $f_{c1} = 50$ Hz.

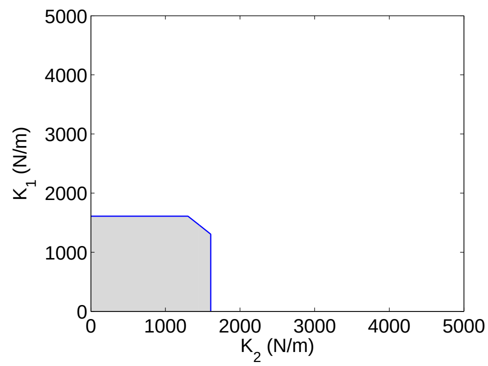

(d) $T_d = T_n$, $f_{c2} = 100$ Hz.

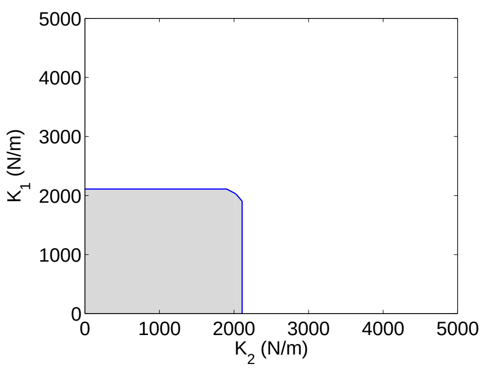

(e) $T_d = 2T_n$, $f_{c1} = 50$ Hz.

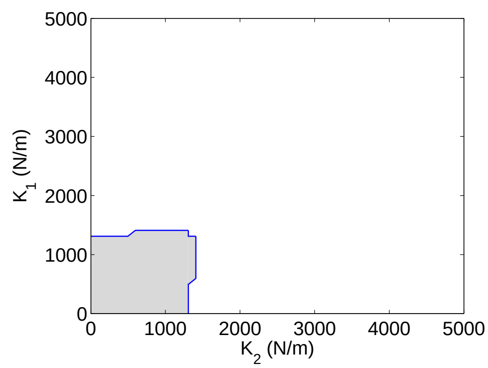

(f) $T_d = 2T_n$, $f_{c2} = 100$ Hz.

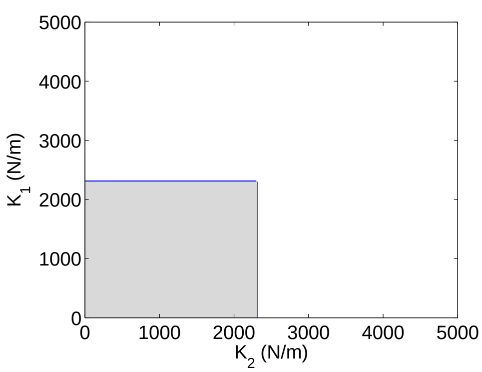

(g) $T_d = 3T_n$, $f_{c1} = 50$ Hz.

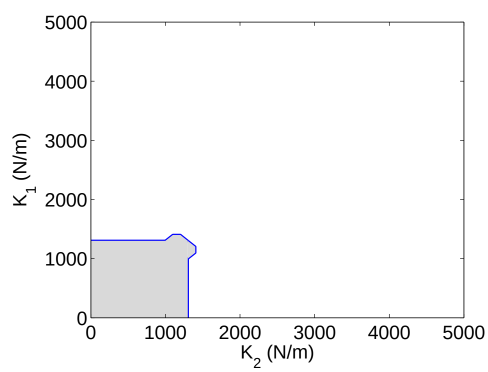

(h) $T_d = 3T_n$, $f_{c2} = 100$ Hz.

Figure 2: Stability region, colored area, for two-users haptic cooperation with centralized passive multirate wave

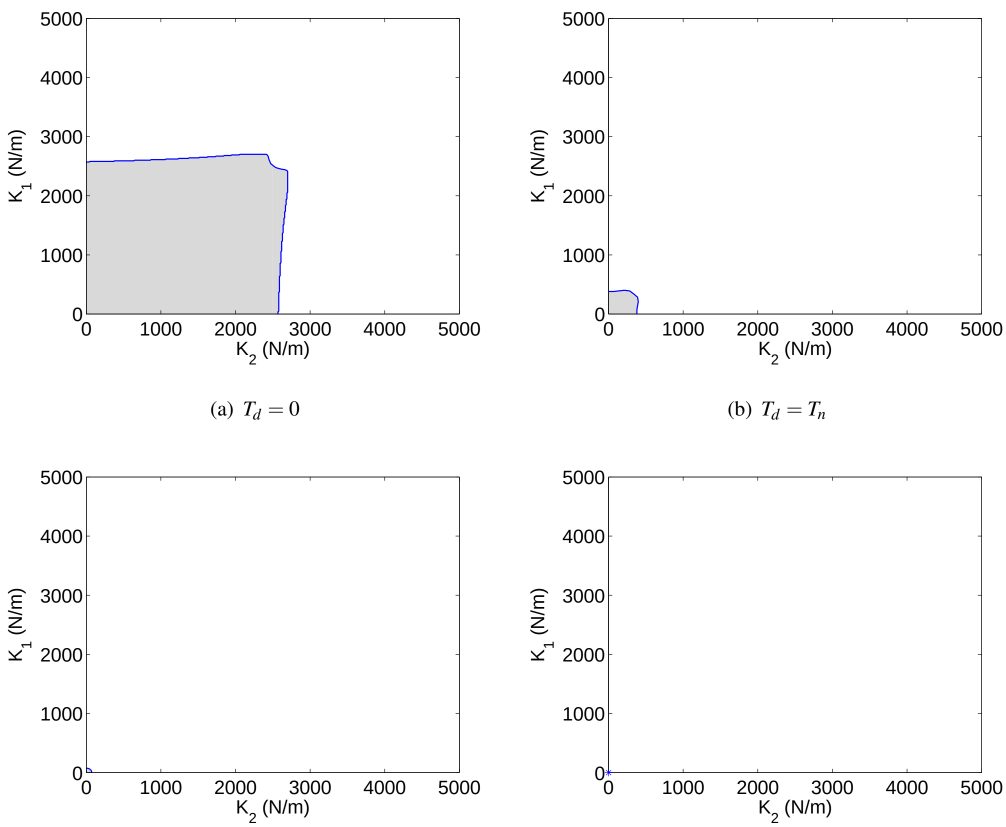

(a) $T_d = 0$

(b) $T_d = T_n$

(c) $T_d = 2T_n$

(d) $T_d = 3T_n$

Figure 3: Stability region, colored area, for two-users haptic cooperation with centralized multirate direct coupling control, for a network packet update interval $T_n = 0.008$ s and four network delays T_d.

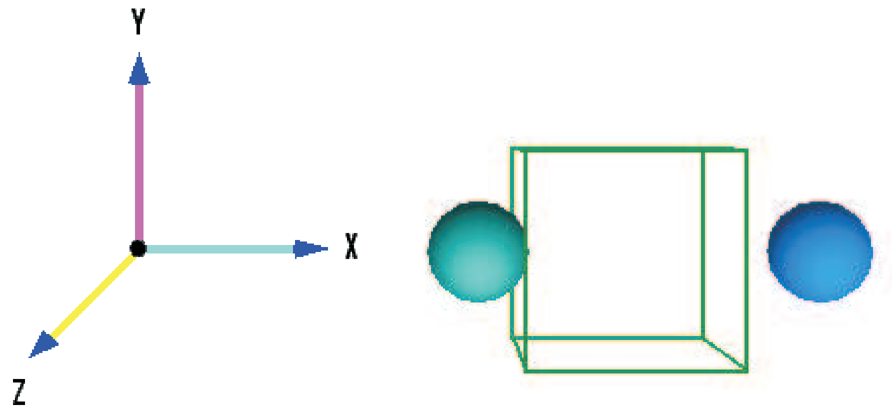

Figure 4: Centralized virtual environment used in the experiments. The two spheres are the avatars of the clients' haptic devices in the virtual environment.

Figure 5 validate that two clients coordinated using passive multirate wave variables control can manipulate in cooperation a centralized virtual cube whose maximum stiffness is unaffected by the network delay.

In the experiments with human users, the clients cooperatively manipulate and move the virtual cube in the virtual environment. To do so, in the first step of the experiments, the users are asked to grip the virtual cube and hold it cooperatively. In the second step they are asked to follow a trajectory which is indicated by a moving arrow in the graphical representation of the virtual environment. The experimental results are presented in Figure 6 for centralized haptic cooperation with passive multirate wave variables control and with various network delays. In Figure 6, solid black lines and dashed black lines demonstrate the center of the virtual cube and the trajectory path respectively, x_1 and x_2 are the positions of the haptic interfaces, x_{s1} and x_{s2} are the position commands in the centralized virtual environment, f_{s1} and f_{s2}, are the interaction forces between the virtual cube and the users' avatars, and f_1 and f_2 are the forces fed back to the two clients. The results in Figure 6 confirm that human users can move together a virtual cube as stiff as the virtual cube that can be cooperatively manipulated through controlled forces applied to the two client haptic devices.

The maximum stiffness of the virtual object for which centralized passive multirate variable control maintains the haptic cooperation stable is $K_{1max} = K_{2max} = 1200$ N/m for $T_d = 0$ ms, and is $K_{1max} = K_{2max} = 600$ N/m for network delays $T_d > 0$ ms. In contrast, the maximum stiffness for which multirate direct coupling control maintains the cooperation stable is $K_{1max} = K_{2max} = 700$ N/m for $T_d = 0$ ms, $K_{1max} = K_{2max} = 60$ N/m $T_d = 8$ ms and $K_{1max} = K_{2max} = 0$ N/m for $T_d = 16$ ms. The maximum virtual stiffness achievable in the experiments differs from the analytical predictions both for passive multirate wave variables control and for multirate direct coupling control. The difference is due to modeling uncertainties, sensor noise and quantization, actuator limitations, and the switching off of the force feedback to the clients when their avatars are not in contact with the virtual object, which all inject energy into the system [34]. Nonetheless, the ratio of the maximum stiffness achievable under passive multirate wave variables control to the maximum stiffness achievable under multirate direct coupling control matches the ratio predicted by the analysis in Section 4 for the respective network delays. Hence, the

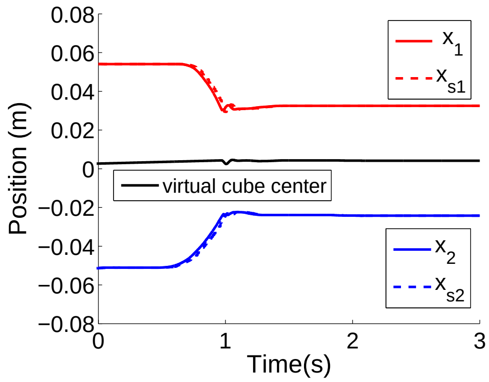

(a) Positions: of haptic devices (solid); of centralized avatars (dotted). $T_d = 0$ ms.

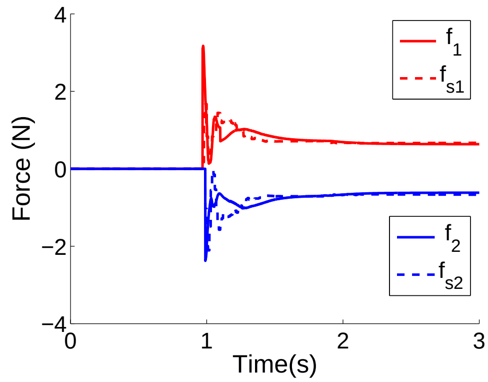

(b) Forces: on haptic devices (solid); on centralized avatars (dotted). $T_d = 0$ ms.

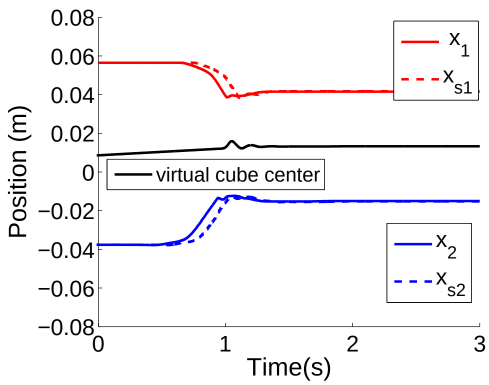

(c) Positions: of haptic devices (solid); of centralized avatars (dotted). $T_d = 16$ ms.

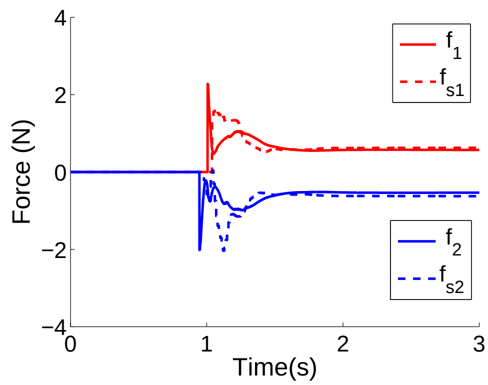

(d) Forces: on haptic devices (solid); on centralized avatars (dotted). $T_d = 16$ ms.

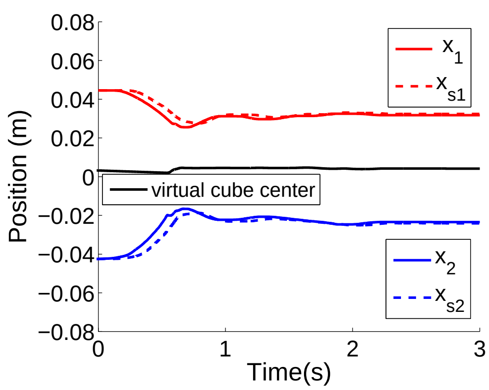

(e) Positions: of haptic devices (solid); of centralized avatars (dotted). $T_d = 24$ ms.

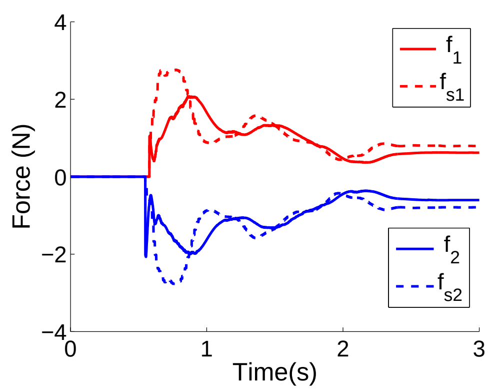

(f) Forces: on haptic devices (solid); on centralized avatars (dotted). $T_d = 24$ ms.

Figure 5: Controlled experiments: cooperative manipulation of a centralized virtual cube with stiffness $K = 500$ N/m, via passive multirate wave variables control with wave impedance $b = 25$ Ns/m, and for different network delays T_d.

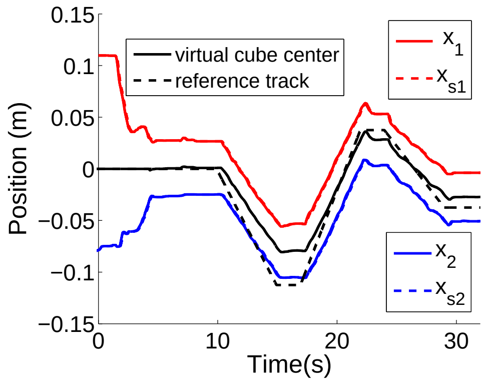

(a) Positions: of haptic devices (solid); of centralized avatars (dotted). $T_d = 0$ ms.

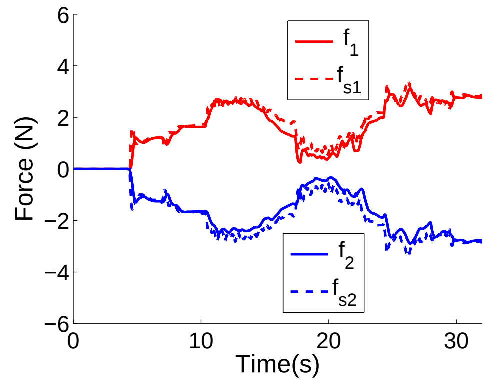

(b) Forces: on haptic devices (solid); on centralized avatars (dotted). $T_d = 0$ ms.

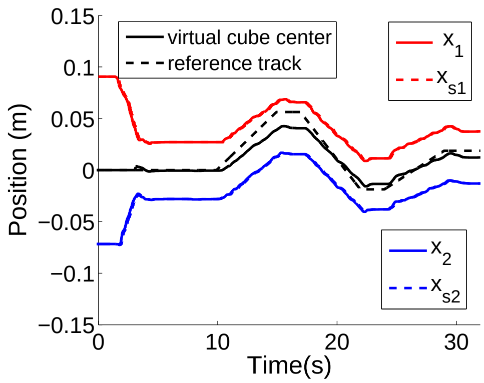

(c) Positions: of haptic devices (solid); of centralized avatars (dotted). $T_d = 16$ ms.

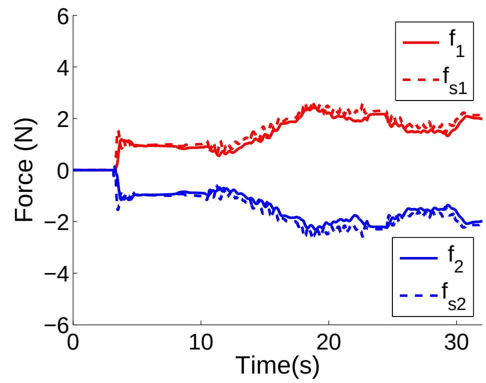

(d) Forces: on haptic devices (solid); on centralized avatars (dotted). $T_d = 16$ ms.

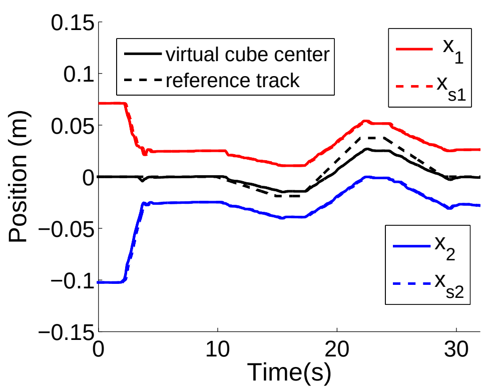

(e) Positions: of haptic devices (solid); of centralized avatars (dotted). $T_d = 24$ ms.

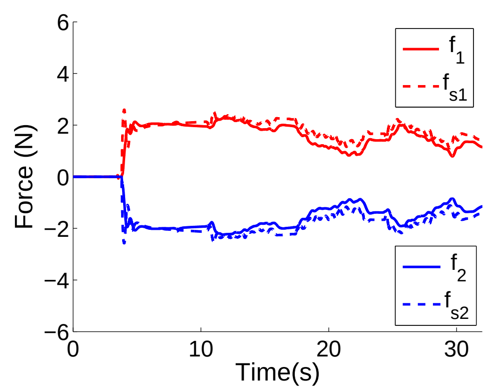

(f) Forces: on haptic devices (solid); on centralized avatars (dotted). $T_d = 24$ ms.

Figure 6: Experiments with human users: cooperative manipulation of a centralized virtual cube with stiffness $K = 500$ N/m, via passive multirate wave variables control with wave impedance $b = 25$ Ns/m, and for different network delays T_{d}. First, the users are asked to grasp and hold the virtual cube, i.e. the forces become non zero for the fisrt time. Then the users are asked to follow the trajectory, black dashed line.

experiments validate two important advantages of passive multirate wave variables control over traditional multirate control of centralized haptic cooperation: (i) it enables the users to manipulate much stiffer virtual objects together and thus, it increases the realism of haptic cooperation in centralized rigid virtual environments; and (ii) it renders a maximum stiffness of the virtual environment that is unaffected by the network delay. These results suggest that passive multirate wave variables control is suitable for providing realistic force feedback during haptic cooperation in centralized rigid virtual environments to which the client users connect across a LAN or a high-speed MAN.

In all experiments, it was investigated that using a zero order hold expander as the upsampler, Figure 1, leads to a noisy force feedback. This is expected because in this case according to Equation (2), the feedback force f_i is a linear combination of two signals with different update rates, i.e., velocity signal updated by control loop rate and incoming wave v_{ci} updated by network updated rate, and the jumps in v_{ci} signal, due to zero order hold expander, result in a noisy force feedback. To cope with this problem, in all experiments a delayed first order hold is used in the place of zero order hold expander. In Section B it is shown that using a delayed first order hold does not affect the passivity of the wave variable communication channel which guarantees the stability of the overall system.

6 CONCLUSIONS

This paper has been concerned with increasing the stiffness of centralized virtual environments in which haptic cooperation can be maintained stable across LANs and high-speed MANs. To this end, it has connected the users to the central server through passive multirate wave variables controllers, and has investigated centralized haptic cooperation with passive multirate wave variables communications both analytically and experimentally. For the stability analysis, the paper has developed the multirate state space model of centralized haptic cooperation with passive multirate wave variables control, and has employed eigenvalue analysis of the closed-loop state transition matrix of the multirate system realization. The analysis has predicted that, compared to traditional multirate control, passive multirate wave variables control has two important advantages: (i)it enables the clients to manipulate much stiffer virtual objects together and thus, it increases the realism of haptic cooperation in centralized rigid virtual environments; and (ii) it renders a maximum stiffness of the virtual environment that is unaffected by the network delay. Both controlled experiments and experiments with human users have been presented to validate the analytical predictions.

Future work will focus on maintaining the haptic cooperation stable in the presence of variable network delays and packet loss in order to permit remote client users to connect to a centralized virtual environment over the Internet.

APPENDIX A

A CONTINUOUS TIME STATE-SPACE MATRICES

For centralized haptic cooperation between two clients, the state-space matrices of the continuous time open loop system in Equation (7) are computed as follows:

$$\mathbf{A}_{n_0\times n_0} = \begin{bmatrix} 0 & 1 & \cdots & 0 & 0 & 0 & 0 \\ 0 & -b_{\mathrm{HD1}}/m_{\mathrm{HD1}} & \cdots & 0 & 0 & 0 & 0 \\ \vdots & & & & & & \\ 0 & 0 & \cdots & 0 & 1 & 0 & 0 \\ 0 & 0 & \cdots & 0 & -b_{\mathrm{HDp}}/m_{\mathrm{HDp}} & 0 & 0 \\ 0 & 0 & \cdots & 0 & 0 & 0 & 1 \\ 0 & 0 & \cdots & 0 & 0 & 0 & -b_{\mathrm{O}}/m_{\mathrm{O}} \end{bmatrix} \tag{22}$$

$$\mathbf{B}_{c_{n_0\times n_{cu}}} = \begin{bmatrix} 0 & \cdots & 0 \\ -1/m_{\mathrm{HD1}} & \cdots & 0 \\ \vdots & & \\ 0 & \cdots & 0 \\ 0 & \cdots & -1/m_{\mathrm{HDp}} \\ 0 & \cdots & 0 \\ 0 & \cdots & 0 \end{bmatrix} \tag{23}$$

$$\mathbf{B}_{n_{n_0\times n_{nu}}} = \begin{bmatrix} 0 & \cdots & 0 & 0 & 0 \\ \sqrt{2b}/m_{\mathrm{HD1}} & \cdots & 0 & 0 & 0 \\ \vdots & & & & \\ 0 & \cdots & 0 & 0 & 0 \\ 0 & \cdots & \sqrt{2b}/m_{\mathrm{HDp}} & 0 & 0 \\ 0 & \cdots & 0 & 0 & 0 \\ 0 & \cdots & 0 & 1/m_{\mathrm{O}} & 1/m_{\mathrm{O}} \end{bmatrix}. \tag{24}$$

The continuous time dynamics of the anti-aliasing wave filters in Equation (15) can be written in the form:

$$\begin{aligned} \dot{\mathbf{x}}_{\mathrm{f}} &= \mathbf{A}_{\mathrm{f}}\,\mathbf{x}_{\mathrm{f}} + \mathbf{B}_{\mathrm{f}}\,\mathbf{u}_{\mathrm{f}} \\ \mathbf{y}_{\mathrm{f}} &= \mathbf{C}_{\mathrm{f}}\,\mathbf{x}_{\mathrm{f}} \end{aligned}, \tag{25}$$

with $\mathbf{A}_{\mathrm{f}_{p\times p}} = -f_c\mathbf{I}_{p\times p}$, $\mathbf{B}_{\mathrm{f}_{p\times p}} = \mathbf{I}_{p\times p}$, $\mathbf{C}_{\mathrm{f}_{p\times p}} = f_c\mathbf{I}_{p\times p}$ and $\mathbf{I}_{p\times p}$ the $p\times p$ unity matrix.

B DISCRETE TIME STATE-SPACE MATRICES

The multirate state-space realization of the anti-aliasing wave filters can be written in the form:

$$\begin{aligned} \mathbf{x}_{\mathrm{Df}}[k+1] &= \mathbf{A}_{\mathrm{Df}}\,\mathbf{x}_{\mathrm{Df}}[k] + \mathbf{B}_{\mathrm{Df}}\,\mathbf{u}_{\mathrm{Df}}[k] \\ \mathbf{y}_{\mathrm{Df}}[k] &= \mathbf{C}_{\mathrm{Df}}\,\mathbf{x}_{\mathrm{Df}}[k] + \mathbf{D}_{\mathrm{Df}}\,\mathbf{u}_{\mathrm{Df}}[k] \end{aligned} \tag{26}$$

with the matrices $\mathbf{A}_{\mathrm{Df}}$, $\mathbf{B}_{\mathrm{Df}}$, $\mathbf{C}_{\mathrm{Df}}$, and $\mathbf{D}_{\mathrm{Df}}$ derived similarly to $\mathbf{A}_{\mathrm{D}}$, $\mathbf{B}_{\mathrm{D}}$, $\mathbf{C}_{\mathrm{D}}$, and $\mathbf{D}_{\mathrm{D}}$ in Equation (8), as described in detail in [29].

The multirate open loop matrices of haptic cooperation with passive wave variables communications are given in the following formulae, in which matrix dimensions have been omitted when they can be easily inferred for clarity of presentation. The state transition matrix is:

$$\mathbf{A}_{\mathrm{Dw}} = \begin{bmatrix} \mathbf{A}_{\mathrm{D}} & \mathbf{0} & \mathbf{0} \\ \mathbf{A}_{\mathrm{Ds}}\mathbf{C}_{\mathrm{D}} & \mathbf{A}_{\mathrm{s}} & \mathbf{0} \\ \mathbf{0} & \mathbf{0} & \mathbf{A}_{\mathrm{Df}} \end{bmatrix}, \tag{27}$$

with:

$$\mathbf{A}_{\mathrm{Ds}_{2p\times(N_c n_{cy}+N_n n_{ny})}} = \begin{bmatrix} 0 & 0 \\ \frac{1}{b}K_1 & \frac{1}{b}B_1 \\ \vdots & \\ 0 & 0 \\ \frac{1}{b}K_{\mathrm{p}} & \frac{1}{b}B_{\mathrm{p}} \end{bmatrix} \mathbf{S}_{\mathrm{VO}} \tag{28}$$

$$\mathbf{A}_{\mathrm{s}_{2p\times 2p}} = \begin{bmatrix} 1 & T_{\mathrm{n}} & \cdots & 0 & 0 \\ -\frac{1}{b}K_1 & -\frac{1}{b}B_1 & \cdots & 0 & 0 \\ \vdots & & & & \\ 0 & 0 & \cdots & 1 & T_{\mathrm{n}} \\ 0 & 0 & \cdots & -\frac{1}{b}K_{\mathrm{p}} & -\frac{1}{b}B_{\mathrm{p}} \end{bmatrix}, \tag{29}$$

and:

$$\mathbf{S}_{\mathrm{VO}_{2\times(N_c n_{cy}+N_n n_{ny})}} = \begin{bmatrix} \mathbf{0}_{2\times(N_c n_{cy}+N_n n_{ny}-2)} & \mathbf{I}_{2\times 2} \end{bmatrix} \tag{30}$$

selects the slowly updated states of the centralized virtual object.

The input matrix is:

$$\mathbf{B}_{\mathrm{Dw}} = \begin{bmatrix} \mathbf{B}_{\mathrm{D}} & \mathbf{0} & \mathbf{0} \\ \mathbf{A}_{\mathrm{Ds}}\mathbf{D}_{\mathrm{D}} & \mathbf{B}_{\mathrm{s}} & \mathbf{0} \\ \mathbf{0} & \mathbf{0} & \mathbf{B}_{\mathrm{Df}} \end{bmatrix}, \tag{31}$$

with:

$$\mathbf{B}_{\mathrm{s}_{2p\times p}} = \begin{bmatrix} 0 & \cdots & 0 \\ \sqrt{\frac{2}{b}} & \cdots & 0 \\ \vdots & & \\ 0 & \cdots & 0 \\ 0 & \cdots & \sqrt{\frac{2}{b}} \end{bmatrix}. \tag{32}$$

The output matrices are:

$$\mathbf{C}_{\mathrm{Dw}} = \begin{bmatrix} \mathbf{C}_{\mathrm{D}} & \mathbf{0} & \mathbf{0} \\ \sqrt{2b}\mathbf{C}_{\mathrm{u}}\mathbf{C}_{\mathrm{D}} & \mathbf{0} & \mathbf{0} \\ \sqrt{\frac{2}{b}}\mathbf{C}_{\mathrm{v}}\mathbf{C}_{\mathrm{D}} & -\sqrt{\frac{2}{b}}\mathbf{C}_{\mathrm{s}} & \mathbf{0} \\ -\mathbf{C}_{\mathrm{v}}\mathbf{C}_{\mathrm{D}} & \mathbf{C}_{\mathrm{s}} & \mathbf{0} \\ \mathbf{0} & \mathbf{0} & \mathbf{C}_{\mathrm{Df}} \end{bmatrix} \tag{33}$$

and:

$$\mathbf{D}_{\mathrm{Dw}} = \begin{bmatrix} \mathbf{D}_{\mathrm{D}} & \mathbf{0} & \mathbf{0} \\ \mathbf{D}_{\mathrm{u}} & \mathbf{0} & \mathbf{0} \\ \sqrt{\frac{2}{b}}\mathbf{C}_{\mathrm{v}}\mathbf{D}_{\mathrm{D}} & \mathbf{I} & \mathbf{0} \\ -\mathbf{C}_{\mathrm{v}}\mathbf{D}_{\mathrm{D}} & \mathbf{0} & \mathbf{0} \\ \mathbf{0} & \mathbf{0} & \mathbf{D}_{\mathrm{Df}} \end{bmatrix} \tag{34}$$

with:

$$\mathbf{C}_{\mathrm{u}_{pN_c\times(N_cn_{cy}+N_nn_{ny})}} = \begin{bmatrix} \mathbf{S}_{1_{1\times n_{cy}}} & \dots & \mathbf{0}_{1\times n_{cy}} & \mathbf{0}_{1\times n_{ny}} & \cdots \mathbf{0}_{1\times n_{ny}} \\ \vdots & & & & \\ \mathbf{0}_{1\times n_{cy}} & \dots & \mathbf{S}_{1_{1\times n_{cy}}} & \mathbf{0}_{1\times n_{ny}} & \cdots \mathbf{0}_{1\times n_{ny}} \\ \vdots & & & & \\ \mathbf{S}_{\mathrm{p}_{1\times n_{cy}}} & \dots & \mathbf{0}_{1\times n_{cy}} & \mathbf{0}_{1\times n_{ny}} & \cdots \mathbf{0}_{1\times n_{ny}} \\ \vdots & & & & \\ \mathbf{0}_{1\times n_{cy}} & \dots & \mathbf{S}_{\mathrm{p}_{1\times n_{cy}}} & \mathbf{0}_{1\times n_{ny}} & \cdots \mathbf{0}_{1\times n_{ny}} \end{bmatrix} \tag{35}$$

$$\mathbf{C}_{\mathrm{v}_{p\times(N_cn_{cy}+N_nn_{ny})}} = \begin{bmatrix} K_1 & B_1 \\ \vdots & \\ K_{\mathrm{p}} & B_{\mathrm{p}} \end{bmatrix} \mathbf{S}_{\mathrm{VO}} \tag{36}$$

$$\mathbf{C}_{\mathrm{s}_{p\times 2p}} = \begin{bmatrix} K_1 & B_1 & \cdots & 0 & 0 \\ \vdots & & & & \\ 0 & 0 & \cdots & K_{\mathrm{p}} & B_{\mathrm{p}} \end{bmatrix} \tag{37}$$

$$\mathbf{D}_{\mathrm{u}_{pN_c\times(pN_c+2pN_n)}} = \sqrt{2b}\mathbf{C}_{\mathrm{u}}\mathbf{D}_{\mathrm{D}} - \begin{bmatrix} \mathbf{0}_{N_c\times pNc} & \mathbf{1}_{N_c\times 1} & \cdots & \mathbf{0}_{N_c\times 1} & \mathbf{0}_{N_c\times pN_n} \\ \vdots & & & & \\ \mathbf{0}_{N_c\times pNc} & \mathbf{0}_{N_c\times 1} & \cdots & \mathbf{1}_{N_c\times 1} & \mathbf{0}_{N_c\times pN_n} \end{bmatrix} \tag{38}$$

and:

$$\mathbf{S}_{\mathrm{i}_{1\times n_{cy}}} = \begin{bmatrix} 0 & 0\cdots & 0 & 1 & \cdots & 0 & 0 \end{bmatrix} \tag{39}$$

has the $2i$-th element equal to one.i-th client from the $n_0 = 2p+2$ continuous time states of the p clients and the centralized virtual object).

Lastly, the feedback matrix $\mathbf{F}_{\mathrm{Dw}}$ is:

$$\mathbf{F}_{\mathrm{Dw}} = \begin{bmatrix} \mathbf{F}_{\mathrm{D}_{N_cp\times(N_cn_{cy}+N_nn_{ny})}} & \mathbf{0}_{N_cp\times N_cp} & \mathbf{0}_{N_cp\times N_np} & \mathbf{0}_{N_cp\times N_np} & \mathbf{0}_{N_cp\times N_np} \\ \mathbf{0}_{N_np\times(N_cn_{cy}+N_nn_{ny})} & \mathbf{0}_{N_np\times N_cp} & \mathbf{I}_{N_np\times N_np} & \mathbf{0}_{N_np\times N_np} & \mathbf{0}_{N_np\times N_np} \\ \mathbf{0}_{N_np\times(N_cn_{cy}+N_nn_{ny})} & \mathbf{0}_{N_np\times N_cp} & \mathbf{0}_{N_np\times N_np} & \mathbf{I}_{N_np\times N_np} & \mathbf{0}_{N_np\times N_np} \\ \mathbf{0}_{N_cp\times(N_cn_{cy}+N_nn_{ny})} & \mathbf{0}_{N_np\times N_cp} & \mathbf{0}_{N_np\times N_np} & \mathbf{0}_{N_np\times N_np} & \mathbf{I}_{N_np\times N_np} \\ \mathbf{0}_{N_cp\times(N_cn_{cy}+N_nn_{ny})} & \mathbf{I}_{N_cp\times N_cp} & \mathbf{0}_{N_cp\times N_np} & \mathbf{0}_{N_cp\times N_np} & \mathbf{0}_{N_cp\times N_np} \end{bmatrix} \tag{40}$$

with:

$$\mathbf{F}_{\mathrm{D}_{N_c p\times(N_c n_{cy}+N_n n_{ny})}} = b\begin{bmatrix} \mathbf{S}_{p\times n_{cy}} & \cdots & \mathbf{0}_{p\times n_{cy}} & \mathbf{0}_{p\times N_n n_{ny}} \\ \vdots & & & \\ \mathbf{0}_{p\times n_{cy}} & \cdots & \mathbf{S}_{p\times n_{cy}} & \mathbf{0}_{p\times N_n n_{ny}} \end{bmatrix} \tag{41}$$

and:

$$\mathbf{S}_{p\times n_{cy}} = \begin{bmatrix} \mathbf{S_1}_{1\times n_{cy}} \\ \vdots \\ \mathbf{S_p}_{1\times n_{cy}} \end{bmatrix}. \tag{42}$$

APPENDIX B

The proof in this section is based on time-domain investigation of the energy balance in the communication channels of wave variables. the claim is to proof that utilizing delayed first order hold expander in the place of zero hold expander does not violate the passivity of the channels. The two-port mechanical system with velocities $\dot{x}_i(t)$ and $\dot{x}_{si}(t)$, forces $f_i(t)$ and $f_{si}(t)$, and initial energy $E(0)$ depicted in Figure 1 is passive iff it obeys [35][2]:

$$\begin{aligned}&\int_0^t \left(f_i(t)\dot{x}_i(t) - f_{si}(t)\dot{x}_s(t)\right)dt + E(0) \geq 0\\ &\forall t, \quad \text{admissible } f_i(t),\, f_{si}(t).\end{aligned} \tag{43}$$

The system in Figure 1 employs wave domain communications. If continuous time implementation is assumed and the communications downsampling and upsampling are ignored, its passivity condition can be written as [35]:

$$\begin{aligned}&\int_0^t \frac{1}{2}\left(u_{ci}^T(t)u_{ci}(t) + v_{si}^T(t)v_{si}(t)\right)dt\\ &\geq \int_0^t \frac{1}{2}\left(u_{si}^T(t)u_{si}(t) + v_{ci}^T(t)v_{ci}(t)\right)dt\\ &\forall t, \quad \text{admissible } u_{ci}(t),\, v_{ci}(t).\end{aligned} \tag{44}$$

In other words, the continuous time wave communications are passive if the energy provided by the output waves is limited by the energy received via the input waves [35].

After defining truncated signals via:

$$u_\theta(\tau) = \begin{cases} 0 & \text{if } \tau < 0 \\ u(\tau) & \text{if } 0 \leq \tau \leq \theta \\ 0 & \text{if } \tau > \theta \end{cases}, \tag{45}$$

the passivity condition in Equation (44) can be written for discrete time wave communications as, by considering the fact that $T_n = l_n T_c = M T_c$:

$$\begin{aligned}\Delta E(t) &= \frac{1}{2}\left[\sum_{k=0}^{N} u_{ci_t}^2(kT_c)\cdot T_c - \sum_{i=0}^{N/M} u_{si_t}^2(iMT_c)\cdot MT_c\right]\\ &+ \frac{1}{2}\left[\sum_{i=0}^{N/M} v_{si_t}^2(iMT_c)\cdot MT_c - \sum_{k=0}^{N} v_{ci_t}^2(kT_c)\cdot T_c\right]\\ &\geq 0 \quad \forall t \geq 0,\end{aligned} \tag{46}$$

[2]The same argument holds for each user therefore for simplicity only one client, i, is considered.

where $\Delta E(t)$ is the energy stored in the multirate wave communications at time t. For simplicity, only MT_c will be used in place of T_n in the remainder of the paper. It is shown in [24] that the first term in Equation (46) is greater than zero, i.e. it is passive, only if the aliasing due to downsampling is prevented, i.e. using a low pass filter. It is also shown [24] that the second term in Equation (46) is passive when zero order hold expander is used, i.e. it is greater than zero. The relation between v_{si_t} and v_{ci_t} in a delayed first order hold, for which v_{si_t} is its input and v_{ci_t} is its output, is as follows:

$$v_{ci_t}(kT_c) = \frac{v_{si_t}(iMT_c) - v_{si_t}(i(M-1)T_c)}{M} N_c + v_{si_t}(i(M-1)T_c) \qquad N_c = 1, 2, \ldots, M \tag{47}$$

where N_c is a counter. Hence, when delayed first order hold is used the energy balance for the second term in Equation (46) becomes:

$$\frac{1}{2}\left[\sum_{i=0}^{N/M} v_{si_t}^2(iMT_c) \cdot MT_c - \sum_{k=0}^{N} v_{ci_t}^2(kT_c) \cdot T_c\right] = \frac{1}{2}\sum_{i=0}^{N/M} v_{si_t}^2(iMT_c) \cdot MT_c - \sum_{i=0}^{N/M}\sum_{N_c=1}^{M}\left[\frac{v_{si_t}(iMT_c) - v_{si_t}(i(M-1)T_c)}{M} N_c + v_{si_t}(i(M-1)T_c)\right]^2 \cdot T_c \tag{48}$$

the inner summaton in Equation (48) is equal to:

$$\sum_{N_c=1}^{M}[\frac{v_{si_t}(iMT_c) - v_{si_t}(i(M-1)T_c)}{M} N_c + v_{si_t}(i(M-1)T_c)]^2 \cdot T_c = \sum_{N_c=1}^{M}[(v_{si_t}(iMT_c) - v_{si_t}(i(M-1)T_c))^2 \cdot \frac{(M+1)(2M+1)}{6M} + (v_{si_t}(iMT_c) - v_{si_t}(i(M-1)T_c)) \cdot v_{si_t}(i(M-1)T_c) \cdot (M+1) + v_{si_t}^2(i(M-1)) \cdot M] \cdot T_c \tag{49}$$

for simplifying the summation in Equation (49) the following relations are used:

$$\sum_{N_c=1}^{M} N_c = \frac{M(M+1)}{2} \qquad \sum_{N_c=1}^{M} {N_c}^2 = \frac{M(M+1)(2M+1)}{6} \tag{50}$$

after substutating Equation (48) in Equation (49) the proof of passivity is equivalent to showing the following inequality holds:

$$\sum_{i=0}^{N/M} v_{si_t}^2(iMT_c) \cdot MT_c \geq \sum_{N_c=1}^{M}[(v_{si_t}(iMT_c) - v_{si_t}(i(M-1)T_c))^2 \cdot \frac{(M+1)(2M+1)}{6M} + (v_{si_t}(iMT_c) - v_{si_t}(i(M-1)T_c)) \cdot v_{si_t}(i(M-1)T_c) \cdot (M+1) + v_{si_t}^2(i(M-1)T_c) \cdot M] \cdot T_c \tag{51}$$

After some algebraic manipulation the problem reduces to:

$$\sum_{i=0}^{N/M} [v_{si_t}^2(iMT_c)\cdot(M-1)\cdot(4M+1) \\ -(v_{si_t}(iMT_c))(v_{si_t}(i(M-1)T_c))\cdot 2\cdot(M-1)\cdot(M+1) \\ -v_{si_t}^2(i(M-1)T_c)\cdot(M-1)\cdot(2M-1)] \geq 0 \tag{52}$$

moreover Equation (52) can be written as:

$$(M-1)\cdot[\sum_{i=0}^{N/M}[(v_{si_t}(iMT_c)-v_{si_t}(i(M-1)T_c))^2\cdot(M+1) \\ +(v_{si_t}^2(iMT_c)-v_{si_t}^2(i(M-1)T_c))\cdot(3M)]] \tag{53}$$

since:

$$(3M)\cdot\sum_{i=0}^{N/M}[v_{si_t}^2(iMT_c)-v_{si_t}^2(i(M-1)T_c)] = (3M)\cdot v_{si_t}^2(NT_c) \geq 0 \tag{54}$$

it can be concluded that Equation (53) is greater than zero and consequently Equation (52) holds and proofs that using delayed fisrt order hold maitain the passivity of the channels □.

REFERENCES

[1] X. Shen, J. Zhou, A. E. Saddik, and N. D. Georganas. Architecture and evaluation of tele-haptic environments. In *8th IEEE International Symposium on Distributed Simulation and Real Time Applications*, pages 53–60, Budapest, Hungary, 2004.

[2] S. J. O'Leary, M. A. Hutchins, D. R. Stevenson, C. Gunn, A. Krumpholz, G. Kennedy, M. Tykocinski, M. Dahm, and B. Pyam. Validation of a networked virtual reality simulation of temporal bone surgery. *The Laryngoscope*, 118(6):1040–1046, 2008.

[3] C.R. Carignan, P.A. Ollson, and J. Tang. Cooperative control of virtual objects using haptic teleoperation over the internet. *Int J Disab Human Dev*, 4(4):261 – 267, 2005.

[4] A. Alamri, M. Eid, R. Iglesias, S. Shirmohammadi, and A. El Saddik. Haptic virtual rehabilitation exercises for poststroke diagnosis. *IEEE Tran Instrum Meas*, 57(9):1876–1884, 2008.

[5] H.-S. Park, Q. Peng, and L.-Q. Zhang. A portable telerehabilitation system for remote evaluations of impaired elbows in neurological disorders. *IEEE Trans Neural Syst Rehab Eng*, 16(3):245–254, 2008.

[6] M. Glencross, C. Jay, J. Feasel, L. Kohli, M. Whitton, and R. Hubbold. Effective cooperative haptic interaction over the Internet. In *IEEE Virt Real Conf*, pages 115–122, Charlotte, NC, 2007.

[7] R. Iglesias, S. Casado, T. Gutierrez, A. Garcia-Alonso, W. Yu, and A. Mrshall. Simultaneous remote haptic collaboration for assembly tasks. *Multimedia*, 13:263–274, 2008.

[8] M. Capps, P. McDowell, and M. Zyda. A future for entertainment-defense research collaboration. *IEEE Comput Graphics Appl*, 21(1):37–43, 2001.

[9] J. Kim, H. Kim, B.K. Tay, M. Muniyandi, M.A. Srinivasan, J. Jordan, J. Mortensen, M. Oliveira, and M. Slater. Transatlantic touch: a study of haptic collaboration over long distance. *Presence: Teleop Virt Envir*, 13(3):328–337, 2004.

[10] J. Cheong, S.-I. Niculescu, A. Annaswamy, and M.A. Srinivasan. Synchronization control for physics-based collaborative virtual environments with shared haptics. *Adv Robot*, 21(9):1001–1029, 2007.

[11] G. Sankaranarayanan and B. Hannaford. Experimental comparison of internet haptic collaboration with time-delay compensation techniques. In *IEEE Int Conf Robotic Autom*, volume 1, pages 206–211, Pasadena, CA, 2008.

[12] K.S. Park and R.V. Kenyon. Effects of network characteristics on human performance in a collaborative virtual environment. In *IEEE Virt Real Conf*, pages 104–111, Huston, TE, 1999.

[13] K. Hikichi, H. Morino, I. Arimoto, K. Sezaki, and Y. Yasuda. The evaluation of delay jitter for haptics collaboration over the Internet. In *IEEE Global Telecom Conf*, pages 1492–1496, Taipei, Taiwan, 2002.

[14] M. O. Alhalabi, S. Horiguchi, and S. Kunifuji. An experimental study on the effects of network delay in cooperative shared haptic virtual environment. *Computers and Graphics*, 27(2):205 – 213, 2003.

[15] G. Sankaranarayanan and B. Hannaford. Experimental Internet haptic collaboration using virtual coupling schemes. *Symposium on Haptic Interfaces for Virtual Environment and Teleoperator Systems*, pages 259–266, 2008.

[16] S. Lee and J. W. Kim. Transparency analysis and delay compensation scheme for haptic-based networked virtual environments. *Computer Communications*, 32(5):992 – 999, 2009.

[17] M. Fotoohi, S. Sirouspour, and D. Capson. Stability and performance analysis of centralized and distributed multi-rate control architectures for multi-user haptic interaction. *International Journal of Robotics Research*, 26(9):977–994, 2007.

[18] O.R. Astley and V. Hayward. Multirate haptic simulation achieved by coupling finite element meshes through Norton equivalents. In *IEEE Int Conf Robotic Autom*, pages 989–994, 1998.

[19] M.C. Cavusoglu, F. Tendick, and S.S. Sastry. Telesurgery and Surgical Simulation: Haptic Interfaces to Real and Virtual Surgical Environments. In M.L. McLaughlin, J.P. Hespanha, and G. Sukhatme, editors, *Touch in virtual environments*. Prentice-Hall, Inc., Upper Saddle River, NJ, 2001.

[20] D. Wang, Y. Zhang, Y. Wang, Y.-S. Lee, P. Lu, and Y. Wang. Cutting on Triangle Mesh: Local Model-Based Haptic Display for Dental Preparation Surgery Simulation. *IEEE Trans Vis Comput Gr*, 11(6):671–683, 2005.

[21] F. Barbagli, D. Prattichizzo, and K. Salisbury. A multirate approach to haptic interaction with deformable objects single and multipoint contacts. *Int J Rob Res*, 24(9):703–715, 2005.

[22] K. Lee and D.Y. Lee. MIMO output estimation with reduced multirate sampling for real-time haptic rendering. *IEEE T Robotics*, 23(3):481 – 493, 2007.

[23] Ch. Cho, J. B. Song, and M. Kim. Stable haptic display of slowly updated virtual environment with multirate wave transform. *IEEE/ASME Transactions on Mechatronics*, 13(5):566–575, 2008.

[24] N. Yasrebi and D. Constantinescu. Passive multirate wave communications for haptic interaction with delayed rigid environments. *IEEE/ASME T ON Mechatronics*, 18(1):328–336, 2013.

[25] R. J. Anderson and M. W. Spong. Bilateral control of teleoperators with time delay. *IEEE Transactions on Automatic Control*, 34(5):494–501, 1989.

[26] G. Niemeyer and J.-J.E. Slotine. Stable adaptive teleoperation. *IEEE J Oceanic Eng*, 16(1):152–162, 1991.

[27] M. Gautier and C. Andriot. 6DOF haptic cooperation over large latency network with wave variables for virtual prototyping. In *IEEE Int Conf Robotic Autom*, pages 2167–2172, 2009.

[28] A. Shahdi and S. Sirouspour. Adaptive/robust control for enhanced teleoperation under communication time delay. In *IEEE/RSJ International Conference on Intelligent Robots and Systems*, pages 2667–2672, San Diego, CA 2007.

[29] M. Araki and K. Yamamoto. Multivariable multirate sampled-data systems: State-space description, transfer characteristics, and Nyquist criterion. *IEEE Transactions on Automatic Control*, 31(2):145–154, 1986.

[30] N. Yasrebi and D. Constantinescu. Centralized multi-user multi-rate haptic cooperation using wave transformation. In *IEEE Int Conf Mechatronics Autom*, pages 3816 –3821, 2009.

[31] S. Hirche and M. Buss. Packet loss effects in passive telepresence systems. In *IEEE Conf Dec Contr*, pages 4010–4015, Paradise Islands, The Bahamas, 2004.

[32] G. Niemeyer and J.-J. E. Slotine. Telemanipulation with time delays. *International Journal of Robotics Research*, 23(9):873–890, 2004.

[33] TATA Consultancy Services. The Wide Area Network emulator.

[34] B. Gillespie and M. Cutkosky. Stable user-specific haptic rendering of the virtual wall. In *ASME International Mechanical Engineering Conference and Exposition*, pages 397–406, Atlanta, GA, 1996.

[35] G. Niemeyer and J.-J.E. Slotine. Telemanipulation with time delays. *Int J Robot Res*, 23(9):873–890, 2004.

Appendix C: Passive Wave Variable Control of Haptic Interaction with an Unknown Virtual Environment

Naser Yasrebi, Daniela Constantinescu

Department of Mechanical Engineering, University of Victoria, Victoria, Canada

E-mail: nyasrebi@uvic.ca, danielac@me.uvic.ca.

Abstract

The wave variable transformation cannot be exploited for the control of sampled-data and discrete-time systems without precaution. This paper shows that connecting a haptic interface to a discrete time virtual environment through a wave variable controller can inject energy into the haptic feedback loop and thus jeopardize the stability of the haptic interaction. The connection involves a one step computational delay when the virtual environment is not known prior to starting the interaction. Using the Jury-Marden stability criterion, the paper investigates the effect of this computational delay on the stability of wave variable control of haptic interaction with a virtual wall. It also develops a time domain passivity analysis to compute the energy injected in the wave variable transformation by the computational delay. Then, it proposes an algorithm for dissipating the extra energy and restoring the passivity of the wave variable transformation. The paper concludes with the experimental validation of the energy dissipating algorithm.

1 Introduction

The wave variable/scattering transformation provides a robust solution for addressing the destabilizing effect of constant or variable time delay in bilateral teleoperation systems [1, 2]. The possibility of utilizing the wave variable transformation as a control strategy in sampled-data and discrete-time systems has also been the focus of recent research because of the similarities between bilateral teleoperation and haptics. In [3], the wave variable transformation has been used to relate the virtual environment force F_s and velocity $\dot{x}_s$ variables to the haptic device force F_m and velocity $\dot{x}_m$ variables. The analysis in [3] has accounted only for reflecting delays, i.e., only for delays in the communications. In [4], the wave variable transformation has been employed to connect the virtual environment variables directly to the motor current i and voltage e_w variables. Because the inductance of motors typically used in haptics provides a stiffness higher than can be obtained through digital control, the approach in [4] has led to stiffer virtual walls being stably rendered to users. Further work is required to apply forces that arise from variable stiffness and along more than one direction. In [5], the wave variable transformation has provided a means to address the computational delay associated with 6 degrees of freedom (DOF) molecular docking

IEEE International Conference on Robotics and Automation, pp.919-924, 9-13 May 2011

simulations. Virtual damping has been added to maintain stability and no stability or performance analysis have been offered in [5].

The use of wave variables in multirate haptic systems has been proposed in [6]. The change of rate between the fast haptic feedback loop and a slow simulation loop has been modeled as downsampling and upsampling of the communications, and wave variables have linked the haptic device and the virtual environment to render their multirate connection passive. The negative impact of aliasing on the passivity of the multirate wave variable transformation has not been considered in [6]. In [7, 8], the aliasing has been eliminated and the passivity of the multirate wave variable transformation has been restored through wave low pass (LP) filtering before downsampling. The work in [7, 8] has restricted the passivity analysis to the wave variable communication channels and has neglected the computational delay that arises when the model of the virtual environment is unknown.

The wave variable/scattering transformation has several practical limitations both in the continuous and in the discrete time domains, including wave reflections and performance degradation due to the limited frequency content of the forces rendered to users. Research has been devoted to alleviating those limitations in continuous time [9, 10, 11], and proposed solutions include low pass filtering the outgoing master wave and integrating the high frequency content of the environment force into the returning wave. Less attention has been paid to the challenges posed by the wave variable transformation in the discrete time domain. Work focusing on wave variables in sampled-data systems has investigated primarily the stability or passivity of haptic interaction. One exception is [3] which has studied the effect of the reflecting delays.

This paper proposes a technique for passively connecting a wave variable controller to an unknown virtual environment. Herein, a virtual environment is considered unknown when the virtual stiffness and damping are computed during the interaction (i.e., simulated at run-time) rather than being known in advance. In such a case, the algebraic loop that arises when computing the virtual environment velocity command cannot be unwrapped. As a result, the virtual environment velocity is decoded using the wave arriving from the haptic device at the current simulation step and the force encoded in the wave sent to the haptic device at the previous simulation step. The paper shows that the one step computational delay incurred in the virtual environment velocity derivation injects energy in the feedback loop and severely shrinks the stability region of haptic interaction with the unknown virtual environment. The Jury-Marden stability criterion is used to analyze the stability of haptic interaction with a virtual wall for the case that: (i) the algebraic loop can be unwrapped, either through iteration or through exploiting the model of the virtual environment; and (ii) the algebraic loop is eliminated through a one step computational delay when the virtual environment is unknown and/or a slow simulation update rate precludes the use of iteration. Similarly to the analysis in [12], the stability analysis in this work assumes that the haptic interaction system is linear. Furthermore, the computational delay is considered constant. The stability analysis predicts that this computational delay significantly decreases the stability region of the haptic interaction system. The paper develops a time domain passivity analysis to derive the energy injected in the feedback loop by the computational delay incurred when connecting the wave variable transformation to an unknown virtual environment. Then,it proposes an algorithm to compensate the destabilizing effect of this delay and to guarantee passive connection of the wave variable transformation to the unknown virtual environment. Lastly, the paper validates the analytical results via controlled experimental haptic interactions with a virtual wall.

In the remainder of the paper, Section 2 introduces the problem associated with passively connecting the wave variable transformation to an unknown virtual environment. Section 3 proposes a stability analysis of haptic interaction with a virtual constraint based on the Jury-Marden criterion. Section 4 presents a time domain investigation of the energetic behavior of the connection of a wave transformation to an unknown virtual environment. It also derives a compensating algorithm to ensure the passivity of this connection. Section 5 validates the performance of the compensating algorithm experimentally. Section 7 summarizes the conclusions of this work and the plans for future work.

2 Problem definition

When wave variable control is used in haptic systems, Figure 1, the haptic device plays the role of the master robot and the virtual environment plays the role of the slave robot in bilateral teleoperation. Therefore, notation is used in accordance with this analogy. When the haptic interface is an impedance-type device, like the Phantom Omni device used in the experimental setup in this paper, the virtual environment ("slave" side) decodes a velocity command $\dot{x}_s$ from the wave signal u_s, according to [1]:

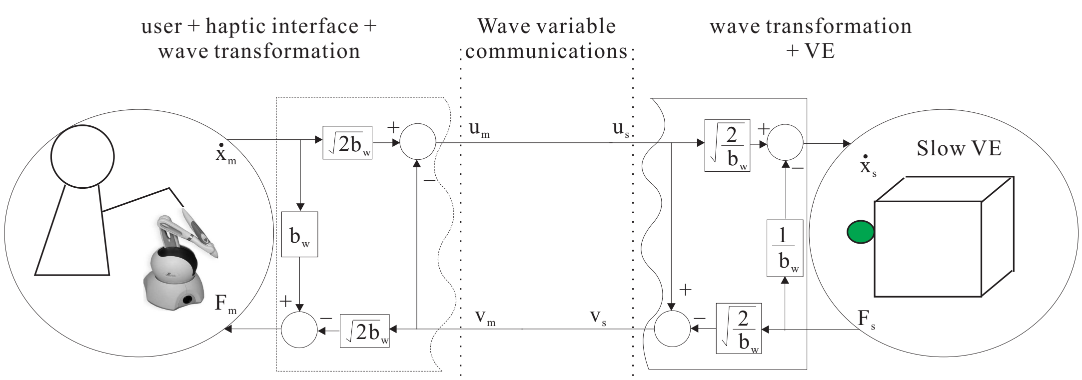

Figure 1: A haptic system with wave control.

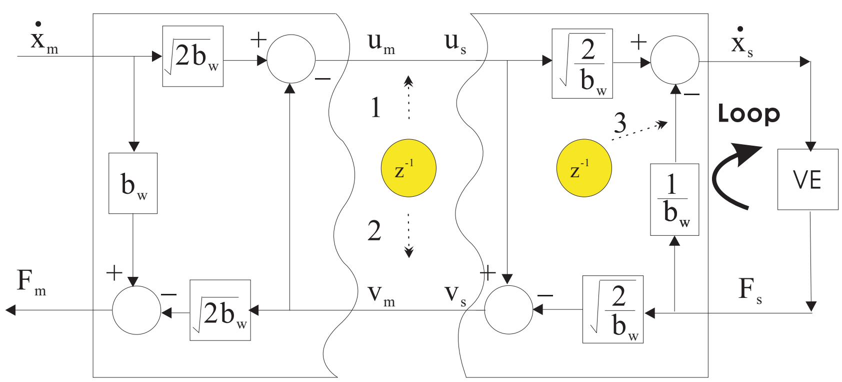

Figure 2: Wave transformation, virtual environment, and algebraic loop arising at the connection between the two.

$$\dot{x}_s(t) = \sqrt{\frac{2}{b_w}} u_s(t) + \frac{-F_s(t)}{b_w} \tag{1}$$

In Equation (1), b_w is the wave impedance and $F_s(t)$ is the force response of the virtual environment, as shown in Figure 2. In discrete time, Equation (1) becomes:

$$\dot{x}_s(nT) = \sqrt{\frac{2}{b_w}} u_s(nT) + \frac{-F_s(nT)}{b_w}, \tag{2}$$

with n being the index of the current time step and T the time step of the virtual environment simulation. In Equation (2), the virtual environment force $F_s(nT)$ depends on the velocity command $\dot{x}_s$:

$$F_s(nT) = h_{VE}(\dot{x}_s(nT)), \tag{3}$$

where h_{VE} is the transfer function of the virtual environment in continuous time. From Equation (3), it follows that the right side is dependent on the left side in Equation (2). In other words, connecting a wave transformation to a virtual environment creates an algebraic loop, as illustrated in Figure 2. This algebraic loop is similar to the algebraic loop that arises in the wave variable control of bilateral teleoperators [13].

When the model of virtual environment is available, i.e. h_{VE} is known prior to starting the interaction, or the virtual environment simulation is sufficiently fast, i.e., T is sufficiently small, the algebraic loop in Equation (2) can be unwrapped, either analytically by using h_{VE} or numerically by iteration. For example, when the virtual environment comprises a constraint with known stiffness K and damping B parameters, Equation (2) becomes:

$$\dot{x}_s(nT) = \frac{\sqrt{2b_w} u_s(nT) - K x_s(nT)}{b_w + B}. \tag{4}$$

When the algebraic loop cannot be unwrapped, i.e. when the virtual environment is unknown or is updated slowly, Equation (2) is implemented via:

$$\dot{x}_s(nT) = \sqrt{\frac{2}{b_w}} u_s(nT) + \frac{-F_s((n-1)T)}{b_w}, \tag{5}$$

which means that the algebraic loop is eliminated through introducing a one step computational delay, as shown in Figure 2. The effect of this delay on the stability of haptic interaction is investigated in the following section based on the Jury-Marden criterion.

3 The effect of the computational delay

In the discrete time implementation of wave variable control, one factor that has a significant impact on the stability of the haptic interaction system is the location of the communication and computational delays associated with the discrete time system. Figure 2 depicts the communication delays in the communication channels, and the computational delay in the local feedback path in the virtual environment. This computational delay creates the algebraic loop described in the previous section.

The passivity of the discrete time implementation of the wave transformation has been analyzed in [3] considering only the delays in the communication channels. To illustrate the importance of the computational delay, this section investigates the stability of haptic interaction with a constraint with stiffness K and damping B via a pure mass haptic device for the case that: 1) the algebraic loop is unwrapped and no delay arises at the connection between the wave transformation and the virtual environment; and 2) the algebraic loop cannot be unwrapped and a one step computational delay needs to be introduced in the local feedback path at the virtual environment side. The stability analysis is performed by deriving the characteristic equations of the closed loop haptic interaction system using Equations (4) and (5) for the case 1) and 2), respectively. The stability regions are obtained using the Jury-Marden criterion and the closed-loop characteristic equation. The characteristic equation is:

$$\begin{aligned}
0 \quad = \quad & (\frac{1}{2}mKT + mB + mb_w)z^4 + \\
& \left(-2mb_w - 4mB + 5b_wTB - mKT + \right. \\
& \qquad \left. \frac{5}{2}b_wT^2K + b_w^2T\right) z^3 + \\
& (-9b_wTB - 3b_w^2T + 6mB + \frac{1}{2}b_wT^2K + 2mb_w)z^2 + \\
& (3b_w^2T - \frac{3}{2}b_wT^2K + 5b_wTB - 4mB - \\
& \quad 2mb_w + mKT)z - \\
& \frac{1}{2}mKT - b_w^2T - b_wTB + mb_w + \frac{1}{2}b_wT^2K + mB
\end{aligned} \tag{6}$$

when the algebraic loop can be unwrapped, and it is:

$$\begin{aligned}
0 \quad = \quad & 2mb_wz^4 + \\
& (4b_wT^2K - 2mB - 2b_w^2T + \\
& \quad 8b_wTB - mKT - 2mb_w)z^3 + \\
& (b_wT^2K - 2mb_w - 14b_wTB + 6mB + \\
& \quad mKT + 4b_w^2T)z^2 + \\
& (2mb_w + mKT - 2b_wT^2K - 2b_w^2T - \\
& \quad 6mB + 8b_wTB)z + \\
& 2mB - mKT + b_wT^2K - 2b_wTB,
\end{aligned} \tag{7}$$

when the algebraic loop is eliminated via a computational delay. In Equations (6) and (7), m is the mass of the haptic device. To simplify the analysis and reduce the number of parameters, the following non-dimensional system parameters are used in the derivations:

$$\begin{aligned}
\alpha &= \frac{KT^2}{m} \\
\beta &= \frac{b_wT}{m} \\
\sigma &= \frac{BT}{m}
\end{aligned} \tag{8}$$

For $\sigma = 0$ and negligible physical damping of the haptic interface, the stability regions for cases 1) (algebraic loop unwrapped) and 2) (algebraic loop eliminated via one step computational delay) are depicted in Figure 3(a) and Figure 3(b), respectively. Figure 3 shows that the stability region for case 2) is significantly smaller (note the different scales used in Figure 3(a) and Figure 3(b)). The major difference between cases 1) and 2) is the one step computational delay in the local feedback path at the simulation side, required when the virtual environment is unknown and the algebraic loop cannot be unwrapped. Hence, Figure 3 illustrates that the computational delay considerably degrades the stability of haptic interaction under wave variable control. Further support for this assertion is provided by [2], which has proven that a discrete time implementation of the wave transformation retains its passivity in the presence of delay in the communication channels.

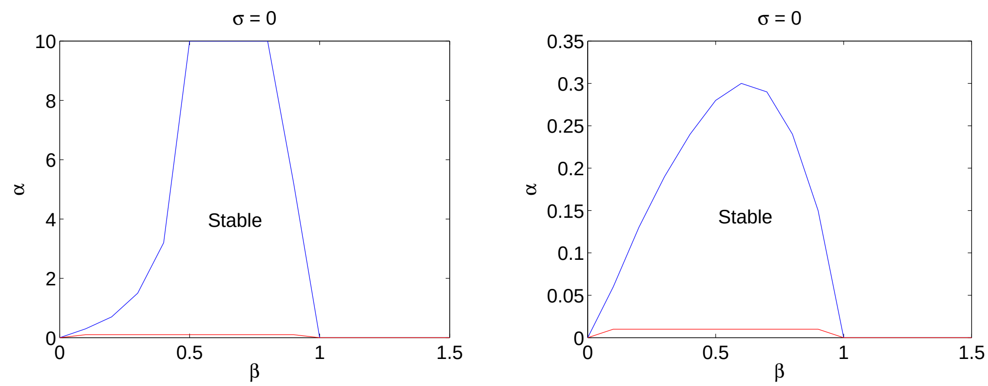

(a) Case 1): algebraic loop unwrapped.

(b) Case 2): algebraic loop eliminated via one step computational delay.

Figure 3: Stability region of haptic interaction with a virtual constraint with no virtual damping, $\sigma = 0$, and using a haptic interface with negligible physical damping. Note that different scales are used in (a) and (b) because of the much smaller stability region of case 2).

The next section develops a time domain passivity analysis to derive the energy generated by the computational delay.

4 Time domain passivity analysis

The energy balance on the right (simulation or "slave") side of Figure 2 is given by:

$$\Delta E = \sum_{n=0}^{n=N_f} \frac{1}{2}[(u_s^T(n)u_s(n)) - (v_s^T(n)v_s(n)]T. \quad (9)$$

where N_f is the current time step of the simulation. When the computational delay is negligible or the algebraic loop shown in Figure 2 can be eliminated through numerical methods or through unwrapping Equation (2), the following equation can be obtained upon suitable substitution of the wave variables:

$$\sum_{n=0}^{n=N_f} \frac{1}{2}[(u_s^T(n)u_s(n)) - (v_s^T(n)v_s(n)]T = \sum_{n=0}^{n=N_f} F_s(n)\dot{x}_s(n)T. \quad (10)$$

When the computational delay cannot be eliminated, $\dot{x}_s(n)$ is computed using Equation (5). Regardless of the computational delay, $v_s(n)$ is given by:

$$v_s(n) = u_s(n) - \sqrt{\frac{2}{b_w}} F_s(n). \tag{11}$$

Pre-multiplication of Equation (1) by $F_s(n)$ followed by integration in discrete time gives:

$$\sum_{n=0}^{n=N_f} F_s(n)\dot{x}_s(n)T = \sum_{n=0}^{n=N_f} [\sqrt{\frac{2}{b_w}} F_s(n)u_s(n) + \frac{-F_s(n)F_s(n-1)}{b_w}]T. \tag{12}$$

After substitution from Equation (11), Equation (9) becomes:

$$\sum_{n=0}^{n=N_f} \frac{1}{2}[(u_s^T(n)u_s(n)) - (v_s^T(n)v_s(n)]T = \sum_{n=0}^{n=N_f} \sqrt{\frac{2}{b_w}} u_s(n)F_s(n) + \frac{-F_s^2(n)}{b_w}, \tag{13}$$

and after subtracting Equation (12), Equation (14) provides the energy generated by the computational delay:

$$\Delta E_{delay}(n) = \sum_{n=0}^{n=N_f} \frac{-F_s^2(n) + F_s(n)F_s(n-1)}{b_w}. \tag{14}$$

Now Parseval's identity can be used to show that $\Delta E_{delay}(n) < 0$ which means that the computational delay always generates energy and thus, destroys the passivity of the wave transformation and threatens the stability of the haptic interaction system in Figure 3. The next section devises an algorithm for dissipating the energy generated by the computational delay.

5 Compensating algorithm

The compensating algorithm proposed in this section assumes that the virtual environment is passive. Work in progress investigates modifications of the compensating algorithm to enable it to handle active virtual environments.

To restore the passivity of the wave transformation, the energy injected in the haptic feedback loop by the computational delay has to be dissipated. The algorithm put forward in this work changes the value of $v_s(n)$ so as to make $\Delta E_{delay}(n) = 0$, as follows:

1. at each simulation step, $\Delta E_{delay}(n)$ is calculated from Equation (14);
2. if $\Delta E_{delay}(n) < 0$, then $v_s(n)$ is changed using:

$$v_{s_{new}}(n) = sgn(v_s(n))\sqrt{v_s^2(n) - 2\Delta E_{delay}(n)}, \tag{15}$$

   where $sgn|.|$ is sign function.

After substituting $v_{s_{new}}(n)$ in Equation (14) and subtracting Equation (12), it follows that $\Delta E_{delay}(n)$ becomes zero. By decreasing the wave command returned to the haptics device, the algorithm effectively decreases the impendance

6 Experiments

This section presents experimental haptic interactions with a virtual wall through a Phantom Omni haptic interface and for two cases: (i) controlled experiments with a constant input as the human input and (ii) experiments with human users. In the experimental setup, the haptic device is connected to a personal computer (PC) running Windows Vista on an Intel Core 2 Duo CPU at 2.67GHz with 2 GB RAM. A simple one degree of freedom virtual environment runs as a C++ console application on the same computer. The console application comprises two loops; (i) a fast loop which includes all control computations at the haptic device ("master") side and the filtering of the outgoing wave $u_m(n)$; and (ii) a slow loop which simulates the virtual environment ("slave" side). The OPENHAPTICS API is used to run the fast loop at 1 KHz and the update rate of the simulation loop is controlled via a counter synchronous with the fast loop. Since the console application runs under the Windows operating system, an exact sampling time cannot be guaranteed. However, the variation of the sampling time is very small and can be neglected. To ensure the "same" user during successive interactions, a constant force is applied to the handle of the haptic interface through commands sent to the motors. The virtual environment is a virtual wall updated every 0.02 s. The wave impedance is $b_w = 25$ Ns/m . An anti-aliasing low-pass filter with cutoff frequency equal to $\frac{1}{2(0.02)\text{ s}} = 25$ Hz is placed in the wave communications to ensure their passivity [7, 8]. The low-pass wave filter is required because the experimental setup is a multirate system, whereas the analysis in Section 3 considers a unirate haptic system.

Figure 4 plots the Z-width of the Phantom Omni interface obtained through controlled experiments for the case that the device is connected to the virtual wall via: (i) direct coupling (black lines); (ii) multirate wave variables free of aliasing (blue stars); and (iii) multirate wave variables free of aliasing and with the proposed energetic compensation of the computational delay (red triangles). The results in Figure 4 demonstrate that multirate wave variable control with the proposed compensating algorithm can render contacts almost twice as stiff as multirate wave control without compensation when users interact with a virtual environment with a simulation step $T = 0.02$ s through a Phantom Omni haptic interface.

Figure 5 depicts the experimental human interaction with a virtual wall with stiffness $K = 500$ N/m and through the same Phantom Omni device and controlled through multirate wave transformation free of aliasing and with energetic compensation of the computational delay. To better illustrate the performance of the proposed algorithm, the damping of the wall was set to zero, $B = 0$ Ns/m. In Figure 5, x_m is the position of the haptic interface, x_s is the position command in the virtual environment (obtained through discrete time integration of the velocity command $\dot{x}_s$ decoded from the u_s wave), F_m is the force fed back to the operator, and F_s is the force computed in the virtual environment. The energy balance at the simulation ("slave") side in Figure 2 before and after the proposed energetic compensation of the computational delay, as well as the energy injected by the computational delay and by the virtual environment, are shown in Figure 5(c). Figure 5 illustrates good force tracking and the ability of the proposed compensation algorithm to restore the passivity of the connection between the wave transformation and the virtual environment in the presence of the computational delay which arises when the algebraic loop in Equation (2) cannot be unwrapped. As shown in Figure 5, the VE is passive, $\Delta E_{VE} > 0$. However, the energy balance for the right side becomes negative, $\Delta E < 0$, at certain time instances

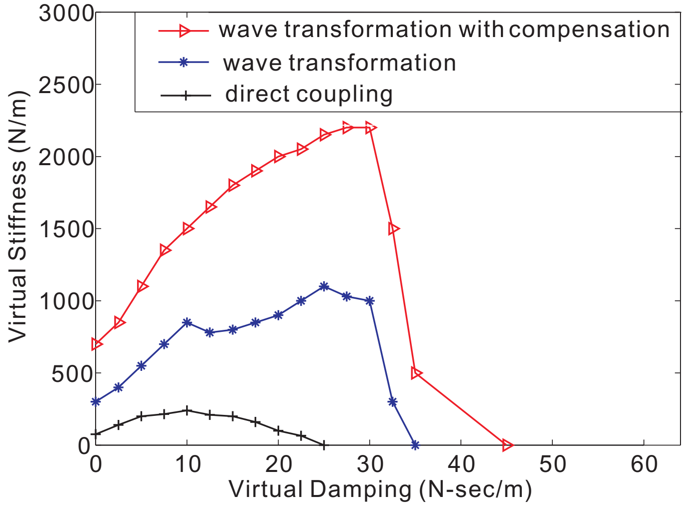

Figure 4: Z-width of the Phantom Omni device derived when (i) direct coupling (black lines), (ii) multirate wave variables free of aliasing (blue stars), and (iii) multirate wave variables free of aliasing and with energetic compensation of computational delay (red triangles) are used to connect the haptic interface to a virtual wall updated every $T = 0.02$ s.

before applying the energetic compensation algorithm. This algorithm appropriately compensates the effect of the computational delay and makes the energy balance of the right side almost equal to the energy balance of the VE, $\Delta E \approx \Delta E_{VE}$.

7 Conclusions and future work

This paper has investigated the stability of haptic interaction with an unknown virtual environment under wave variable control. First, the paper has shown that connecting a wave variable controller to an unknown virtual environment introduces a one step computational delay in the local feedback path at the simulation side. Then, it has used the Jury-Marden criterion to show that this computational delay injects energy into the haptic feedback loop and severely restricts the stability of the haptic interaction. Based on a time domain passivity analysis, the paper has derived the energy generated by the computational delay and has proposed a simple algorithm to dissipate it and restore the passivity of the wave transformation. Lastly, the paper has validated the analytical results and the performance of the proposed energy compensation algorithm through experiments. The experiments have shown that the proposed algorithm doubles the Z-width of a Phantom Omni interface in interaction with a virtual environment updated every $T = 0.02$ s. This means that stiffer contact is achievable in the virtual environment when the energy injected in the haptic system is dissipated as suggested in this work.

Although the proposed compensating algorithm improves the Z-width of the haptic interface, our on-going investigations show that the wave impedance considerably influences the impedance transmitted to the user. Therefore, upcoming work focuses on the performance analysis that will inform a robust controller design. The extension of the algorithm to handle active virtual environments is also underway.

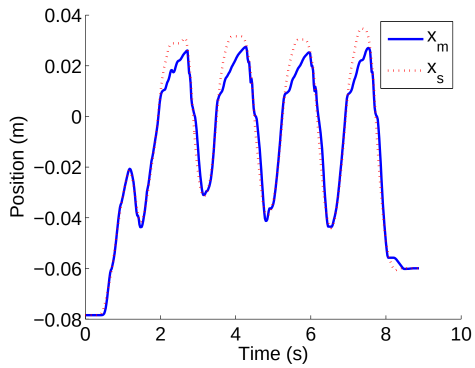

(a) Positions of the interface x_m, and commanded in the virtual environment x_s.

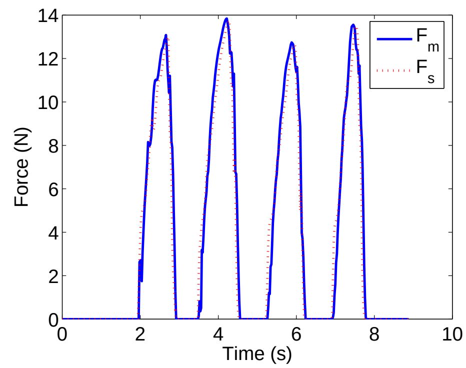

(b) Forces applied to the user F_m, and computed in the virtual environment F_s.

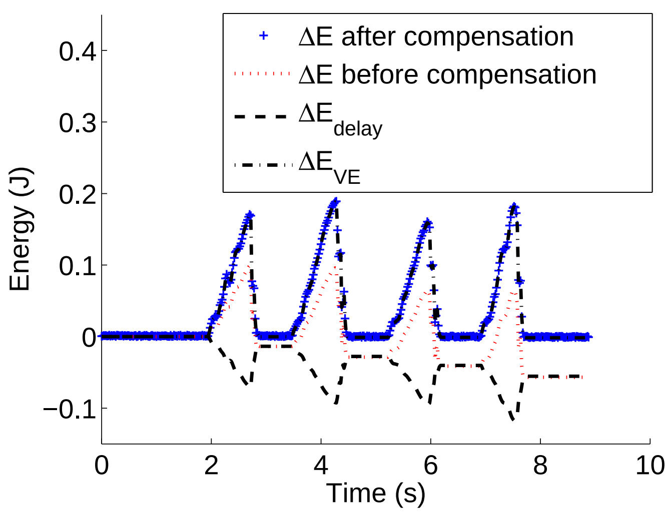

(c) Energy balance for the virtual environment ΔE_{VE}, for the computational delay ΔE_{delay}, and for the connection of the wave transformation to the virtual environment before and after energetic compensation of the computational delay.

Figure 5: Experimental interaction with a virtual wall ($K = 500$ N/m, $B = 0$ Ns/m, $T = 0.02$ s) under multirate wave variable control with energetic compensation of the computational delay.

REFERENCES

[1] G. Niemeyer and J.-J.E. Slotine. Stable adaptive teleoperation. *IEEE Journal of Oceanic Engineering*, 16(1):152–162, 1991.

[2] P. Berestesky, N. Chopra, and M. W. Spong. Discrete time passivity in bilateral teleoperation over the Internet. In *IEEE International Conference of Robotics and Automation*, pages 4557– 4564, New Orleans, LA, 2004.

[3] J. H. Lee, C. H. Cho, M. Kim, and J. B. Song. Haptic interface through wave transformation using delayed reflection: Application to a passive haptic device. *Advanced Robotics*, 20(3):305–322, 2006.

[4] N. Diolaiti, G. Niemeyer, and N. A. Tanner. Wave haptics: Building stiff controllers from the natural motor dynamics. *International Journal of Robotics Research*, 26(1):5–21, 2007.

[5] B. Daunay, A. Abbaci, A. Micaelli, and S. Regnier. Wave variables, a solution for stable haptic feedback in molecular docking simulations. In T. Sobh, K. Elleithy, A. Mahmood, and M. Karim, editors, *Innovative Algorithms and Techniques in Automation, Industrial Electronics and Telecommunications*. Springer, Netherlands, 2007.

[6] C. Cho, M. Kim, C. S. Hwang, J. Lee, and J. B. Song. Stable haptic display of slowly updated virtual environment with multirate wave transform. In *IEEE International Conference of Robotics and Automation*, pages 2465– 2470, Barcelona, Spain, 2005.

[7] N. Yasrebi and D. Constantinescu. Centralized multi-user multi-rate haptic cooperation using wave transformation. In *IEEE International Conference on Mecahtronics and Automation*, pages 3816 –3821, 2009.

[8] N. Yasrebi and D. Constantinescu. Passive multirate wave communications for haptic interaction with delayed rigid environments. *In review at the IEEE Transactions on Mechatronics*, 2010.

[9] N. A. Tanner and G. Niemeyer. Online tuning of wave impedance in telerobotics. In *IEEE Conference on Robotics, Automation and Mechatronics*, pages 7–12, Singapore, 2004.

[10] N.A. Tanner and G. Niemeyer. Practical limitations of wave variable controllers in teleoperation. In *IEEE Conference on Robotics, Automation and Mechatronics*, pages 25–30, 2004.

[11] N. A. Tanner and G. Niemeyer. Improving perception in time-delayed telerobotics. *International Journal of Robotics Research*, 24(8):631–644, 2005.

[12] J. J. Gil, E. Sánchez, T. Hulin, C. Preusche, and G. Hirzinger. Stability boundary for haptic rendering: influence of damping and delay. *J Comput Inf Sci Eng*, 9(1):8, 2009.

[13] G. Niemeyer. *Using wave variables in time delayed force reflecting teleoperation*. PhD thesis, MIT, 1996.

IEEE International Conference on Robotics and Automation, pp.919-924, 9-13 May 2011

Appendix D: Passive velocity Filtering for Haptic Applications with Wave Control

Naser Yasrebi, Daniela Constantinescu

Department of Mechanical Engineering, University of Victoria, Victoria, Canada

E-mail: nyasrebi@uvic.ca, danielac@me.uvic.ca.

Abstract

This work proposes a passive velocity filtering for both unirate and multirate haptic application with wave control to remove noise and improve the transparency of the system. In this method the velocity is computed by using simple Euler velocity estimation and the filtering is performed in wave domain which is robust again constant lag or time delay. A filterbank-like structure in wave domain is introduced to filter both the outgoing wave variable and the velocity signal. The passivity condition for the proposed scheme including the filters is derived by considering the energy balance in communication channels of the wave variables. This passivity condition is used as the design criterion which is formulated as a minimax optimization problem. The performance of the proposed method in terms of transparency is studied in frequency domain. Experimental results prove the appropriate performance of the filtering method and confirms the analytical results.

1 INTRODUCTION

Digital velocity estimation by using position samples always has been a challenging task in different applications. There are several methods available for velocity computation each of which is suitable for a specific kind of application. Good reviews on these methods are presented in [1–3].

In haptic applications the velocity of the manipulandum is used to compute the virtual environment (VE) force and stabilize the system as the controller input, e.g. in virtual coupling or wave control methods. Hence, estimating accurate velocity is crucial for haptic applications. A suitable differentiator on one hand should be accurate and on the other hand should not endanger the stability of the haptic system. Also the estimated velocity must be noise free as much as possible since the human operator feels the nosily force feedback.

Wave transformation is widely used in teleoperation and haptic systems. It provides a robust solution for constant communication delay [4] and/or slowly updated VEs [5]. When wave control is used, the velocity estimation becomes more critical due to the fact that the velocity signal is directly used in feedback signal mostly with large gains, i.e.

American Control Conference, pp.3477-3483, 27-29 June 2012

wave impedance. This large gain while is desirable for the transparency of the system in low frequencies, brings about two problems: i) amplifies noise and ii) affects the transparency of the system in high frequencies.

There are few works that trying to address the need of a suitable differentiator for haptic applications and up to our knowledge there is no work related to velocity estimation or filtering for applications with wave transformation. Related works fall into two main categories. Some of them such as [6–10] demand a new haptic interfaces design which are not commercially available or requires an accurate model of the haptic device which such an accurate and reliable model is not available [11, 12].

Beside these works, there are some works that provide software solution for haptic application by introducing new algorithms for calculating velocity. [13] proposes an adaptive windowing for velocity estimation. Their results show that the proposed method has poor performance for low frequency sampling rates. Also the stability and transparency of the system with this velocity estimator is not clear. In [14] designing a suitable Finite Impulse Response (FIR) differentiator for haptic application is studied. This differentiator is designed in a way that enhance the passivity of the system but still suffers form the noisy output.

In this paper a new filter bank-like architecture Figure 1 involving passive multirate wave control [5,15] and passive velocity filtering Figure 2 is presented. Beside removing noise, the proposed passive filtering improves the transparency of the haptic system, especially in high frequencies.

As it is elucidated in Figure 1, the outgoing wave variable, u_m is split into two parts by using lowpass (LP) and highpass (HP) filters. The first part of the wave signal, the output of LP, is fed to the virtual environment (VE) and the output of the HP is used to filter the input velocity signal. The presented configuration in Figure 1 as it is discussed later, is converted to an equivalent scheme shown in Figure 2. The role of the LP filter is threefold: i) removes noise, ii) reduces wave reflection, and iii) by avoiding aliasing guarantees the passivity of the transmission lines in the presence of any rate change. The rate change might be due to the computer network limitations or a slow VE.

Since available filters are not ideal, the design of the filters are formulated as a minimax problem based on the passivity criterion. The performance of the proposed architecture is study in frequency domain and it is shown that the proposed structure improves the performance of the system in high frequencies. The analytical results are confirmed experimentally, especially the effectiveness of the proposed design method and appropriate performance of the filtering scheme.

The rest of this paper is structured as follows: Section 2 introduces the problem associated with the passive multirate wave control. The passivity discussion about the proposed architecture and passive velocity filtering is presented in Section 3. The filter design problem formulated in Section 4. The performance of the new architecture is investigated analytically in Section 5 and Section 6 presents the experimental results. Finally Section 7 is devoted to the conclusions and the future works.

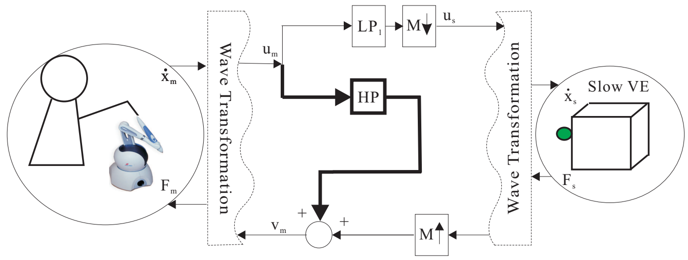

Figure 1: The filter bank-like structure of proposed method

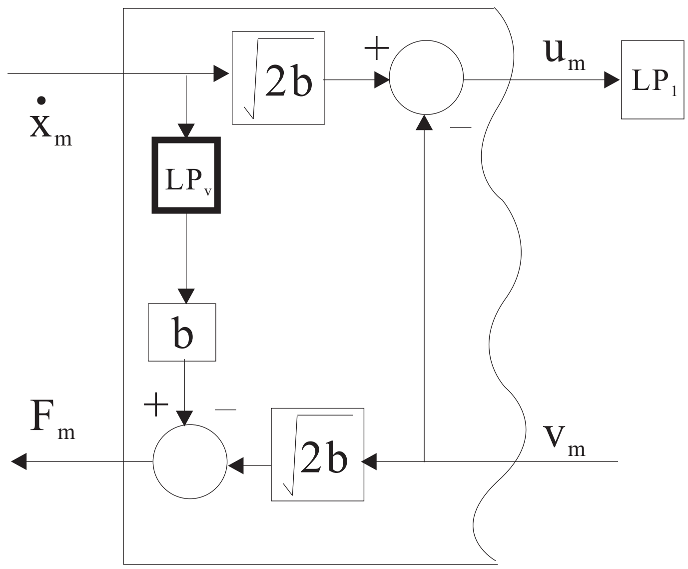

Figure 2: Master side with velocity filter

2 Problem definition

For an impedance haptic interface with wave control the feedback force is computed by:

$$F_m = b\dot{x}_m - \sqrt{2b}v_m \tag{1}$$

where b is wave impedance, $\dot{x}_m$ is the velocity of the haptic interface, and v_m is incoming wave variable.

As it is shown later on in this section, in high frequencies the first term in Equation (1) becomes dominant and it generates a large feedback force, i.e F_m, especially when wave impedance is large. On the other hand a large wave impedance improves the performance of the system in low frequencies. Furthermore, due to noisy velocity signal, which is computed from position signal, the feedback force becomes too noisy.

Utilizing a lowpass filter to filter the velocity signals provides a solution for these problems. It is a well-known fact that filtering in power domain due to the imposed phase lag might make the system unstable. On the other hand designing suitable velocity observer or filter in power domain demands an accurate model of the haptic interface. Such a model due to nonlinearities in available commercial haptic devices and the change of physical properties usually is not available.

This work proposes a passive velocity filtering method which can be designed independent of haptic interface and wave impedance.

Consider the second branch of outgoing wave variable u_m, which is the output of the HP filter, v_{HP}. Since u_m is found by:

$$u_m = \sqrt{2b}\dot{x}_m - v_m \tag{2}$$

and on the other hand v_m mostly involves low and medium frequencies, it can be concluded that the main signal that contributes to v_{HP} is the velocity signal. Hence, by feeding back v_{HP} and dividing this signal by 2 and by some manipulation Equation (1) in frequency domain can be written:

$$F_m(z) = b\dot{X}_m(z)(1 - HP(z)) - \sqrt{2b}V_m(z) \tag{3}$$

$(1 - HP(z))$ actually is a low pass filter which removes high frequency content and noise from the velocity signal x_m . This explains how the structrue shown in Figure 1 is equivalent to the structure shown in Figure 2 where $LP_v = (1 - HP(z))$ As it is shown in the next section, this lowpass filter also takes care of the significant deviation from the ideal response in high frequencies.

The same argument hold for admittance type haptic interface. By this difference that the HP feedback in this case is used to filter the measured force.

2.1 Frequency Domain Analysis

In our earlier works [5,15], we have shown that in order to guarantee the passivity of the communication channels a low pass filter with a cutoff frequency less than the update frequency of the VE should be used before the downsampler. The aliasing due to the rate change might inject energy to the system and violate the passivity of the communication channel. To better show the shortcomings of the multirate passive wave transformation without velocity filter, its performance is studied by using frequency domain analysis.

Lifting [16] is used to convert the multirate feedback system, Figure 1 without HP, to a unirate system in order to find the transmitted admittance:

$$H(z) = \frac{X_m(z)}{F_h(z)}, \tag{4}$$

The VE is a virtual wall where its virtual damping and virtual stiffness are $B_{VE} = 10\ Ns/m$ and $K_{VE} = 2000$ N/m respectively. The VE is updated every 0.02 s. The frequency response of the resultant transfer function in Equation (4) is compared with the frequency response of the transfer function of the ideal case. The ideal case is considered to be the transmitted admittance when direct coupling is used. Figure 3 plots the frequency response of the transmitted admittance in low frequencies and for different wave impedances. In this frequency range, when the hand input can be considered as a constant input, increasing wave impedance improves the perception. This is expected because for constant input and in steady state, the low pass filter used in communication channels behaves like a virtual coupler with the following spring stiffness [17]:

$$K_{filter} = 2b\lambda, \tag{5}$$

where λ is the cutoff frequency of the lowpass filter. Hence it can be concluded that increasing wave impedance in low frequencies, improves the perception. On the other hand increasing wave impedance in high frequency has an adverse effect on the transparency of the system, Figure 4. In this frequency range increasing wave impedance is similar to adding damping to the system which results in decreasing the first natural frequency of the system. It can be shown that by increasing the cutoff frequency of the lowpass filter, it is possible to get closer to the ideal case at the expense of the stability of the system [5]. In order to improve the performance in high frequency and remove noise, the filterbank-like structure in Figure 1 is used instead. Filtering the velocity signal makes it possible to use larger wave impedances which in turn improves the performance of the system in low frequencies as well.

In the next sections passivity analysis for the proposed architecture is presented and filter design problem is introduced.

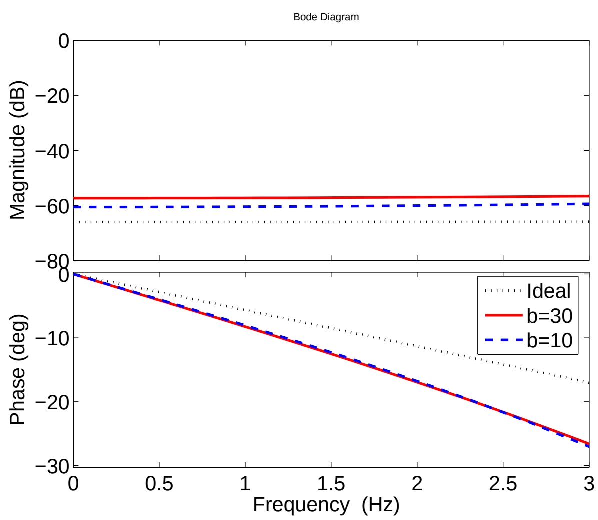

Figure 3: Frequency responses of transmitted admittance for different wave impedances and in low frequencies for $B_{VE} = 10\ Ns/m$ and $K_{VE} = 2000$ N/m

3 Passivity analysis

Consider the passivity condition for the right side of the haptic system in Figure 1:

$$\Delta E\,(t) = \frac{1}{2}\left[\sum_{k=0}^{N} u_{m_t}^2(k)\cdot T - \sum_{k=0}^{N} v_{m_t}^2(k)\cdot T\right] \geq 0$$
$$\forall t \geq 0, \tag{6}$$

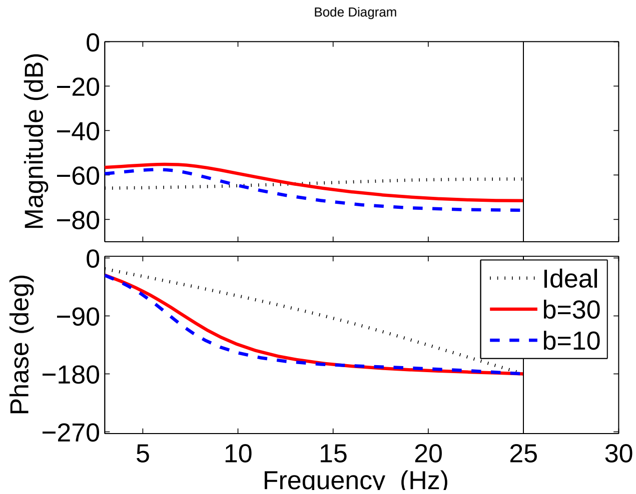

Figure 4: Frequency responses of transmitted admittance for different wave impedances and in high frequencies for $B_{VE} = 10\ Ns/m$ and $K_{VE} = 2000$ N/m

where u_{m_t} and v_{m_t} are truncated signals defined as:

$$u_\theta(\tau) = \begin{cases} 0 & \text{if } \tau < 0 \\ u(\tau) & \text{if } 0 \le \tau \le \theta \\ 0 & \text{if } \tau > \theta \end{cases}, \tag{7}$$

Considering Equation (7), Equation (6) can be written as:

$$\Delta E\,(t) = \frac{1}{2}\left[\sum_{k=0}^{\infty} u_{m_t}^2(k)\cdot T - \sum_{k=0}^{\infty} v_{m_t}^2(k)\cdot T\right] \ge 0 \quad \forall t \ge 0, \tag{8}$$

Using Parseval's theorem, the second term in Equation (8) can be written as:

$$\frac{1}{2}\left[\frac{TM}{2\pi}\int_{-\pi}^{\pi} |U_m(e^{j\omega})|^2 - V_m(e^{j\omega})|^2 d\omega\right], \tag{9}$$

where U_m and V_m are the discrete-time Fourier transform of u and v respectively. Moreover, u_m is split into two signals by using LP and HP filters.

$$\begin{cases} U_{LP} = H_{LP}U \\ U_{HP} = H_{HP}U \end{cases}, \tag{10}$$

The first output of the filters, u_{LP}, is fed to the VE and the output of HP filter is used to filter the velocity as explained earlier in Section 2. On the other hand v_m is generated by adding the outputs of VE and HP:

$$v_m = v_{LP} + v_{HP}, \tag{11}$$

where v_{LP} and v_{HP} are the outputs of the VE and HP respectively. Hence Equation (9) can be written as:

$$\frac{1}{2}\left[\frac{TM}{2\pi}\int_{-\pi}^{\pi}|U_m(e^{j\omega})|^2 - |\left[V_{LP}(e^{j\omega}) + V_{HP}(e^{j\omega})\right]|^2 d\omega\right], \tag{12}$$

Assuming that the VE is passive and by some manipulations Equation (12) becomes:

$$\frac{1}{2}\left[\frac{TM}{2\pi}\int_{-\pi}^{\pi}|U_m(e^{j\omega})|^2\left[1 - \left[|H_{LP}|^2 + \frac{|H_{HP}|^2}{4} + 2Real\left[H_{LP}H_{HP}^*/2\right]\right]\right]d\omega\right], \tag{13}$$

where H_{HP}^* denotes complex conjunction of H_{HP}. It can be concluded that the passivity condition is:

$$1 > \left[|H_{LP}|^2 + \frac{|H_{HP}|^2}{4} + 2Real\left[H_{LP}H_{HP}^*/2\right]\right], \tag{14}$$

Equation (14) provides the passivity condition independent of VE and haptic interface, provided they are passive. If LP and HP are ideal, Equation (14) is always satisfied. For practical filters Equation (14) gives passivity condition which can be used to design the filters.

In the next section the design problem is formulated as a minimax problem to obtain the filter coefficients.

3.1 Passive velocity Filter

4 Filters design

The filter design problem is formulated as a constrained minimax optimization problem. The VE which is used in this paper for analytical and experimental performance evaluation, is a slow VE with an update rate equal to 50 Hz. For this VE, the LP_1 filter, Figure 1, is designed based on the passivity analysis which is presented in [5], i.e. for avoiding aliasing the cutoff frequency should be less than $50/2 = 25\ Hz$. Hence, the LP_1 filter is considered to be a first order filter with the following transfer function:

$$H_{LP}(z) = \frac{0.05}{z - 0.95} \tag{15}$$

Also the following structure is assumed for H_{HP}:

$$H_{HP}(z) = \frac{z-1}{z-\alpha} \tag{16}$$

where α is the optimization variable. The error function is defined by using right hand side of Equation (14) and by evaluating it in 512 different frequency points. The constraint is defined in a way that guarantees the stability of the filter and prevents the overlapping of the frequency bandwidth of the LP and HP filters, i.e. $0 < \alpha < 0.95$.

Matlab Optimization toolbox is used to solve the problem. Figure 5 demonstrates the evaluated error function with optimized variable which found to be $\alpha = 929.134319755588e - 003$.

5 Frequency domain analysis

Figure 6 and Figure 7 demonstrates the frequency response of transmitted admittance in low and high frequency with the designed velocity filter. As it is cleared in these figures the new architecture significantly improves the performance

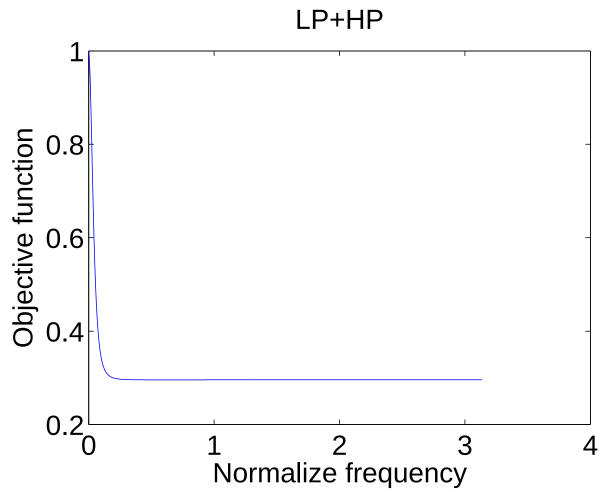

Figure 5: Evaluated objective function in different frequencies

of the system in high frequencies. In high frequency the significant deviation from the ideal case is removed which makes it possible to utilize larger wave impedances in order to improve the low-frequency response.

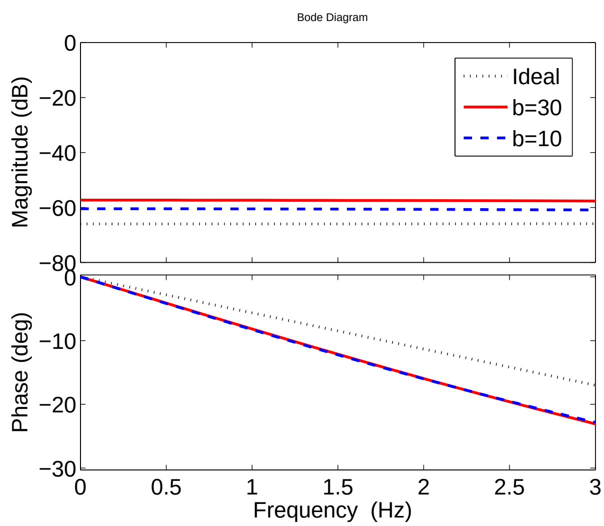

Figure 6: Frequency responses of transmitted admittance for different wave impedances and with velocity filter in low frequencies for $B_{VE} = 10\ Ns/m$ and $K_{VE} = 2000$ N/m

To confirm the analytical results, experimental results are provided in the next section.

6 Experiments

This section presents experimental interactions with a slow virtual wall through a Novint Falcon haptic interface which is connected to a personal computer (PCs) running Windows Vista on Intel Core 2 Duo CPU at 2.67GHz with 2 GB

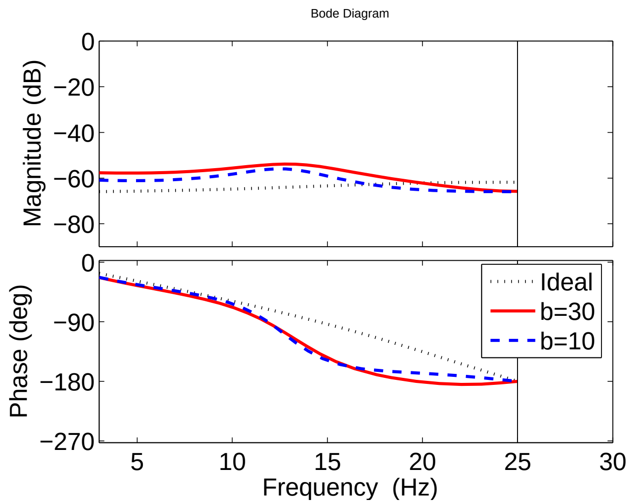

Figure 7: Frequency responses of transmitted admittance for different wave impedances and velocity filter in high frequencies for $B_{VE} = 10\ Ns/m$ and $K_{VE} = 2000$ N/m

RAM. The one degree of freedom virtual environment runs as a C++ console application on the same computer. The console application hast two loops; i) fast loop which comprises the master side and the filtering of the outgoing wave variable, u_m and velocity filter and ii) slow loop which consists of the slave side and runs inside the fast loop. Novint Falcon API is used to run the fast loop at 1 KHz and the update rate of the slow loop is controlled by a counter inside this fast loop. Since the console application runs on the Windows operating system, no exact sampling time could be guaranteed but the variation of the sampling times is negligible. The slow virtual wall is updated every 0.02 s. The wave impedance is $b = 30$ Ns/m. The stiffness of the VE is equal to 2000 N/m.

Two sets of experiments are conducted. In the first set of experiments a sinusoidal hand input is used. The frequency of the hand input is set to 5 Hz and its amplitude is 1 N. The main goal of this experiment is to show the performance of the designed filter in terms of noise attenuation. The result of three different experiments are provided: i) without using velocity filter, ii) with a velocity filter which differs form the designed velocity filter, and iii) with the designed velocity filter. Figure 8, Figure 9, and Figure 10 plot the results of the first set of experiments for these cases respectively.

Comparing Figure 8(b) and Figure 10(b), reveals how noise affects the force applied on the user. For the experiment shown in Figure 8 the following filter is used:

$$H_{LP}(z) = \frac{0.05}{z - 0.95} \tag{17}$$

instead of the designed filter which is:

$$H_{LP}(z) = \frac{0.071}{z - 0.929} \tag{18}$$

the result in Figure 8 demonstrate how the stability of the system is sensitive to the filter parameters and using wrong filters makes the system unstable. The results prove the effectiveness of the filter design method in Section 4.

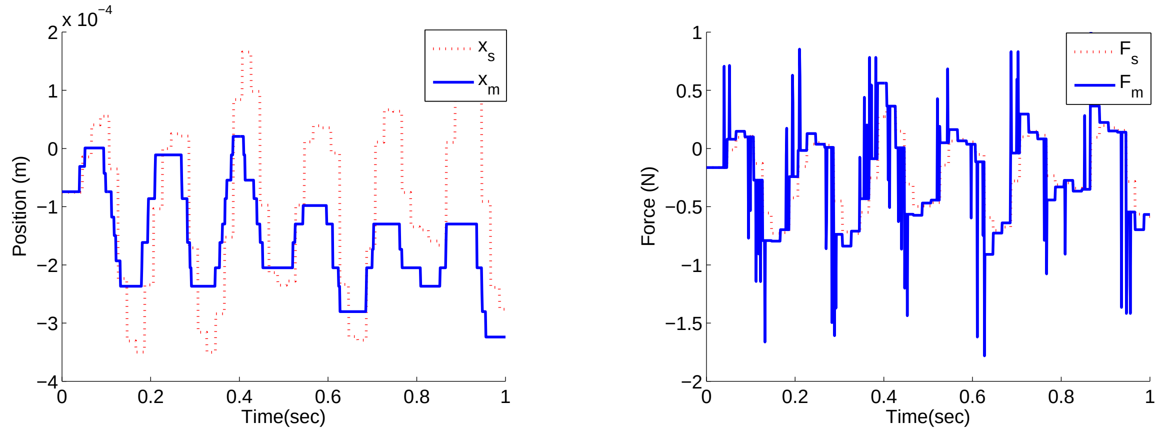

(a) Position of the haptic interface (solid line) and the command position in the VE (dotted).

(b) Feedback force (solid line) and the force in the VE (dashed line).

Figure 8: Experimental interaction with a slow virtual wall ($K = 2000$ N/m, $B = 10$ Ns/m, $T_{VE} = 0.02$ s) via passive multirate wave communications and without velocity filter. The frequency of sinusoidal hand input is 5 Hz.

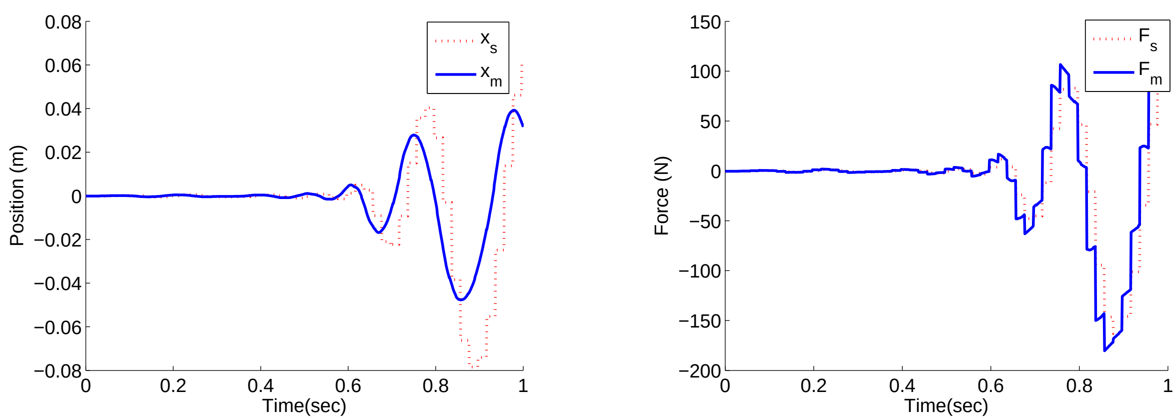

(a) Position of the haptic interface (solid line) and the command position in the VE (dotted).

(b) Feedback force (solid line) and the force in the VE (dashed line).

Figure 9: Experimental interaction with a slow virtual wall ($K = 2000$ N/m, $B = 10$ Ns/m, $T_{VE} = 0.02$ s) via passive multirate wave communications and with an impropriate velocity filter. The frequency of sinusoidal hand input is 5 Hz.

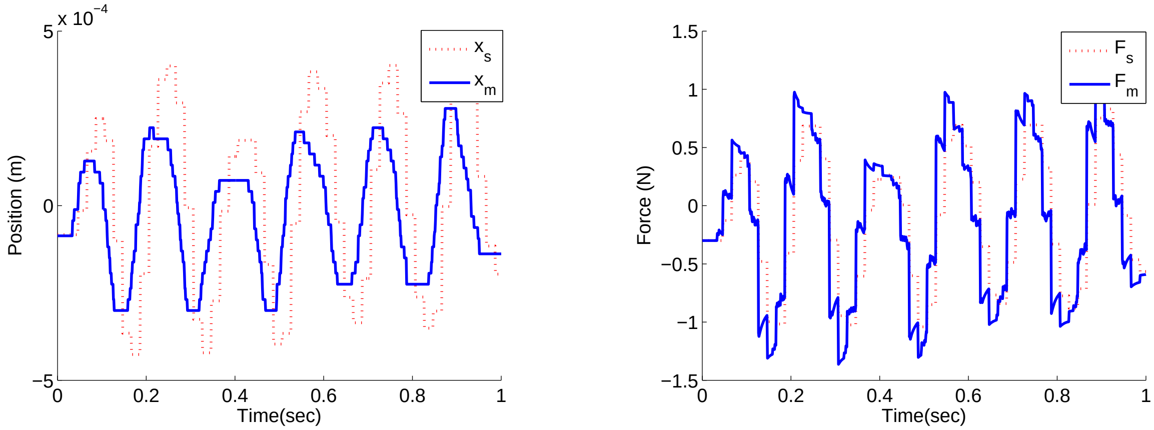

(a) Position of the haptic interface (solid line) and the command position in the VE (dotted).

(b) Feedback force (solid line) and the force in the VE (dashed line).

Figure 10: Experimental interaction with a slow virtual wall ($K = 2000$ N/m, $B = 10$ Ns/m, $T_{VE} = 0.02$ s) via passive multirate wave communications and with the designed velocity filter. The frequency of sinusoidal hand input is 5 Hz.

In the second set of experiments a step input is used as the human hand input to investigate the transient response of the system. The results are presented in Figure 11 and Figure 12 for two cases i) without velocity filter and ii) with velocity filter respectively. Beside the noisy force, note that the first peak of the applied force on the user in Figure 11(b) is almost twice greater than the first peak of the force in Figure 12(b). This fact shows that using velocity filter improves the performance of the system in high frequencies. The results confirms the analytical results in Section 5.

7 Conclusions

This work proposes a new filter bank-like architecture for improving the performance of multirate wave control of haptic system and filtering the input signal. The filters of proposed structure are designed based on passivity. Both analytical and experimental results are provided to confirm the performance of proposed architecture. Advantages of the proposed method is as follows:

1- the performance can be evaluated and improved. Unlike most time domain passivity based methods,

2- it can used for different haptic interface types and VEs, admittance or impedance,

3- controller, i.e. filters, design is independent of the haptic interface and VE.

4- noisy velocity input can be filtered passively.

5- filters design is a unirate problem

future works seeks two lines of research i) extending the results to passive position filtering which makes the proposed method a general way of passive filtering and ii) the possibility of adding a local model to the proposed

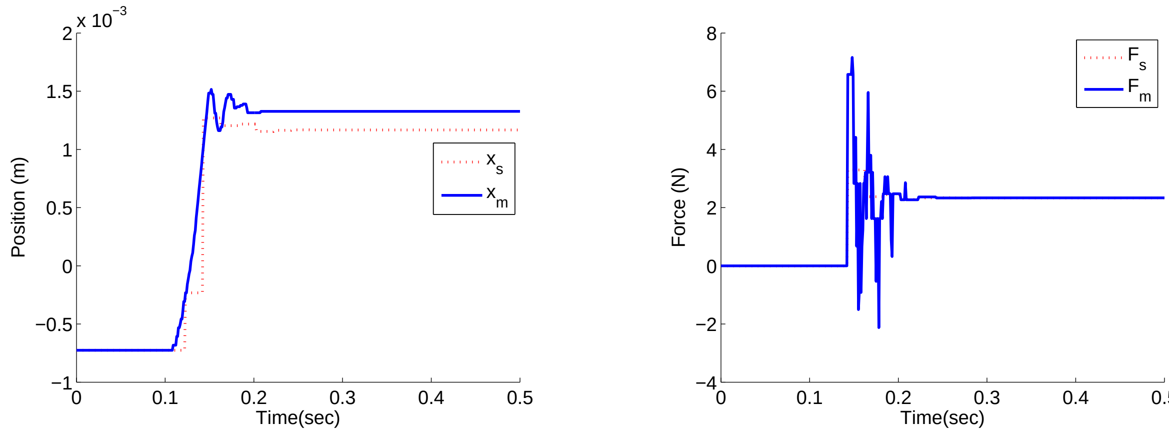

(a) Position of the haptic interface (solid line) and the command position in the VE (dotted).

(b) Feedback force (solid line) and the force in the VE (dashed line).

Figure 11: Experimental interaction with a slow virtual wall (K = 2000 N/m, B = 10 Ns/m, T_{VE} = 0.02 s) via passive multirate wave communications and without velocity filter. The hand input is a unit step.

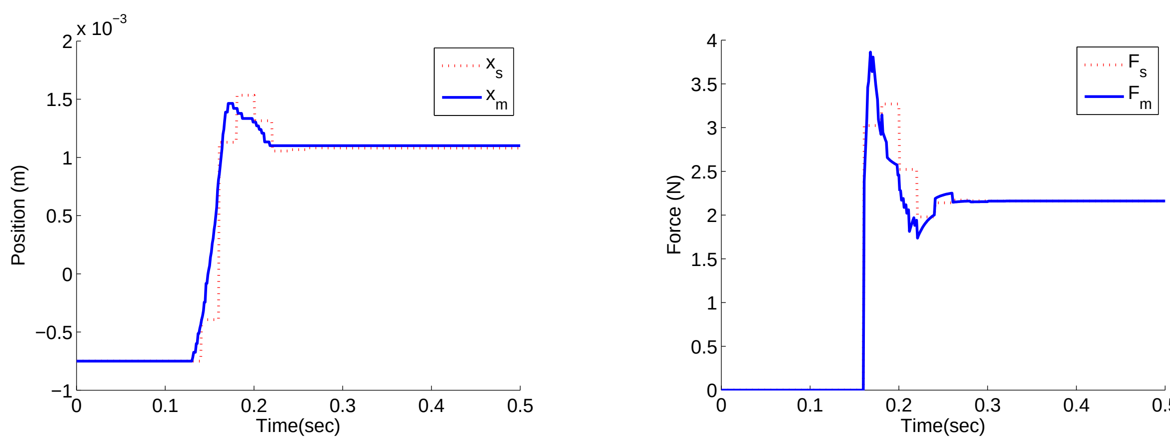

(a) Position of the haptic interface (solid line) and the command position in the VE (dotted).

(b) Feedback force (solid line) and the force in the VE (dashed line).

Figure 12: Experimental interaction with a slow virtual wall (K = 2000 N/m, B = 10 Ns/m, T_{VE} = 0.02 s) via passive multirate wave communications and with the designed velocity filter. The hand input is a unit step.

filterbank-like structure to improve performance of the system.

8 ACKNOWLEDGMENTS

The authors gratefully acknowledge the contribution of National Research Organization and reviewers' comments.

REFERENCES

[1] L. Bascetta, G. Magnani, and P. Rocco. Velocity estimation: Assessing the performance of non-model-based techniques. *Control Systems Technology, IEEE Transactions on*, 17(2):424 –433, march 2009.

[2] R.H. Brown, S.C. Schneider, and M.G. Mulligan. Analysis of algorithms for velocity estimation from discrete position versus time data. *Industrial Electronics, IEEE Transactions on*, 39(1):11 –19, feb 1992.

[3] Yuhua Li, Fengshou Gu, Georgina Harris, Andrew Ball, Nick Bennett, and Ken Travis. The measurement of instantaneous angular speed. *Mechanical Systems and Signal Processing*, 19(4):786 – 805, 2005.

[4] G. Niemeyer. *Using wave variables in time delayed force reflecting teleoperation.* PhD thesis, MIT, 1996.

[5] N. Yasrebi and D. Constantinescu. Passive multirate wave communications for haptic interaction with delayed rigid environments. *In review at the IEEE Transactions on Mechatronics*, 2010.

[6] N. Yasrebi and D. Constantinescu. Extending the Z-Width of a haptic device using acceleration feedback. In *EuroHaptics*, pages 157–162, Madrid, Spain, 2008.

[7] M. C. Chavushoglu, D. Feygin, and F. Tendick. A Critical Study of the Mechanical and Electrical Properties of the PHANToM Haptic Interface and Improvements for Highperformance Control. *Presence: Teleoperators and Virtual Environments*, 11(6):555–568, 2002.

[8] Wen-Hong Zhu and T. Lamarche. Damping enhancement of haptic devices by using velocities from accelerometers and encoders. In *Decision and Control, 2009 held jointly with the 2009 28th Chinese Control Conference. CDC/CCC 2009. Proceedings of the 48th IEEE Conference on*, pages 7515 –7520, dec. 2009.

[9] Andrew H. C. Gosline and Vincent Hayward. Dual-channel haptic synthesis of viscoelastic tissue properties using programmable eddy current brakes. *The International Journal of Robotic Research*, 28(10):1387–1399, 2009.

[10] Beibei Han and Jee-Hwan Ryu. An injecting method of physical damping to haptic interfaces based on fpga. In *Control, Automation and Systems, 2008. ICCAS 2008. International Conference on*, pages 1835 –1840, oct. 2008.

[11] Jilin Zhou, Xiaojun Shen, E.M. Petriu, and N.D. Georganas. Linear velocity and acceleration estimation of 3 dof haptic interfaces. In *Haptic Audio visual Environments and Games, 2008. HAVE 2008. IEEE International Workshop on*, pages 137 –142, oct. 2008.

[12] Z. Jabbour, S. Moreau, A. Riwan, and G. Champenois. Speed estimation comparison between full order state observer kalman filter for a haptic interface. In *IEEE International Symposium on Industrial Electronics, 2009*, pages 1482 –1487, july 2009.

[13] F. Janabi-Sharifi, V. Hayward, and C.-S.J. Chen. Discrete-time adaptive windowing for velocity estimation. *Control Systems Technology, IEEE Transactions on*, 8(6):1003 –1009, nov 2000.

[14] Naser Yasrebi and Daniela Constantinescu. Velocity estimation for haptic applications. In *CSME Forum 2010*, jun. 2010.

[15] N. Yasrebi and D. Constantinescu. Centralized multi-user multi-rate haptic cooperation using wave transformation. In *IEEE International Conference on Mechatronics and Automation*, pages 3816 –3821, aug. 2009.

[16] B.A. Francis and T.T. Georgiou. Stability theory for linear time-invariant plants with periodic digital controllers. *IEEE Transactions on Automatic Control*, 33(9):820–832, 1988.

[17] G. Niemeyer and J.-J.E. Slotine. Telemanipulation with time delays. *International Journal of Robotic Research*, 23(9):873–890, 2004.

American Control Conference, pp.3477-3483, 27-29 June 2012

Appendix E: Wave Filter Bank for High Fidelity Passive Multirate Haptic Interaction with Slowly Updated Virtual Environments

Naser Yasrebi, Daniela Constantinescu

Department of Mechanical Engineering, University of Victoria, Victoria, Canada

E-mail: nyasrebi@uvic.ca, danielac@me.uvic.ca.

Abstract

This paper proposes a filter bank-like structure with a local model of interaction for improving the performance of passive multirate wave variable control of haptic interaction with a slowly updated virtual environment. In the proposed structure, the low frequency component of the outgoing wave at the user's side is sent to the slow virtual environment, and the high frequency component is sent to a local model of interaction. Low-pass and high-pass filters separate the outgoing wave into the two components. Frequency domain analysis tools and lifting are used to investigate the effect of utilizing a local model of interaction in conjunction with the slow virtual environment. The analysis shows that: (1) the proposed control structure significantly improves the admittance transmitted to the user at both low and high frequencies; and (2) the parameters of the local model have little impact on the stability of the haptic system, unlike the parameters of local models developed in the power domain. Experiments with a Phantom Omni haptic device probing a slowly updated virtual wall validate the analytical results.

1 Introduction

The human touch requires a force refresh rate of about 1 KHz for convincing haptic interaction with virtual environments [1, 2, 3]. Yet, physically-based virtual environments oftentimes cannot be simulated at the speed needed for high-fidelity force control because they involve complex dynamics and/or collision detection computations. The delay of computationally demanding virtual environments is a well-recognized factor degrading the stability or passivity of haptic interaction [4, 5]. Providing stable and transparent haptic feedback to users interacting with slowly updated virtual environments is a challenging issue in haptic systems research.

A key approach to enabling a fast force control loop in the presence of computational delay of the virtual environment exploits a fast local model of interaction either in conjunction with the original slow virtual environment [1, 6] or in its place [7, 3, 8]. In essence, the fast local model is a simulation with reduced numerical complexity that computes the force feedback at typical haptic frequencies and thus, increases the stability and

IEEE Haptics Symposium, pp.105-110, 4-7 March 2012

transparency of the haptic interaction. Local models of interaction have been proposed for haptic manipulation both of rigid [9] and of deformable [10, 1, 7, 11, 3] virtual environments. Since this paper does not address the development of a local model of interaction, the reader is referred to [7] for a recent comprehensive overview.

A local model can be used in various architectures in conjunction with diverse control strategies. In [1], a local model comprising a fixed stiffness has been used together with virtual coupling [12, 5] control. Lifting [13] has been employed to derive the closed loop stability of a multirate simulation with the constant stiffness local model [1], and to show that the simulation loop is stable if the local stiffness is lower than the stiffness of the slow virtual environment. The results in [1] indicate that a fixed stiffness local model cannot be used to increase the gain of the force feedback loop and thus, to increase the range of contact impedances that can be rendered to users interacting in slowly updated virtual environments. In [3], pre-computed passive local models have substituted the slow virtual environment and a switching between the local models has been devised to passively activate them. The resulting passive interaction forces guarantee stable interaction, and the physical accuracy of the pre-specified local models ensures fidelity. The passive activation of the local models [3] guarantees the stability of the haptic manipulation of any slowly updated deformable virtual environment but requires passive local models to be pre-defined. In [6, 7], a real-time technique has been offered to generate a lower-order approximation of a full order virtual environment model. The lower-order-approximation local model has been used in conjunction with the full-order virtual environment in [6], and has been used in place of the full-order environment in [7]. Substituting a local model for a slow virtual environment improves the stability of the haptic interaction [3], but the transparency of the interaction hinges on the accuracy of the local model. Oftentimes no guarantee is provided for such accuracy. Using a local model in conjunction with the slow virtual environment may threaten the stability of the haptic system [1].

This paper introduces a novel filter bank-like haptic control architecture which combines passive multirate wave communications [14, 15] and a local model of interaction. The proposed architecture is shown to impose few restrictions on the parameters of the local model and to improve the transparency of passive multirate wave-based control of haptic interaction with a slowly updated virtual environment. The paper starts by investigating the limitations of the passive multirate wave communications [14, 15] in terms of transparency. It then proposes the new architecture, and contrasts its transparency to the transparency of the passive multirate wave control strategy. Lastly, the paper presents experimental results which validate the increased transparency of the haptic interaction with a slowly updated virtual environment through the novel filter bank-like architecture and the local model of interaction. Frequency domain tools alongside lifting enable the performance analyses and comparisons presented in this paper.

In the remainder, Section 2 introduces the performance limitations of passive multirate wave control of a haptic system with a slow virtual environment. Section 3 introduces the new filter bank-like architecture with local model, and investigates its performance. Section 4 presents the experimental performance validation. Section 5 summarizes the conclusions of this work.

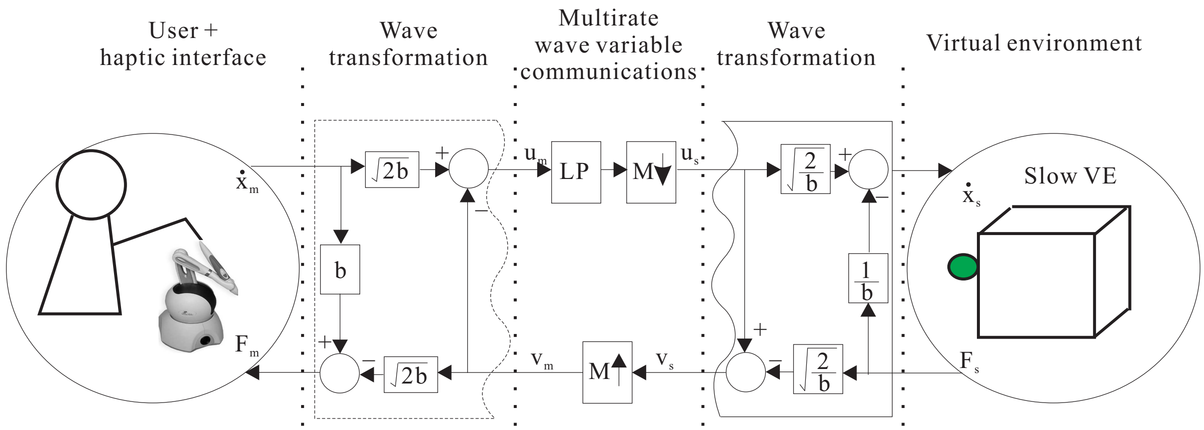

Figure 1: Passive multirate wave transformation with downsampling and upsampling in the communication channels, and with anti-aliasing low-pass filter in the wave sent from the user to the slow virtual environment.

2 Performance of passive multirate wave control of haptic interaction with slow virtual environments

This section investigates the performance of the passive multirate wave variable transformation depicted in Figure 1. In this figure: a downsampler M↓ and an upsampler M↑ are placed in the communications to model the rate change imposed on the haptic system by the slowly updated virtual environment; b is the wave impedance; $\dot{x}_m$ is the velocity of the user's hand; F_m is the force feedback applied to the user through control; u_m and u_s are the outgoing wave at the user and the virtual environment side, respectively; and F_s is the force response of the slow virtual environment. We have shown in prior work [14, 15] that wave aliasing due to downsampling may inject energy into the haptic system and destroy the passivity of multirate wave communications. To eliminate aliasing and guarantee the passivity of the multirate wave transformation, a low pass wave filter *LP* with cutoff frequency less than half the update frequency of the virtual environment is placed before the downsampler in the communication channel.

Lifting [13] is used to convert the multirate feedback system to a unirate system whose admittance transmitted to the user can be computed according to:

$$H(z) = \frac{X_m(z)}{F_h(z)}. \tag{1}$$

Note that the hand position rather than the hand velocity is used to compute the admittance transmitted to the user. Therefore, the DC transmitted admittance provides a direct indication of the environment stiffness transmitted to the user. After simplification of the control loop, the frequency response of the admittance transmitted to the user by passive multirate wave control is contrasted with the frequency response of the admittance transmitted by direct coupling control, hereafter considered the ideal response. Throughout the analysis, the haptic device is considered to have mass $m_{HD} = 0.1$ kg and damping $b_{HD} = 1.5$ ns/m, and the slowly updated virtual environment comprises a virtual wall with stiffness $K_{VE} = 500$ N/m, damping $B_{VE} = 1$ Ns/m, and sampling interval $T_{VE} = 0.02$ s. Figure 2 illustrates the frequency response of the transmitted impedance for various wave impedances. The low frequency response is depicted in Figure 2(a) and the high frequency response is shown in Figure 2(b).

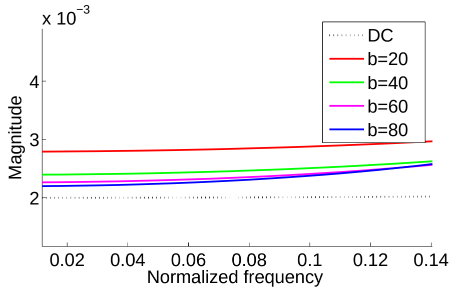

(a) Low frequencies.

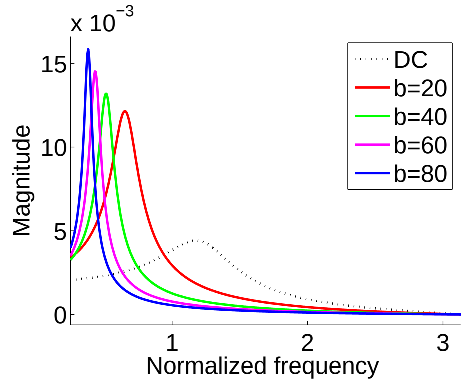

(b) High frequencies.

Figure 2: Frequency responses of the admittance transmitted to the user through direct coupling (DC) control and through passive multirate wave control for different wave impedances b and for a virtual wall with stiffness $K_{VE} = 500$ N/m, damping and $B_{VE} = 1$ Ns/m, and sampling interval $T_{VE} = 0.02$ s.

Figure 2(a) demonstrates that increasing the wave impedance improves transparency in the low frequency range, where the user's input can be considered constant. This is expected because the low-pass anti-aliasing filter behaves like a virtual coupler with spring stiffness [16]:

$$K_{filter} = 2b\lambda \tag{2}$$

in the low frequency range. In Equation (2), λ is the cutoff frequency of the low-pass filter.

On the other hand, Figure 2(b) illustrates that passive multirate wave control adversely affects the transmitted admittance in the high frequency range. Increasing the wave impedance is similar to adding damping to the haptic system. Added damping decreases the first natural frequency of the system and thus degrades transparency. It can be shown [15] that the transmitted admittance approaches the ideal transmitted admittance at the expense of stability when the cutoff frequency of the low pass filter increases. To overcome this performance shortcoming of passive multirate wave control without sacrificing stability, the next section proposes a novel filter bank-like architecture with a local model of interaction.

3 Passive multirate wave control with filter bank and local model of interaction

Figure 3 depicts the proposed architecture with filter bank and a local model of interaction. In this figure: LP_1 is the low-pass anti-aliasing filter which ensures the passivity of the multirate wave transformation; HP is the high-pass wave filter whose decoded output is passed to the local model of interaction LM; and LP_2 is a low pass wave filter which reduces the wave reflections in the feedback loop which comprises the local model. The filter bank divides the outgoing wave at the user's side u_m into a low-frequency wave, which it sends to the slowly updated virtual environment, and a high-frequency wave, which it passes along to the local model. It can be shown that this filter bank structure maintains the passivity of the wave-based communication channels.

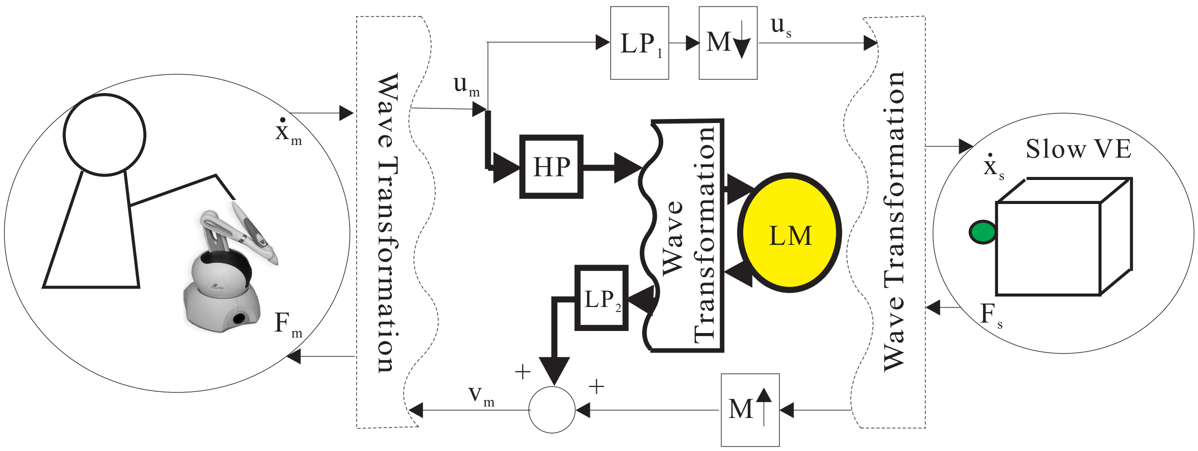

Figure 3: Proposed wave-based haptic control architecture with filter bank and local model of interaction.

The filter bank and local model shown in Figure 3 improve the transparency of the passive multirate wave control of haptic interaction with a slowly updated virtual environment in the high frequency range, but have little effect on the performance of the system in the low-frequency range. Increased transparency in low frequencies is achieved via adding an additional term to the returning wave at the user's side v_m [17]:

$$v_m = v_m - K_p(x_m - x_s), \tag{3}$$

where K_p is a constant gain, and x_m and x_s are the position of the haptic device and the position of its avatar in the virtual environment, respectively. The additional term in Equation (3) makes the low-frequency control performance independent of the wave impedance.

The following section uses frequency domain analysis to derive the performance of the proposed wave-based haptic control architecture with filter bank and local model of interaction, and to demonstrate that the local model stiffness K_{LM} and and the gain of the term added to the returning wave K_p do not affect the stability of the haptic system.

3.1 Stability analysis

In this section, lifting is used to convert the wave-based haptic multirate system with filter bank and local model of interaction into a unirate system and to derive its stability region. Figure 4 shows the Z-width of the haptic interface with passive multirate wave control. This figure illustrates that the haptic device can stably render a maximum environment stiffness $K_{VE} = 800$ N/m for an environment damping $B_{VE} = 1$ Ns/m.

Figure 5 plots the stability region of haptic interaction with a slowly updated virtual environment controlled via passive multirate waves with filter bank and local model of interaction, for various values of the virtual environment stiffness K_{VE}, of the local model stiffness K_{LM}, and of the gain K_p (Equation (3)). The wave impedance is $b = 25$ Ns/m, and the damping of the virtual environment is $B_{VE} = 1$ Ns/m for all stiffness combinations depicted in Figure 5. All filters are IIR-Butterworth filters. They are designed using the Digital Filter Design toolbox in Matlab, and according to the specifications in Table 1. As shown in Figure 5, the proposed passive

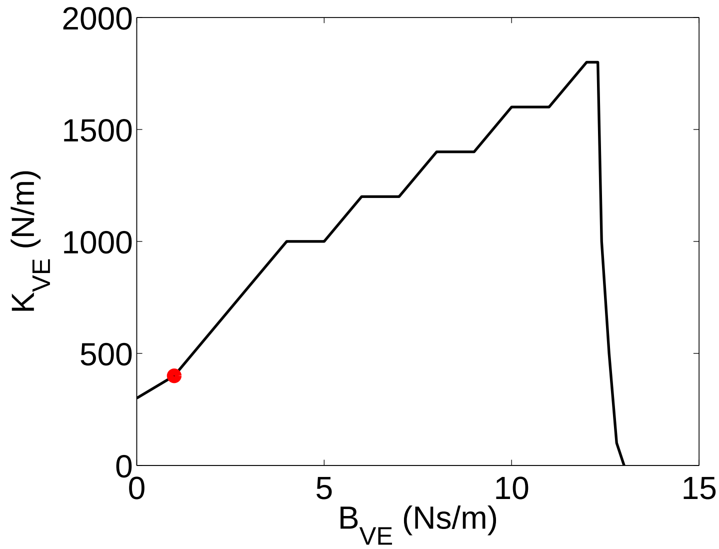

Figure 4: Z-width of the haptic interface with passive multirate wave control.

multirate wave control with filter bank, local model and position feedback improves the stability of the system, too. The improvement is largely brought about by the damping injected through the low-pass filter LP_2. This filter has been introduced to reduce the wave reflections caused by the feedback loop closed through the local model of interaction.

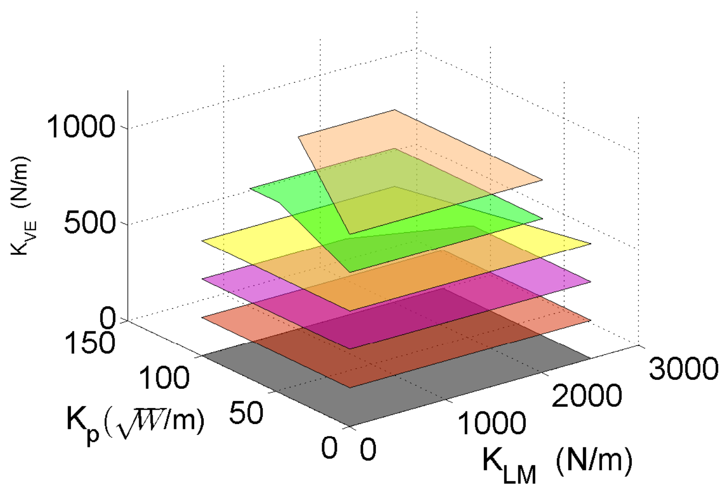

Figure 5: Stability region of the proposed wave-based haptic control architecture with filter bank and local model of interaction for various values of the virtual environment stiffness K_{VE}, of the local model stiffness K_{LM}, and of the gain K_p (Equation (3)).

Table 1: Filter specifications for analysis and experiments

Filter	Passband Freq (Hz)	Stopband Freq (Hz)	Passband Amp (dB)	Stopband Amp (dB)
LP_1	25	50	20	10
LP_2	300	600	1	40
HP	40	70	40	20

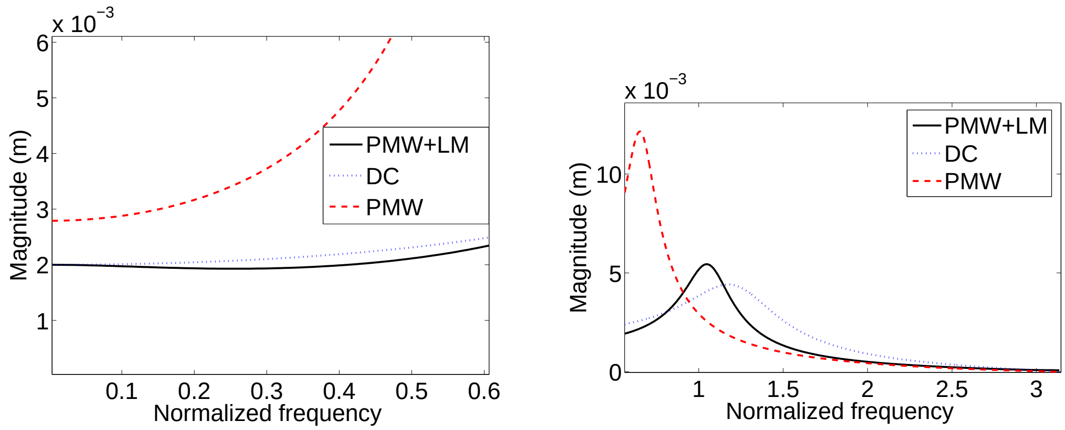

(a) Low frequencies.

(b) High frequencies.

Figure 6: Frequency responses of the admittance transmitted to the user by: passive multirate wave control with filter bank and local model(PMW+LM); direct coupling (DC); passive multirate wave control (PMW). The wave impedance is $b = 25$ Ns/m both for PMW+LM and for PMW.

3.2 Performance analysis

Figures 6(a) and 6(b) plot the low and high frequency responses of the admittance transmitted to the user: by the wave-based haptic control architecture with filter bank and local model of interaction (PMW+LM); by direct coupling control (DC), herein considered the ideal response; and by passive multirate wave control (PMW). Note in these figures that the passive multirate wave control with filter bank and local model of interaction (PMW+LM) has much better performance that passive multirate wave control (PMW) both at low and at high frequencies. In the low frequency range, the amplitude response of PMW+LM is much closer to the ideal response (DC). In the high frequency range, the natural frequency approaches the natural frequency of the ideal system (DC). In other words, the proposed architecture can render stiffer contact than the passive multirate wave controller without local model of interaction.

The analytical results obtained in this section are validated experimentally in the following section.

4 experiments

The experimental interactions involve controlled haptic contact with a delayed virtual wall through a Phantom Omni haptic interface. The haptic device is connected to a personal computer which runs Windows Vista on an

Intel Core 2 Duo CPU at 2.67GHz with 2 GB RAM. The virtual environment runs as a C++ console application on the same computer. The console application has two loops: a fast loop that implements the device control, the filtering of the outgoing wave variable u_m, the filter bank and the local model; and a slow loop that runs the virtual environment simulation. OPENHAPTICS API is used to run the fast loop at 1 KHz and the slow loop at 50 Hz. Since the console application runs on Windows, no exact sampling time can be guaranteed, but the variation of the sampling time is negligible. A sinusoidal force is used to excite the system and to determine its frequency response. The frequency of the sinusoidal input is variable and bounded in the $[0, 50]$ Hz interval. The stiffness of the virtual environment and of the local model are $K_{VE} = K_{ML} = 500$ N/m, the wave impedance is $b = 25$ Ns/m, and the gain in Equation (3) is $K_p = 20\ \frac{\sqrt{W}}{m}$. A virtual wall with $K_{VE} = 500$ N/m, $B_{VE} = 1$ Ns/m, and an update rate of 1 kHz is considered the ideal case in the experiments.

Figure 7 depicts the experimental frequency response of transmitted admittance for three control strategies: passive multirate wave control with filter bank and local model (PMW+LM); direct coupling (DC); passive multirate wave control (PMW). Note in this figure that the proposed architecture PMW+LM: (i) increases the first natural frequency of the system and thus, can be used to render stiffer contacts then passive multirate wave control; and (ii) at low frequency, approaches the ideal transmitted admittance regardless of the low update rate of the virtual environment (equal to 0.02 s) compared to the fast update rate of the ideal virtual environment (equal to 0.001 s).

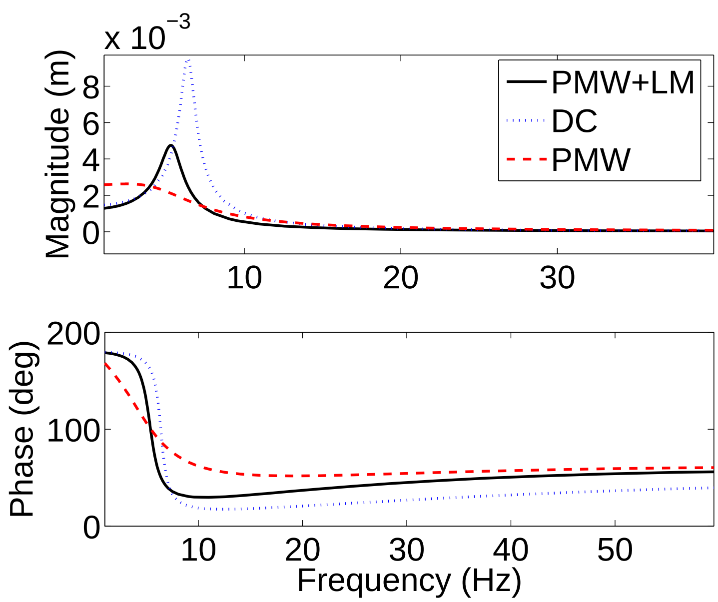

Figure 7: Experimental frequency responses of transmitted admittance for: passive multirate wave control with filter bank and local model(PMW+LM); direct coupling (DC); passive multirate wave control (PMW).

Figure 8 depicts the impedance transmitted to the user $\frac{F_m}{X_m}$ by the three control strategies: passive multirate wave control with filter bank and local model (PMW+LM); ideal direct coupling to fast virtual environment (DC); passive multirate wave control (PMW). Note that the proposed architecture transmits to users an environment impedance which is much closer to the virtual environment stiffness $K_{VE} = 500$ N/m. compared to the passive multirate wave control strategy.

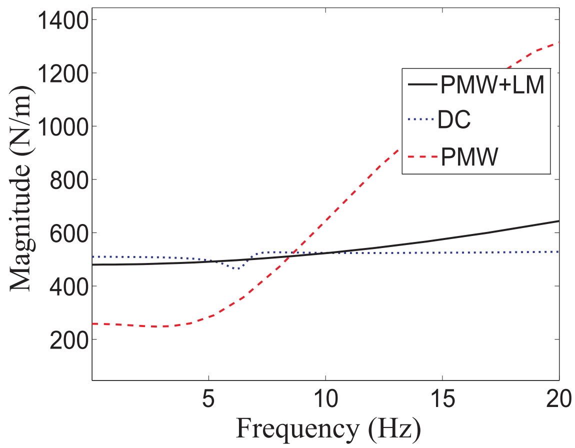

Figure 8: The impedance transmitted to the user by: passive multirate wave control with filter bank and local model(PMW+LM); direct coupling to fast virtual environment (DC); passive multirate wave control (PMW).

5 Conclusions and future work

This paper has aimed to improve the performance of a passive multirate wave variable controller for haptic interaction with slowly updated virtual environments previously developed by the authors [14, 15]. To this end, it has proposed a filter bank-like structure with local model of interaction in which low-pass and high-pass filters have separated the wave leaving the haptic interface side into two components. The low-frequency component of the outgoing wave has been sent to the slow virtual environment, and the high frequency component has been sent to a local model of interaction. Frequency domain analysis and lifting have been used to derive the stability and performance of the local model alongside the slow virtual environment. The filter bank together with the local model of interaction have been shown to improve the admittance transmitted to the user by the passive multirate wave controller both at low and at high frequencies. Further, the parameters of the local model have been shown to affect little the stability of the haptic system, unlike the parameters of local models developed in the power domain. Experiments with a Phantom Omni haptic device probing a slowly updated virtual wall have been presented to validate the analytical results.

Upcoming work will investigate the formulation of the filter design problem as a multirate robust loop-shaping problem. Robust control should decrease the sensitivity to changes in the virtual environment and/or in the haptic interface, and should allow the haptic feedback system to cope with the errors involved in approximating the virtual environment parameters in the local model.

Acknowledgment

This work has been supported through an NSERC Discovery Grant.

IEEE Haptics Symposium, pp.105-110, 4-7 March 2012

REFERENCES

[1] F. Barbagli, D. Prattichizzo, and K. Salisbury. A multirate approach to haptic interaction with deformable objects single and multipoint contacts. *International Journal of Robotic Resesearch*, 24(9):703–715, 2005.

[2] M. Fotoohi, S. Sirouspour, and D. Capson. Stability and performance analysis of centralized and distributed multi-rate control architectures for multi-user haptic interaction. *International Journal of Robotics Research*, 26(9):977–994, 2007.

[3] M. Mahvash and V. Hayward. High-fidelity passive force-reflecting virtual environments. *IEEE Transactions on Robotics*, 21(1):38–46, 2005.

[4] J. E. Colgate and J. M. Brown. Factors affecting the Z-Width of a haptic display. In *IEEE Conference on Robotics and Automation*, pages 3205–3210, San Diego, CA, 1994.

[5] J. E. Colgate and G. G. Schenkel. Passivity of a class of sampled-data systems: application to haptic interfaces. *Journal of Robotic Systems*, 14(1):37–47, 1997.

[6] M. C. Cavusoglu. Multirate simulation for high fidelity haptic interaction with deformable objects in virtual environments. In *IEEE International Conference on Robotics and Automation*, pages 2458–2465, 2000.

[7] Paul Jacobs, Michael J. Fu, and M. Cenk Čavuåoäglu. High fidelity haptic rendering of frictional contact with deformable objects in virtual environments using multi-rate simulation. *International Journal of Robotics Research*, 0(0):1–15, 2010.

[8] Daniel Wang, Yuru Zhang, Yuhui Wang, Yuan-Shin Lee, Peijun Lu, and Yong Wang. Cutting on triangle mesh: Local model-based haptic display for dental preparation surgery simulation. *IEEE Transactions on Visualization and Computer Graphics*, 11:671–683, 2005.

[9] D. Constantinescu, S.E. Salcudean, and E.A. Croft. Local model of interaction for haptic manipulation of rigid virtual worlds. *International Journal of Robotic Research*, 24(10):789–804, 2005.

[10] R. Balaniuk. A differential method for the haptic rendering of deformable objects. In *ACM Symposium on Virtual Reality and Software Technology*, pages 297–304, Limassol, Cyprus, 2006.

[11] K. Lee and D.Y. Lee. MIMO output estimation with reduced multirate sampling for real-time haptic rendering. *IEEE Transactions on Robotics*, 23(3):481–493, 2007.

[12] R. J. Adams and B. Hannaford. Stable haptic interaction with virtual environments. *IEEE Transactions on Robotics and Automation*, 5(3):465–474, 1999.

[13] B.A. Francis and T.T. Georgiou. Stability theory for linear time-invariant plants with periodic digital controllers. *IEEE Transactions on Automatic Control*, 33(9):820–832, 1988.

IEEE Haptics Symposium, pp.105-110, 4-7 March 2012

[14] N. Yasrebi and D. Constantinescu. Centralized multi-user multi-rate haptic cooperation using wave transformation. In *IEEE International Conference on Mechatronics and Automation*, pages 3816 –3821, aug. 2009.

[15] N. Yasrebi and D. Constantinescu. Passive multirate wave communications for haptic interaction with delayed rigid environments. *In review at the IEEE Transactions on Mechatronics*, 2010.

[16] G. Niemeyer and J.-J.E. Slotine. Telemanipulation with time delays. *International Journal of Robotic Research*, 23(9):873–890, 2004.

[17] N. Diolaiti, G. Niemeyer, and N. A. Tanner. Wave haptics: Building stiff controllers from the natural motor dynamics. *International Jornal of Robotics Reseasrch*, 26(1):5–21, 2007.